Myoelectric Signal Monitoring System

Fabiano Reis Mendes

Departamento de Engenharia Electrotécnica

Mestrado em Engenharia Electrotécnica e de Computadores

Área de Especialização em Automação e Sistemas

2015

This report satisfies partially the requirements to the subject of Thesis / Dissertation of Electrical and Computer Engineer MSc.

Candidate: Fabiano Reis Mendes, nº 1091170, 1091170@isep.ipp.pt

Supervisor: José Alberto Machado da Silva, jms@fe.up.pt

Co-supervisor: Gustavo Alves, gca@isep.ipp.pt

Departamento de Engenharia Electrotécnica

Mestrado em Engenharia Electrotécnica e de Computadores

Área de Especialização em Automação e Sistemas

2015

In memory of

Mário de Almeida Mendes

Acknowledgments

I would like to thank everybody who helped me along the development of this work. In particular, I am grateful to:

- whom made it possible for me to come and stay in Portugal: my parents Doralice and Joaquim, my uncle Mário, my aunt Isabel, my brother Mário and my sister Izabel, my cousin Doris and her husband Francisco, the marital Flávia and Leonardo;

- friends from the laboratory: Eng. Helder, Eng. João, Eng. Nuno, Eng. João Loureiro, Eng. Ruben;

- all friends that provided help in any way: Fernando, Carlos and the marital Paulo and Angelúzia;

- professor João Canas Ferreira for providing the microprocessor development kit;

- professors Machado da Silva and Gustavo Alves for their receptiveness, availability and patience.

Thank you all.

Abstract

The *Electromyography* (EMG) is an important tool for gait analyzes and disorders diagnoses. Traditional methods involve equipment that can disturb the analyses, being gradually substituted by different approaches, like wearable and wireless systems. The cable replacement for autonomous systems demands for technologies capable of meeting the power constraints. This work presents the development of an EMG and kinematic data capture wireless module, designed taking into account power consumption issues.

This module captures and converts the analog myoeletric signal to digital, synchronously with the capture of kinetic information. Both data are time multiplexed and sent to a PC via Bluetooth link. The work carried out comprised the development of the hardware, the firmware and a graphical interface running in an external PC. The hardware was developed using the PIC18F14K22, a low power family of microcontrollers. The link was established via Bluetooth, a protocol designed for low power communication. An application was also developed to recover and trace the signal to a *Graphic User Interface* (GUI), coordinating the message exchange with the firmware. Results were obtained which allowed validating the conceived system in static and with the subject performing short movements. Although it was not possible to perform the tests within more dynamic movements, it is shown that it is possible to capture, transmit and display the captured data as expected. Some suggestions to improve the system performance also were made.

Keywords:

Electromyography, microcontroller, Bluetooth, low power.

Resumo

A eletromiografia constitui uma importante ferramenta de diagnóstico na avaliação de patologias relacionadas à marcha. Os métodos tradicionais usam equipamento que pode prejudicar a análise e que vem gradualmente sendo substituído por sistemas sem fios e que proporcionam melhor conforto durante a análise. A substituição de sistemas com cablagem por sistemas autónomos requer o uso de tecnologias voltadas para o baixo consumo de energia. Este trabalho tem por objetivo apresentar uma solução alternativa de captura e transmissão de dados sem fios, desenvolvida tendo em consideração questões de consumo e portabilidade, recorrendo as soluções disponibilizadas no mercado com base no uso de microprocessadores.

O sistema projetado tem como função converter o sinal mioelétrico de analógico para digital, multiplexá-lo com os dados cinéticos e enviá-los para um terminal remoto. O trabalho consiste no desenvolvimento do Hardware, do Firmware e de uma interface gráfica. Para o desenvolvimento do Hardware foi usado o PIC18F14K22, que pertence a família de microcontroladores de baixo consumo. O Bluetooth, que é um protocolo de comunicação desenvolvido para aplicações de baixo consumo, foi usado para o estabelecimento do enlace. A aplicação desenvolvida tem a função de recuperar os dados e exibí-los em uma interface gráfica, além de coordenar a troca de mensagens com o Firmware. Embora não tenha sido possível executar os testes dinamicamente, mostra-se com os testes realizados em regime estático ou com movimentos curtos, que os dados foram capturados, transmitidos e reproduzidos de forma fidedigna e de acordo com o esperado. Finalmente são feitas algumas sugestões que podem melhorar o desempenho do sistema projetado.

Palavras chaves:

Eletromiografia, microcontrolador, Bluetooth, baixo consumo.

Table of Contents

List of Figures

List of Tables

Acronyms and Abbreviations

ACC	-	*Accelerometer*
ACL	-	*Asynchronous Connectionless*
AD	-	*Analog – Digital*
ADC	-	*Analog – Digital Converter*
AFE	-	*Analog Front End*
API	-	*Application Programming Interface*
ASIC	-	*Application Specific Integrated Circuit*
BAN	-	*Body Area Network*
BRG	-	*Baud Rate Generator*
BSN	-	*Body Sensor Network*
BT-LE	-	*Bluetooth Low Energy*
Bth	-	*Bluetooth*
Ckt	-	*Circuit*
CMRR	-	*Common-Mode Rejection Ratio*
CPU	-	*Central Processing Unit*
CTP	-	*Cordless Telephony Profile*
CU	-	*Central Unit*
DA	-	*Digital – Analog*
DAC	-	*Digital – Analog Converter*
DC	-	*Direct Current*
DLS	-	*Double Limb Support* stage
DNP	-	*Dial-up Networking Profile*
DSC	-	*Digital Signal Controller*
DSP	-	*Digital Signal Processor*
EEPROM	-	*Electrically Erasable Programmable Read-Only Memory*
ECCP	-	*Enhanced Capture / Compare / Pulse Width Modulation*
ECG	-	*Electrocardiography*
EDR	-	*Enhanced Data Rate*
EEG	-	*Electroencephalography*
EMG	-	*Electromyography*
EUSART	-	*Enhanced Universal Synchronous - Asynchronous Receiver – Transmitter*
FEC	-	*Forward Error Correction*
FFT	-	*Fast Fourier Transforming*
FIFO	-	*First Input – First Output*

FP - *Fax Profile*

FTP - *File Transfer Profile*

GAP - *Generic Access Profile*

GOEP - *Generic Object Exchange Profile*

GUI - *Graphic User Interface*

HCI - *Host Controller Interface*

HS - *Headset*

I²C - *Integrated Interconnect*

I/O - *Input / Output*

ICSP - *In-Circuit Serial Programming*

IDE - *Integrated Development Environment*

IEEE - *Institute of Electrical and Electronics Engineers, Inc*

IP - *Intercom Profile*[1]

IP - *Internet Protocol*[1]

IrMC - *Infrared Mobile Communication*

ISM - *Industrial, Scientific and Medical*

L2CAP - *Logical Link and Control Adaptation Protocol*

LAN - *Local Area Network*

LAP - *Local Area Network Profile*

LED - *Light Emission Diode*

LMP - *Link Manager Protocol*

LSb - *Least Significant bit*

LSB - *Least Significant Byte*

MAC - *Medium Access Control layer*

MBAN - *Medical Body-Area Networks*

MCU - *Microcontroller Unit*

MISO - *Master Input Slave Output*

MOSI - *Master Output Slave Input*

MIP - *Million Instructions per Second*

MSb - *Most Significant bit*

MSB - *Most Significant Byte*

MSSP - *Master Synchronous Serial Port*

MU - *Motor Unit*

MUAPT - *Motor Unit Action Potentia*l

NRZ - *Non-Return-to-Zero*

OBEX - *Object Exchange Protocol*

[1] These two acronyms are identical; however they are both standard and able to be distinguished, according to the context.

OPAMP(s) - *Operational Amplifier*(*s*)

OS - *Operating System*

OSI - *Open System Interconnection*

P2P - *Peer-to-Peer*

PC - *Personal Computer*

PCB - *Printed Circuit Board*

PHY - *Physical layer*

PLL - *Phase Lock Loop*

PPP - *Point-to-Point Protocol*

PSD - *Power Spectrum Density*

PWB - *Printed Wire Board*

PWM - *Pulse Width Modulation*

R/W - *Read and Write*

RAM - *Random Access Memory*

RCU - *Recording Central Unit*

RF - *Radiofrequency*

RFCOMM - *Radio frequency communication protocol*

RISC - *Reduced Instruction Set Computer*

RMS - *Root Mean Square*

RX - *Reception*

SCI - *Serial Communications Interface*

SCO - *Synchronous Connection-Oriented*

SDAP - *Service Discovery Application Profile*

SDP - *Service Discovery Protocol*

SEMG - *Surface Electromyography*

SIG - *Special Interest Group*

SLS - *Single Limb Support stage*

SNR - *Signal Noise Ratio*

SP - *Synchronization Profile*

SPI - *Serial Peripheral Interface*

SPP - *Serial Port Profile*

TCS - *Telephony Control Specifications*

TCP - *Transport Control Protocol*

TX - *Transmission*

UART - *Universal Asynchronous Receiver - Transmitter*

UDP - *User Datagram Protocol*

UHF - *Ultra High Frequency*

USART - *Universal Synchronous - Asynchronous Receiver - Transmitter*

UWB	-	*Ultra Wideband*
VHF	-	*Very High Frequency*
WAE	-	*Wireless Application Environment*
WAP	-	*Wireless Application Protocol*
WGN	-	*White Gaussian Noise*
WiFi	-	*Wireless Fidelity*
WLAN	-	*Wireless Local Area Network*
WPAN	-	*Wireless Personal Area Network*
WSN	-	*Wireless Sensor Network*
µC	-	*Microcontroller*

1. INTRODUCTION

Myoeletric signals are the result of membrane depolarization during muscular activity that generates a weak, but detectable electric field. Different concentrations of ions K^+, Ca^{++} and Na^+ cause a difference of potential through muscular and nervous cell membranes. The propagation of a stimulus occurs with a temporary altering of concentration between inner and outer of cells environment. By its biological origin, the myoeletric signal can be included into the set of biosignals that can provide information about the physiological state [1].

The Electromyography is the act of recording the myoeletric signals through sensors and display by a graphical interface. Analyses involving EMG are reported since 1849, when surface electrodes sensors were used to capture the myoeletric signal from a muscle. Thereafter, at 1929, a concentric needle was used that allowed to detect the signal from a single *Motor Unit*[2] (MU) [2]. These early studies were improved by enhancement of techniques like noise filtering, signal processing, sensing; being widely used in many fields, especially on medicine with clinical, research, rehabilitation and sportive purposes. "Clinically EMG is used to determine the function of muscle groups following trauma. It may also be used to assess muscle function following suspected neurological damage." [1]

The association with mechanical sensors such as accelerometers or gyroscope is relatively recent and most applied to upper limbs than to lower limb, in which the usage of cameras and feet platforms is still predominant to kinesiological pattern analysis. The usage of multichannel sensing it is necessary to generate a spatial and temporal representation of a movement pattern and associate it to a muscle or to a muscular group activity [3].

Nowadays efforts have been focused on the development of nonintrusive techniques, through innovative surface detection systems, that avoid complications inherent to the invasive techniques. Some works have been conducted in this field leading to studies to

[2] It is called Motor Unit a single nervous pathway that controls one or more muscular fiber(s).

develop wearable sensors clothes with the purpose of measuring the biosignal generated by the body. These clothes have the promise to be used to diagnosis motor-neural illness associated, although it represents more complex and expensive method [4] [5].

It is possible to identify three main conditions in which the *Surface EMG* (SEMG) is commonly applied. The first one is done under static posture to evaluate a possible impairment on a specific peripheral nerve. In this case the SEMG is used as a complementary way to the intrusive EMG. The second is done in the same static condition than the first one but directly applied over one whole nervous arc to assess a potential neuromotor disorder along the stimulus-reflex response pathway. The third condition is that the signal is recorded during an intentional motor action with the purpose of evaluating cyclical movement patterns. If applied jointly with kinesiological sensing it will be possible to relate a motion disturbance to an individual muscle [3].

The SMEG is limited to the more superficial and larger muscles because it is more liable to the adjacent muscles interference when applied to smaller or deeper muscles, but is more efficient to global analysis of movement [3]. The accuracy of intrusive EMG evaluation is hindered by limitations of movements during a motor task, achieving thus, the same conditions of accuracy than SEMG. Different membranes elasticity affects both recording methods, with noise added by electrodes displacement from target on SEMG and the discomfort caused by the needle on intrusive EMG. In this regard two techniques have different indications [3].

On the analysis of human gait the SEMG is indicated because allows more movement freedom, but in a complete analysis in which it is required kinetic and kinesiological data, cables and increased amount of sensors can also affect the natural flow of gait and return altered results. The replacement of cables by wireless connection is the traditional solution. Some dedicated protocols have been proposed in some studies but the trend it is the usage of standardized protocols, mainly the WiFi, the Bluetooth and the ZigBee. Another possible solution is on standalone scenario, in which data is recorded to a card memory. The size and the weight of the apparatus is a solved question with the devices miniaturization. Portability, mobility, and comfort are issues to be thought to conceive non-intrusive methods and thus, to get trust results [3].

In any choice for wireless communication it is necessary to consider the power supply to ensure the device's autonomy during a time enough to perform the desired evaluation. The wireless component has been identified as a major power consumer in programmable smart devices. These devices are supplied with batteries that must satisfy the size and weight constrains for the portability [6].

The efforts to solve the supply issues, which are common to all electric and electronic apparatus, are concentrated on three research branches: the energy density and storing, energy source and energy saving. The first branch goes to increase chemically the power density and the efficiency, like the addition of graphite, silicon or boron to lithium batteries, being a field of engineer of materials. The second branch is concentrated in manners to convert the energy using alternative sources to (re)charge and its reusing, for example photovoltaic microcells, piezoelectric materials or biological heating. The third branch focuses systems designed to save and manage the power consumption, at semiconductor and programming levels. Some solutions are strongly present nowadays although yet in maturing process to its consolidation, being objects of constants efforts to improvements.

The most usual configuration of the EMG system uses a *Central Unit* (CU) based on Microcontroller or on *Digital Signal Processor* (DSP) to collect and process data from sensors. Several manufacturers provide devices that meet the EMG system constrains what explain their widely acceptance. These devices are designed for minimum power consumption and are flexible and versatile to allow operating with many standardized communication protocols. Although can perform the role of data center recover the great trend is the usage like a node, intermediating the EMG system to another remote point that can be a Data Base, a *Local Area Network* (LAN), Internet or other device. The link is made essentially by Bluetooth or ZigBee protocols, which are designed to establish communication routines thought in minimum effort along link that allow more power efficiency to implement a network than *Wireless Fidelity* (Wi-Fi).

The network architecture is other aspect that can be handled to improve the energy efficiency affecting the sensors configuration and the data exchange. Sensor's amount and disposal can drain energy as autonomous as they are and as linked as they are to

others components. The simplicity of the network of sensors implies delegation of more working to the *Recording CU* (RCU). The ideal topology is subject of studies that bring the concept of *Body Sensor Network* (BSN) [7].

This issue becomes so important that The *Institute of Electrical and Electronics Engineers, Inc* (IEEE) introduces the concept of *Body Area Network* (BAN) and since 2008 creates a task group to specify the standard 802.15/6™, "(…) optimized for low power devices and operation on, in or around the human body (but not limited to humans)(…)" [8]. The BSN takes part in medical applications but the BAN predicts other applications like "consumer electronics / personal entertainment (…)" [8]. More generally, the standard 802.15™ cares every kind of *Wireless Personal Area Network* (WPAN) that treats all kind off network nearby human body.

1.1. CONTEXT

ProLimb is a project developed at *INESC Porto* with the purpose of developing a 'knit of sensors'. The result was a wearable legging incorporating a system that is capable of recording EMG signals of both legs during gait. The matching with a personal interest in this area has motivated to present the theme of the thesis like a partial requirement for the Master in Electronic Computer Engineering in branch Automation and Systems (MEEC / AS) at *Instituto Superior de Engenharia do Porto* (ISEP).

1.2. OBJECTIVE

This work aimed at designing a portable low power system to capture the myoeletric and mechanical signals through sensors and send them to a terminal computer, where the waveform will be displayed. The first purpose of this system is the prophylaxis of lower limb diseases after the extraction of relevant features of the signals. A requirement is the usage of non intrusive techniques that suggests the usage of surface electrodes to get myoeletric signals. The assessment is done during a movement task, in which was chosen the human gait to be evaluated because it is the most common and evident motor action.

To achieve this objective, the work was subdivided in some partial goals that started by study of the signals to be monitored and also about the dynamic of the target movement. It followed the implementation of sensors module meant to condition the captured signals and the development of a central unit based on microprocessor to capture the signals. This central unit has the purpose of multiplexing signals from different muscles and sensors before sending them through the wireless link. It is proposed to establish the wireless connection with a communication module, that the Bluetooth is suggested because its widely usage and acceptance. A *Personal Computer* (PC) will receive, demultiplex and display the data by an application, in which is suggested the deployment of a user interface software. The developed system must be validated through tests and reported.

1.3. ORGANIZATION OF THE DISSERTATION

Regarding the goals of the work, it is possible divide the tasks in some steps and present them in six chapters:

In this first chapter is described how this report is organized, the workflow and the organization of tasks as well its scheduling. A brief introduction about the theme exposing the assumption and the aim of the work are also given.

At the second chapter the theme will be unfolded, highlighting important issues necessary to understand the nature of signals and to get necessary expertise to develop the work. Physiological and biomechanical aspects will be addressed to identify the physical features that carry recoverable information. The sensing process is described to understand how the noise inserted affects the system. Filters must be applied to remove or reduce these noises and they will be mentioned in this topic too.

The third chapter makes a review in the used platforms, common architecture, the topologies network and protocols. Communication options and protocols capable to satisfy system conditions will be discussed. The proposed devices that will compose the system and their features will be presented, giving a previewing of the system's architecture and its operation.

The fourth chapter is dedicated to the mounting and to the final conceiving of the system in its two levels, hardware and software. The firmware to run in the hardware and the graphical interface to run in the user terminal will take part in this chapter along with their algorithms. The communication between points will obey some rules to ensure the correct message exchange, in which will be clear by a handshaking scheme.

The fifth chapter brings the tests to be made onto the system and the results to be obtained, with the purpose to evaluate and validate the system. The plotting of the obtained waveform must be shown highlighting relevant characteristics to allow a user identifying a possible disturbance.

The thesis is finalized with the sixth chapter, in which are discussed the obtained results and the conclusions are shown. At this time may be enumerated the difficulties to achieve the results and, based on them and on the conclusions, it is intended doing suggestions to following studies and to improve the system.

1.4. SCHEDULING

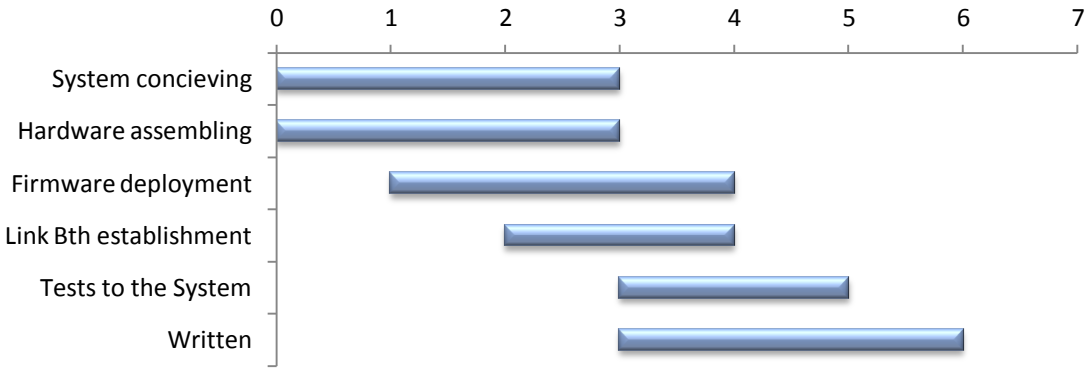

Figure 1 – Planned workflow.

The process of development of the system can be divided into six main stages. Figure 1 depicts how these stages are divided and the presumptive relative time for their execution. It begins with the system conceiving and the hardware implementation. With initial hardware it is possible to start the firmware deployment. The link establishment involves two parts, being the stage that follows the firmware deployment. When done, it is allowed starting the first tests and their documentation. The final task is the report written.

2. HUMAN GAIT ANALYSIS AND THE CHARACTERISTICS OF MYOELETRIC SIGNALS

The SEMG is a powerful tool to record the neurophysiologic responsible for the movement. The gait analysis involves the correlation between the generated signal and the obtained kinesiological response. A possible pathology can be present when this response does not correspond to an expected movement pattern or when an unexpected behavior is seen in the myoeletric waveform. Amid to these procedures the signal must be recorded and treated in order to delivery readable parameters for comparison. Sensors are used to capture the electric stimulus which contains myoeletric information and noise. Some different types of sensors are available with specific purpose and response to the input signal. Before performing any analysis, the noise, which is originated from several sources, must be extracted from the signal to turn it comparable to electrical and kinetic standards parameters. In this regard, this section reviews theses standards for the cyclical event analysis and waveform analysis before describe the electrical characteristic and forms of to capture and treat the myoeletric signal.

2.1. HUMAN GAIT

The simple analyses of lower limb in human gait can be reduced to three main joints: the hip, the knee and ankle. Theses joints are formed by four segments: the pelvis, the thigh, the shank and the foot, and the angles between segments are used to compute the kinematic data of gait [9]. The movement is done over three dimensional Cartesians planes of these segments. Anatomically these planes are known as sagittal plane, which crosses vertically the body on back-front direction and coincides with plane **xz** (Figure 2); the frontal plane that crosses vertically the body side to side

direction, represented on **yz** Cartesian plane; and transverse plane, that crosses the body horizontally, viewed in the Figure 2 on **xy** plane [10].

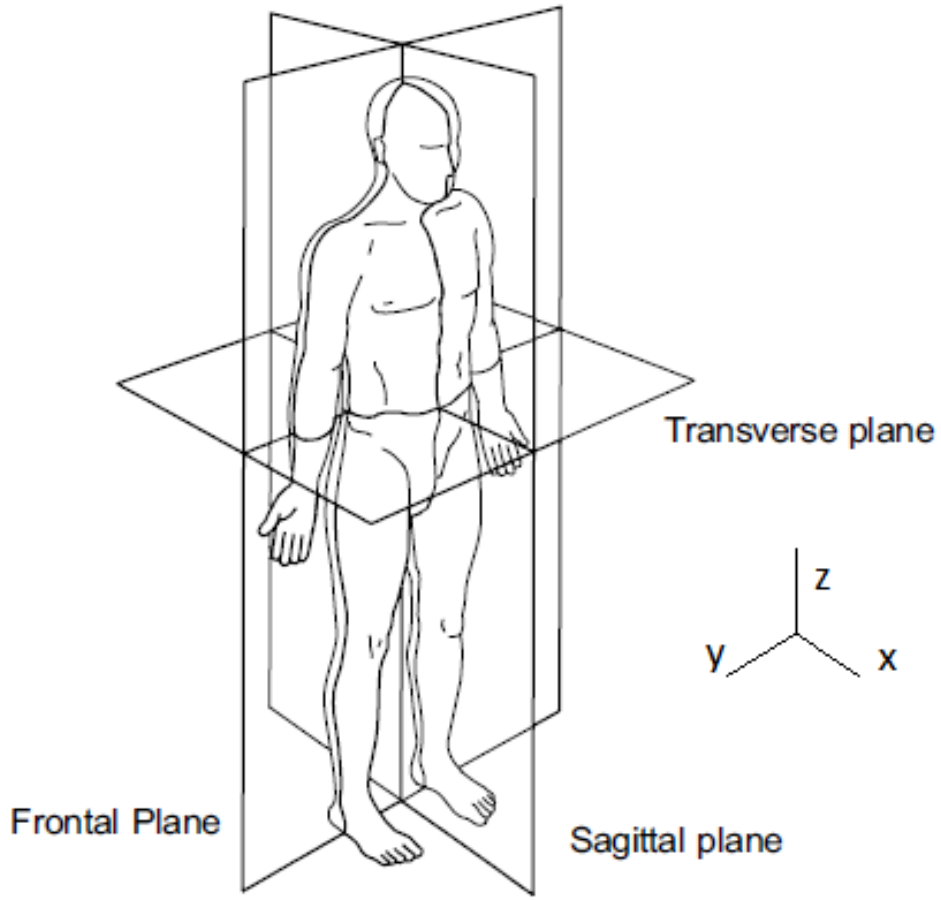

Figure 2 - The reference planes of the human body in the standard anatomical position. [9] This figure was edited to add the Cartesian reference.

2.1.1. KINETIC ANALYSES.

The analysis of gait is made over each cycle in comparison with a standard gait cycle. One cycle comprises one stride or two alternated steps. The moment of initial contact of one limb with floor marks the beginning of the cycle and will be completed with the next initial contact of the same limb with floor (Figure 3). Although the analysis over the tree planes is relevant to describe the gait accurately, most of the analyses just assess the movement over sagittal plane, which is regarded as the most important [10].

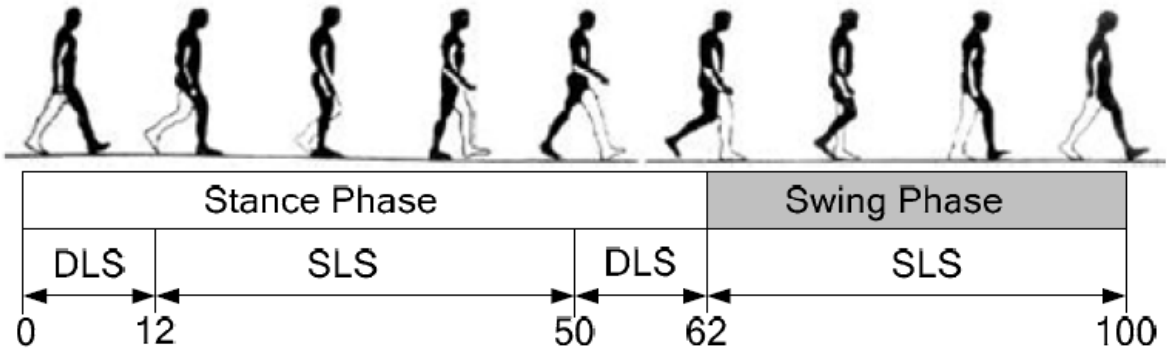

Figure 3 - "Division of normal gait cycle (illustration of right leg). Numbers indicate percent of gait cycle." [11]

The cycle is divided in two phases in function of the contact of each limb with the floor: the stance phase, when a certain limb sustains the weight, and the swing phase, when this limb takes off the contact and moves forward. The Figure 3 depicts both phases on a complete stride, represented in percentage values. The stance phase represents 62% of pace and the swing phase represents another 38%. Globally, it is possible to identify two stages during the march: the *Single Limb Support* stage (SLS) and the *Double Limb Support* stage (DLS) (Figure 3). The DLS is an intermediate stage and takes about 12% of the cycle between each step [11].

2.1.2. MUSCULAR ACTIVITY DURING GAIT.

The activation of muscles and muscular groups happens in specifics stages of gait. The muscular recruitment occurs in coordinated way, moving each segment in appropriate time. Figure 4 shows the activity of major muscles and the expected stage of this activity is described in percentage values. By the waveform it is possible to determine onset-offset activation information. The amplitude reflects roughly the activation intensity denoting the stage of more or less intensity of muscular activity. By the instant it is possible to associate the muscular activity to one phase. The occurrence of mistimed muscle recruitment characterizes a gait abnormality. The Figure 5 maps the location the muscles listed on Figure 4. The dots are positioned in way to match the medial third of each mentioned muscle and the direction of the double dotted points matches with the fibers direction.

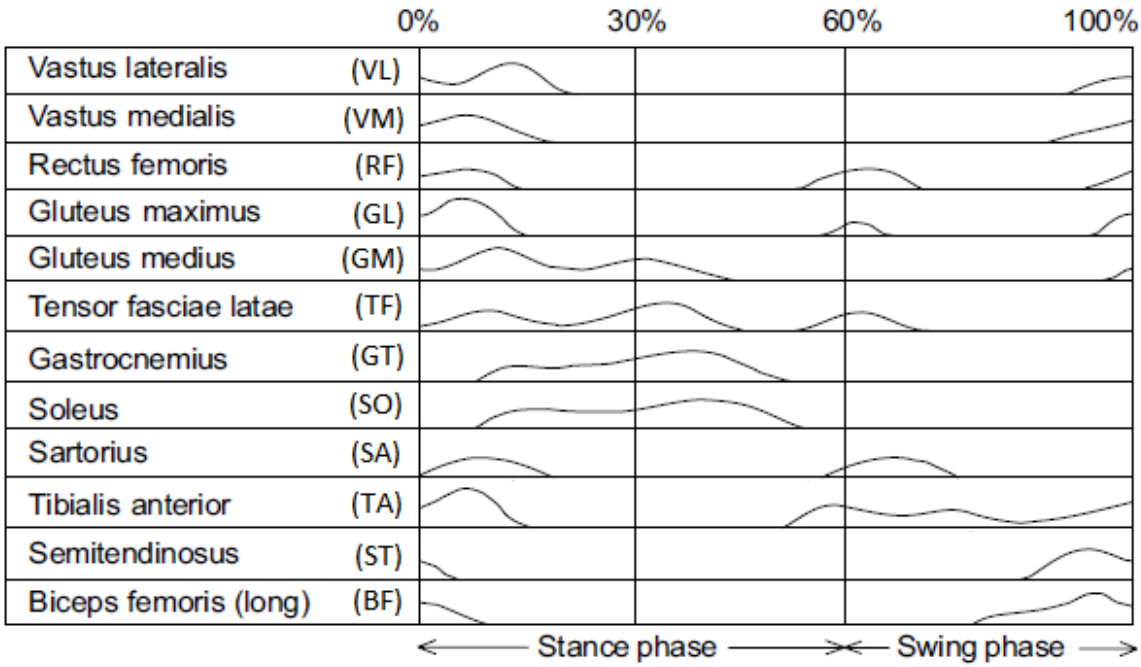

Figure 4 - Expected muscle activation of major lower limb muscles in function of the gait. [9]

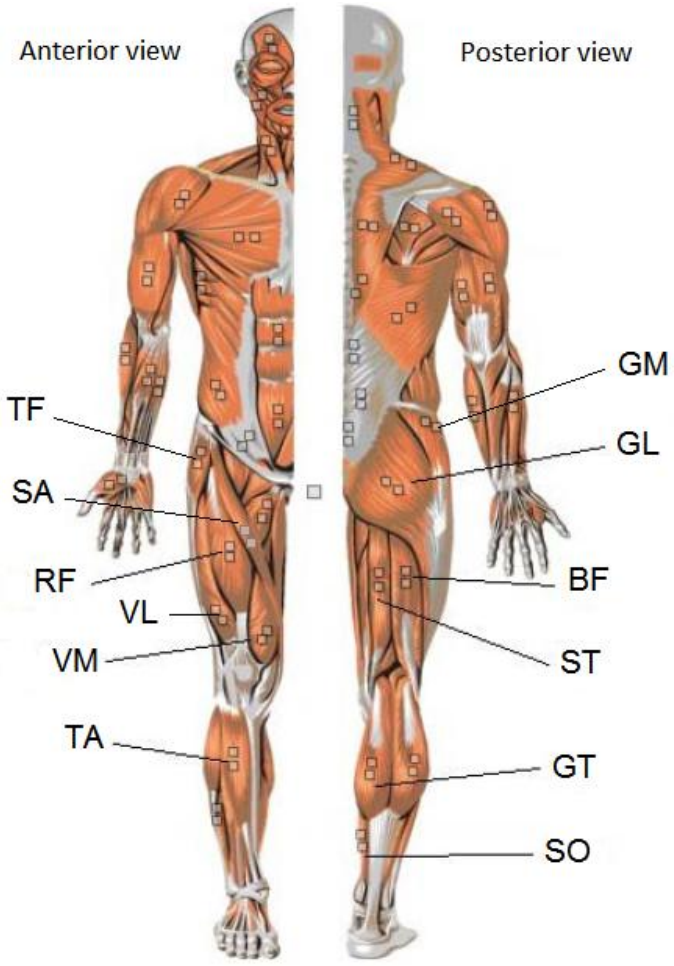

Figure 5 - Major lower limb muscle identification [12].

2.2. THE MYOELETRIC SIGNAL

The stimulation of muscle fiber membrane is done in any point by a motoneuron, commonly nearby at mid distance. The depolarization propagates in both directions along the fiber to repolarize in the end. The complete electric phenomenon is known as action potential and its duration ranges from 2 ms to 6 ms.

Figure 6 illustrates the situation in which an indwelling electrode is placed at different side reference of fiber innervations. Thus the recorded directions are sometimes opposed and the action potentials have inverted phases. The attenuation due the distance from fibers to the electrode is illustrated too with smaller amplitude. *h(t)* is the resultant action potential present at the recording site and constitutes a spatial-temporal superposition of the contributions of the *n* individual action potentials [13].

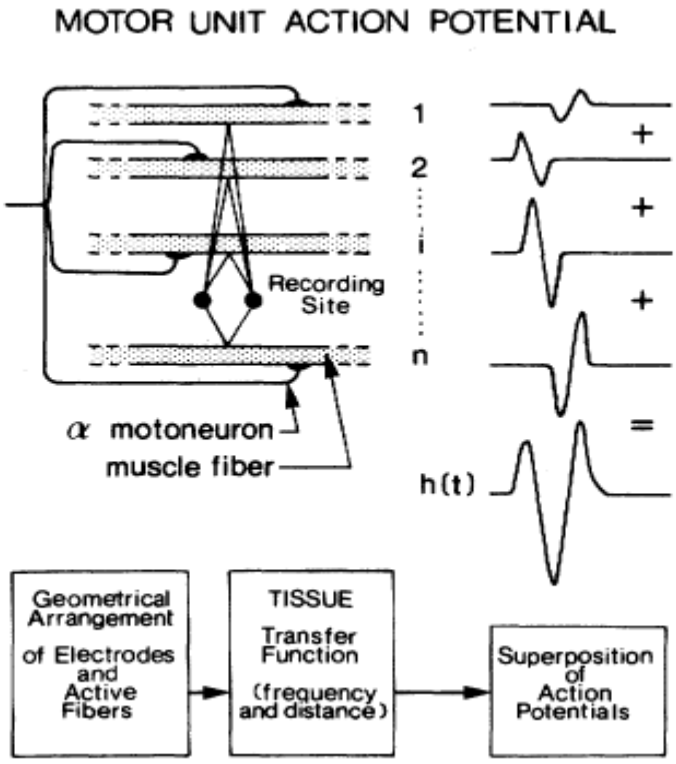

Figure 6 - "Schematic representation of the generation of the MUAP." [13]

"In order to sustain a muscle contraction, the motor units must be repeatedly activated" [13], resulting a train of *MU Action Potential* (MUAPT). The observed waveform of EMG is the summation of multiple MUAPT. Figure 7 is an example of a raw SEMG with three contractions intervals.

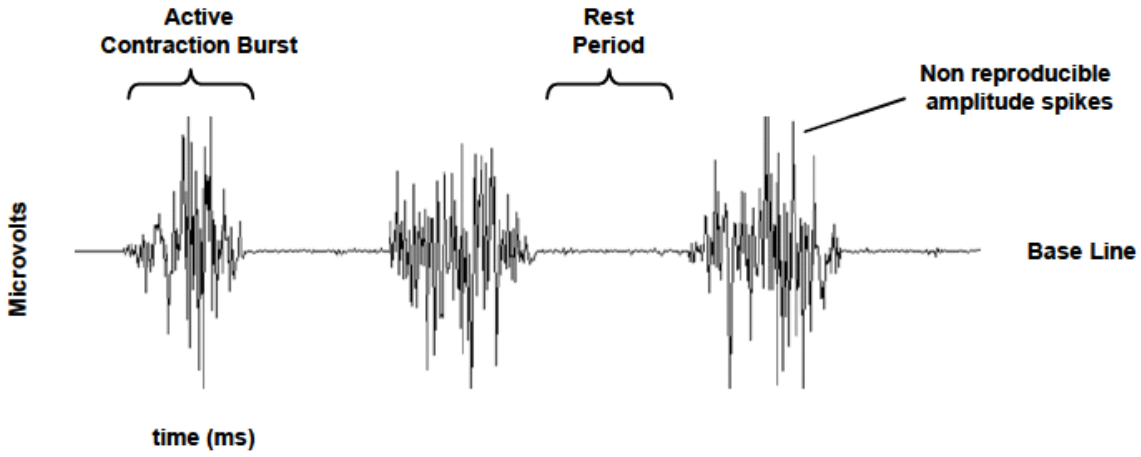

Figure 7 - "The raw EMG recording of 3 contractions bursts of the M. biceps br." [14]

Others physical aspects affect the final waveform of *h(t)*. One is the orientation of the recording electrode contacts with respect to the active fibers. Another relevant aspect is the presence of the fascia and intramuscular tissue that creates a low-pass filtering effect with bandwidth inversely proportional to the distance. The filtering effect is much more pronounced for surface electrodes recordings [13], resulting "in a signal with frequency content below 300 to 400 Hz". The effect to intramuscular recording is regarded negligible and the signal bandwidth is up to 1 to 5 kHz [15]. Most of the SEMG frequency power is located between 10 and 250 Hz [14]. The peak frequency is typically located between 50 and 150 Hz [13].

The amplitude is directly affected by theses aspects. It is possible to find in literature values ranging from 0.01 mV ~ 0.1 mV to upper limit of 0.5 mV ~ 5 mV [16], [1], [4]. The Table 1 [17] details the expected value regarding the application and qualifies useful values in accordance to the situation.

Table 1 – Dynamic Voltage Range for some EMG application. This table was edited from the original [17].

	Kind of electrode	**Dynamic Range**
Single-fiber EMG	Needle	1 – 10 µV
MUAPT	Needle	100 µV – 2 mV
SEMG Skeletal muscle	Surface	50 µV – 5 mV
SEMG Smooth muscle	Surface	-

2.3. NOISE SOURCES

Figure 8 depicts some examples of noise which can affect the myoeletric signal. The first trace is a normal reference signal. The second trace is a simulation of distortion caused by sensor drift and saturation. Noise due a small drift can be removed easily by a high-pass filter, but bigger drift or contact lost causes the saturation of signal with significant lost of information. The value of 40% in the figure represents the amplitude of saturation normalized to 100 mV_{pp}. The third trace shows a *White Gaussian Noise* (WGN) of 5 dB added to the signal. The WGN is inherent to the environment and to the thermal noise. The firth and fifth trace simulate the amplification and attenuation that affect the amplitude of the signal, which have as possible causes the displacement of electrodes, changing at bipolar electrode orientations, altering on the inter-pole distance and changing on components frequencies.

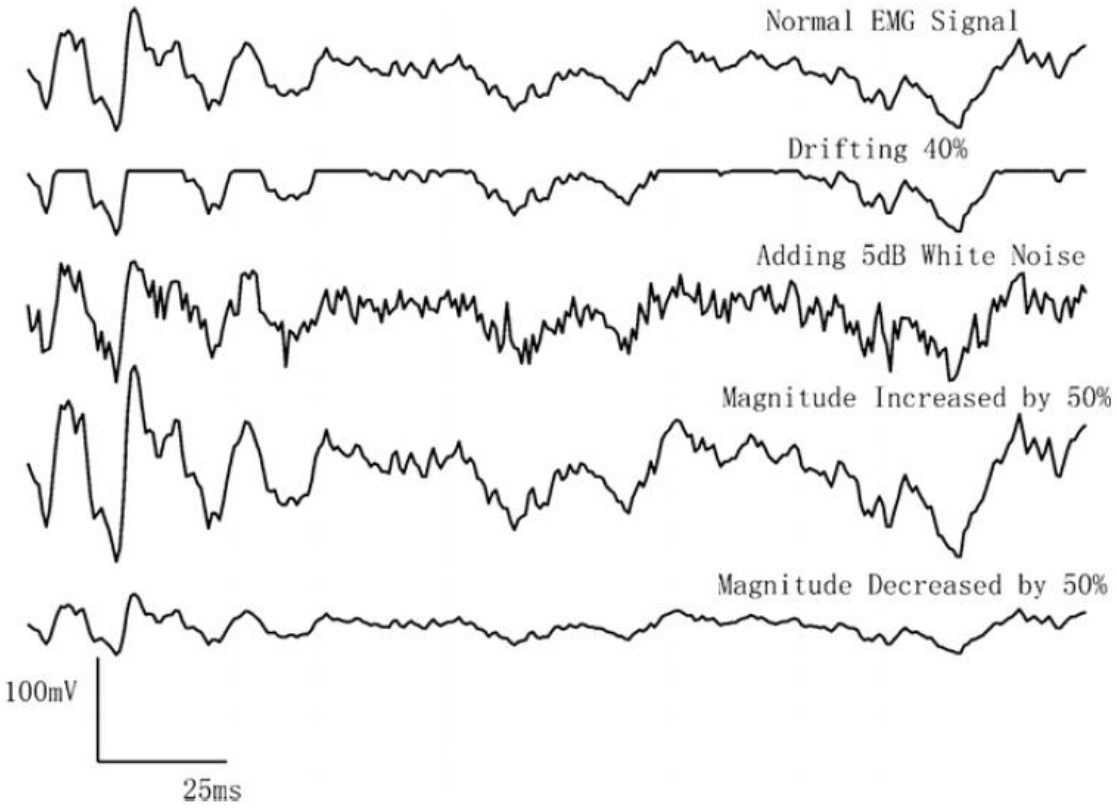

Figure 8 - Examples of 200 ms of simulated EMG signals with different distortions[18].

Other noise sources like the offset inserted by equipment and power line interferences can be added to the signal [4]. The first is easily removed with a low pass filter. The

second noise affects the 50 – 60 Hz frequencies, which is a range of *Power Spectrum Density* (PSD) of myoeletric signals with significant energy. Thus, this noise can't be removed by a notch filter without some loss of information.

2.4. SIGNAL CONDITIONING AND INPUT STAGE

The obtained signal, beyond the noise inserted, is very weak and need be conditioned with amplification and filtering stages. Most of the input stage is designed with filters and amplifiers circuitry based on *Operational Amplifiers* (OPAMPs), in which two or more amplification stages are combined and, in some cases, with adjustable gain and bandwidth.

Typically the input stage uses differential amplification in common mode, wherein just the potential difference between electrodes is measured, rejecting all common signal components (the same phase and amplitude). It means that the environmental noise that affects both input channel, including the power line, is rejected [16]. Both potentials are measured with respect to a third body location that serves as a common point of reference [4].

A band-pass filter follows the differential amplification stage. The low cut-off frequency aims removing DC offset. If the amplified DC offset passes to the next stages it reduces the useful dynamic range or even saturates the signal. For the SEMG applied to the movement analysis the suggested low cut-off frequency ranges 10 – 20 Hz (Table 2). This frequency value also filters the drift artifact noise. The high cut-off frequency ranges between 400 and 500 Hz. Frequencies above do not have relevant information and just degrades the *Signal Noise Ratio* (SNR) [16].

There are some recommended characteristics for amplifiers to ensure a good response from input stage [4]:

- "Gains of 10^3 to 10^4"
- "Amplifier broad-spectrum noise less than 20 nV/Hz"
- "Input impedance greater than $10^8\ \Omega$ "
- "*Common-Mode Rejection Ratio* (CMRR) greater than 100 dB"

It is advisable using instrumentation amplifiers for differential amplification "because they combine low-noise, high-impedance buffer input stages and high-quality differential amplification stages" [4]. A simple example of the implementation of the input stage is given by Figure 9, in which is used an instrumentation amplifier in the first stage and an on OPAMP based band-pass filter in the second stage. Components and values on figure are merely illustrative.

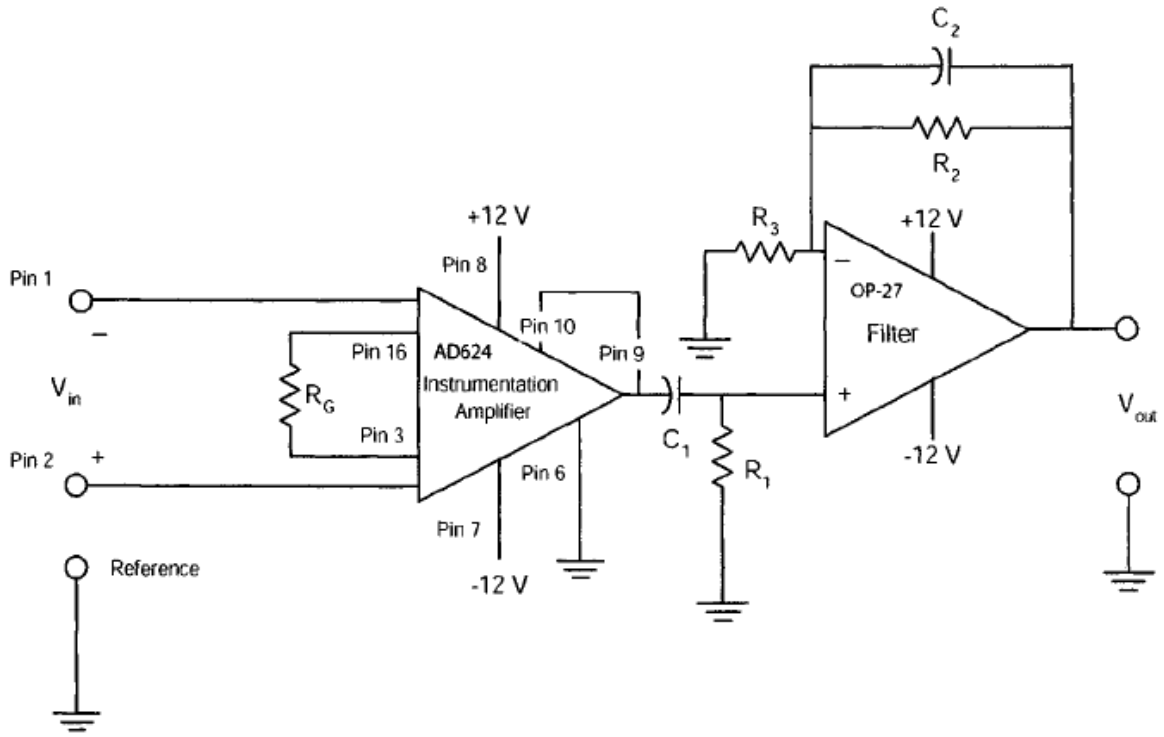

Figure 9 - "A simple biopotential amplifier design based on an integrated-circuit instrumentation amplifier" [4].

Resistors and Capacitors values can be computed in accordance to the application and the used apparatus (Table 2). For the design of the filter the Butterworth profile is commonly used because these show the best balance in selectivity and phase linearity responses [16].

2.5. MYOELETRIC SENSORS

There are two main groups of sensors that can be used to record the myoelectrical signal: superficial and intramuscular. Both are composed by electrodes and the first ones are used for general evaluation and the seconds are commonly used to detect specifics muscular

motor features by intramuscular sensing. “An electrode is the transducer that converts the ionic current generated by the muscle contraction into electrical current.” [16]

Table 2 – “Recommended Bandwidth for EMG Amplifiers” [15].

Electrode Type and application	Recommended High-pass filter	Recommended Low-pass filter
Surface electrode		
EMG spectral analysis	< 10 Hz	400 – 500 Hz
Movement analysis	10 – 20 Hz	400 – 500 Hz
Special wideband applications	10 – 20 Hz	1000 Hz
Wire electrode		
General application	20 Hz	1000 Hz
Signal decomposition	1000 Hz	10 kHz
Monopolar and bipolar needle electrode		
General application	20 Hz	1000 Hz
Signal decomposition	1000 Hz	10 kHz
Single fiber electrode	20 Hz	10 kHz
Macroelectrode	20 Hz	10 kHz

Principals advantages of intramuscular electrode are the strength of the signal recorded and lower noise incidence, getting thus, great SNR, and the accuracy to detect signals from a restrict area. These reasons make this kind of sensor more suitable to clinical purposes. Through observation of features and shape of MU potentials it is possible to diagnose some neurogenic and myogenic pathologies. On the other hands, the insertion of a needle limits the amplitude movement and thus, the assessment capability. The usage of wired sensors rather than needles minimizes the discomfort caused onto movement and allows more freedom and stability.

Surface electrodes have the advantage of being more comfortable and allow wide movements, although its displacement generates noise. Arrangements in line or array are used to improve the selectivity and serves to evaluate the velocity of impulse propagation. In this kind of sensor, shape, dimensions and material are determinant for skin-electrode impedance and noise reduction.

Different configurations of sensors can facilitate the arrangements and turn possible new perspectives of assessment. The most common configuration is on the monopolar, bipolar and quadripolar sensors. Figure 10 depicts the basic electrodes used on EMG and arrangements.

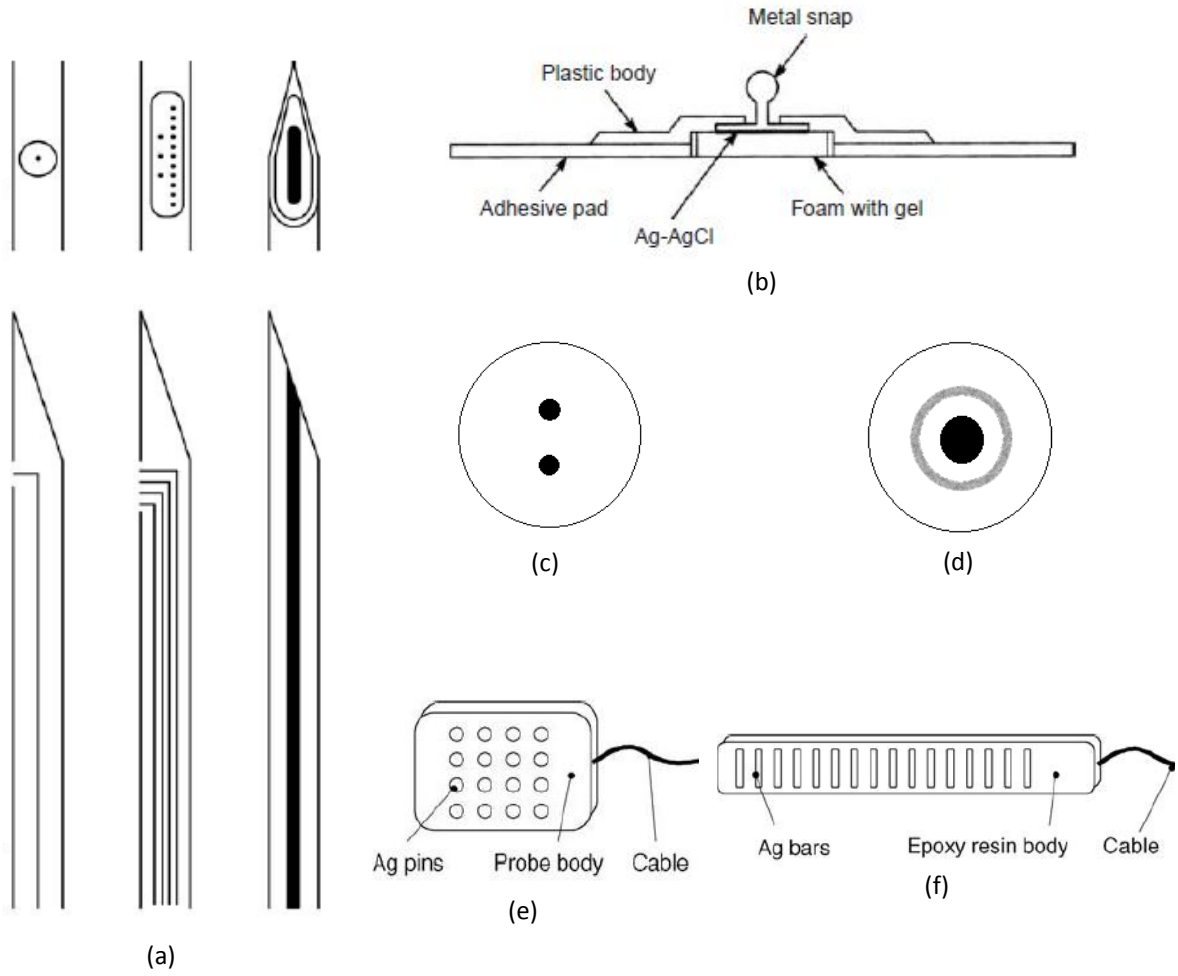

Figure 10 – Representation of main types of electrodes used in EMG. (a) respectively: the monopolar needle, the multipolar needle and the concentric needle [16]. (b) surface electrode and its cut view [15]. The bipolar and monopolar configuration of this electrode is represented in (c) and (d) respectively. (e) represents a surface electrode grid [15] and (f) represents a surface electrode array [15].

With the linear arrangement it is possible to obtain information about properties from a single MU, such as the location of innervations zones or the length of muscle fiber, as well the impulse propagation from beginning on the MU to the end on tendon (Figure 11). The array arrangement allows computing maps to assess the distribution of muscle activities in different tasks, which is very important for clinical applications [16]. This kind of

evaluation using surface electrodes is possible thanks to more powerful mathematical tools [14].

In general, the interface with electrodes delivers a signal with amplitude of 5 – 6 mV with noise inserted due the intrinsic thermal noise and the ionic exchanges, which are strongly related to electrodes geometry and arrangement. The impedance can vary from 10 kΩ to 1 MΩ with capacitive and resistive characteristics [4].

2.6. MATHEMATICAL TREATMENT

The visual inspection of raw signals is regarded imperative to EMG analysis because these signals carry all relevant information and highlights the presence of noises[14]. The most important information to be extracted from EMG to perform the human gait analyses is the on-off timing. In this sense, the exact waveform fidelity does not need to be maintained [4].

Mathematical resources are used to alter the waveform and thus, deliver more readable signals to a user interface with a more evident on-off timing. The most applied techniques are amplitude normalization, the *Root Mean Square* (RMS) timing window, and filtering. The amplitude normalization just turns the signal denser and it is prerequisite for others techniques. The RMS is the most widely used approach, in which a timing window, generally with length from 20 ms to 500 ms, is used to turn the signal smoother [14][19]. The filtering can be used with same purpose, in which a 2^{nd} order or higher, 9 Hz of cut off frequency or higher low-pass filter of is applied [3].

Frequency analyses like *Fast Fourier Transforming* (FFT), Wavelet Transforming, are sometimes used to obtain the PSD and time-frequency varying analyses. The FFT is used to determine the PSD and assess regions of great energy. Some noise affecting the signal will be visible on the PSD. The frequency analysis in locomotor tasks is not frequently applied due the non-stationary nature of the myoeletric signal. To extract information about it is necessary applying techniques like Wavelet Transforming. This technique returns a time-frequency representation of the signal and its recent application brings promising results, particularly in fatigue analysis [3].

2.7. MEASURING THE VELOCITY

The latency is the time between nerve excitation and the muscle response. To measure the velocity of propagation it is necessary to record the muscle response at two different points to the same stimulus. The difference on the time recorded between theses points is used to estimate the velocity of propagation of the signal and the latency does not matter to the peripheral nerve velocity computing. “Measurement of peripheral nerve velocity may be useful in determining the extent of nervous damage following trauma.” [1]. Figure 11 illustrates the propagation of the wave in the time, remarked by dotted line. Each channel takes the peak of the wave on a previous known distance among electrodes.

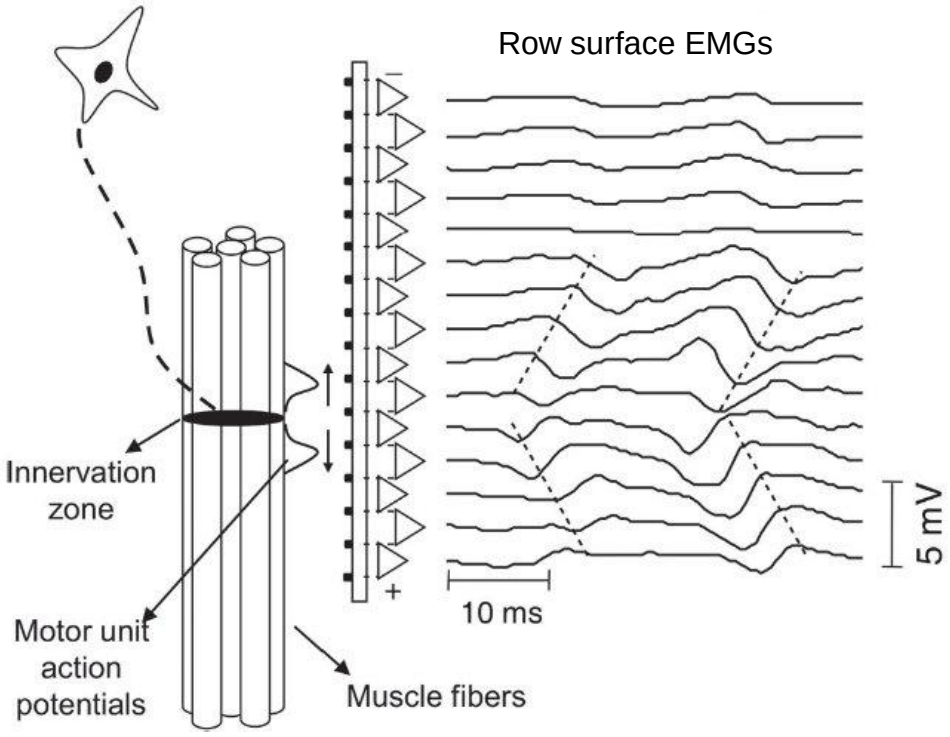

Figure 11 – Measurement of speed of signal propagation by row surface EMG. [20]

2.8. CONCLUSION

Myoeletric signals convey essential information to understand muscular activity during gait. Intra-muscular and surface electrodes are used to capture the electrical activity generated in the muscular fibers. Surface myoelectrical signals are those mostly often used, being intra-muscular detection used only in specific cases.

Myoeletric signals present specific frequency and amplitude characteristics which, although not very demanding, require the use of specific conditioning circuits and processing operations.

This chapter presents a brief overview on the origin of myoeletric signals, its characteristics as well as their use for gait analysis, which helps understanding the context on which the present work has been developed and provides preliminary information to better understand next chapters.

3. TECHNOLOGIES

This chapter provides an introduction to the main technologies involved in the design of the data capture and transmission system developed in this dissertation. This system can be seen as part, a node, of a wireless sensor network and thus the technologies being described here are in fact those commonly found in these wireless systems.

The concept of *Wireless Sensor Network* (WSN) applied to BSN has been developing, mainly since the 1990 decade. The architecture of each node of a sensor network comprises mainly a unit processor, sensor interface, power supply, memory, wireless connection, and an *Operating System* (OS) (Figure 12).

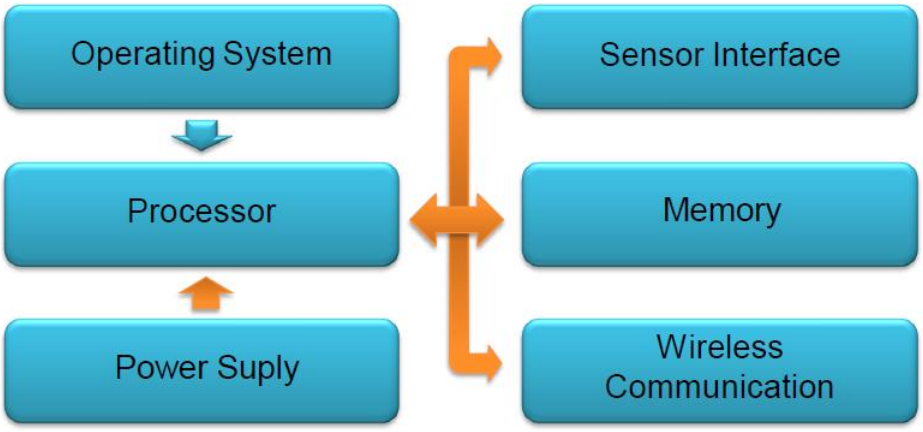

Figure 12 - The main components of common WSN nodes.

- Processor

The devices used in a WSN are required to present low processing power due to constraints in size and power consumption. For this reason, simple *Microcontroller Units* (MCUs) are used in the WSN sensor nodes.

- Memory

Memory is useful in embedded systems to store configuration information, programs images or as an immediate buffer to store data sampled from sensors. Sometimes it is necessary to overcome the limited *Random Access Memory* (RAM) present on the MCU with some additional external memory, typically a flash memory or an *Electrically Erasable Programmable Read-Only Memory* (EEPROM). The advantage of using this kind of memory is that it does not need power to retain the stored data.

- Sensors interface

Sensors can delivery either analogue readings, requiring the existence of an *Analog - Digital Convertor* (ADC) interface for data sampling and acquisition, or digital data, requiring the usage of a protocol to establish a communication with MCU. The most widely used communication protocols are *Serial Peripheral Interface* (SPI), *Integrated Interconnect* (I^2C) and *Universal Asynchronous Receiver - Transmitter* (UART).

- Power supply

The power supply is the main determining factor of the size, volume, and autonomy of the WSN hardware [21]. More popular power sources are Li-ion batteries, zinc-air batteries and rechargeable batteries. Different energy harvesting schemes have also been proposed to increase the operation autonomy of remotely deployed sensor nodes [22].

- Operating system

Usually a proprietary developed firmware is used in many cases, but when the complexity of the system increases it is required the usage of an OS. Despite the widely introduction of proprietary OS, the open source OS is yet the mostly used for embedded systems, mainly the C-based OS.

- Wireless Communication

Usually the wireless communication is the operation that requires the highest power consumption. In some cases this component is responsible for even more than 50% of whole power required by the sensor node. For that reason a significant effort has been concentrated on the development of efficient-energy protocols and routing strategies.

> "For many WSNs, node size and power consumption are often considered more important than the actual processing capacity because in most applications the amount of processing involved is relatively light." [21]

The architecture adopted depends mainly on the WSN application. What different architectures have in common is the needs of low power consumption, being the differences related to number of sampling channels, sampling rate and the amount of data processing. These variables affect the choice of the MCU in terms of power processing, data rate, clock frequency, required peripherals, and number of *Input* /

Output (I/O), determining what node platform to be adopted. Nowadays there are several different architectures found in WSN applications. Some are more notable either by their pioneering or by their wide referencing. Table 3 lists some of them and their features.

Table 3 – Most notorious WSN node platform with their features. [21].

Platforms	**CPU**	**Clock (**MHz**)**	**RAM / Flash / EEPROM**	**Transceiver**	**Bandwidth (**kHz**)**	**Frequency (**MHz**)**	**OS**
BSN node	TI MSP430F190	8	2*k* / 60k / 512k	Chipcon CC2420	250	2400	Tiny OS
BT node	Atmel Atmega 128L	8	4k / 128k / 4k	ZV4002 BT/CC1000	1000	2400	Tiny OS
Dot	Atmel Atmega 163	8	1k / 16k / 32k	RFM TR1000	10	916.5	Tiny OS
EnOcean TCM120	PIC18F452	10	1.5k / 32k / 256	Infineon TDA5200	120	868	Tiny OS
EyesIFX v2	TI MSP430F1611	8	10k / 48k	Infineon TDA5250	64	868	Tiny OS
iMote1	Zeevo ZV4002 (ARM)	12 - 48	64k / 512k	Zeevo BT	720	2400	Tiny OS
iMote2	Intel PXA 271	13-140	128k / 32M	CC2420	250	2400	Tiny OS
Mica	Atmel Atmega 128L	4	4k / 128k / 512k	RFM TR1000	40	916.5	Tiny OS
Mica2	Atmel Atmega 128L	8	4k / 128k / 512k	Chipcon CC1000	38.4	900	Tiny OS
Mica2Dot	Atmel Atmega 128L	4	4k / 128k / 512k	Chipcon CC1000	38.4	900	Tiny OS
MicaZ	Atmel Atmega 128L	8	4k / 128k / 4k	Chipcon CC2420	250	2400	Tiny OS
Nynph	Atmel Atmega 128L	4	4k / 128k	Chipcon CC1000	38.4	900	Mantis
Particle2/29	PIC18F6720	20	4k / 128k / 512k	RFM TR1001	125	868.35	Smart-its
Rene	Atmel AT90LS8535	4	512 / 8k / 32k	RFM TR1000	10	916.5	Tiny OS
Sun Spot	Atmel AT91FR40162S	75	256k / 2M	CC2420	250	2400	Squawk VM(Java)
Telos	TI MSP430F149	8	2k / 60k / 512k	Chipcon CC2420	250	2400	Tiny OS
T-Mote Sky	TI MSP430F1611	8	10k / 48k / 1M	Chipcon CC2420	250	2400	Tiny OS
U3	PIC18F452	0.031-8	1k / 32k / 256	CDC-TR-02B	100	315	Pavenet
XYZ	OKI ML67Q500x (ARM/THUMB)	1.8 - 57.6	4k / 256k / 512k	Chipcon CC2420	250	2400	SOS
Wec	Atmel AT90LS8535	4	512 / 8k / 32k	RFM TR1000	10	916.5	Tiny OS

3.1. NETWORK TOPOLOGIES

Concerning communications topologies two terms can be distinguished: the physical topology refers to the structure of connection, and the logical topology refers to the data and packed exchange way. Within the *Open System Interconnection* (OSI) model "the physical layer and data link layer, define the physical topology of a network, while the network layer is responsible for the logical topology." [7]

In the physical topology the participants can be connected in a point-to-point framework, star, mesh, star-mesh hybrid and cluster tree framework. Figure 13 illustrates each one of these topologies.

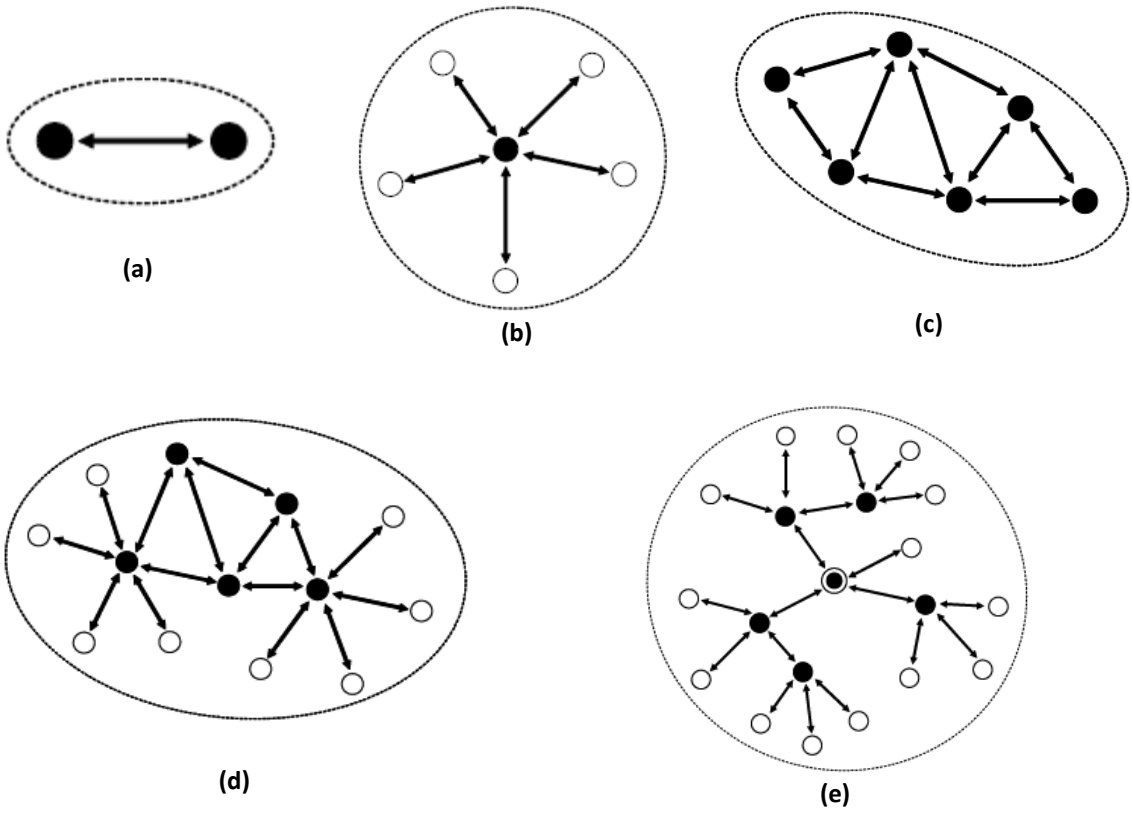

Figure 13 - Basic network topologies: (a) Point-to-point, (b) Star, (c) Mesh, (d) Star-Mesh hybrid, (e) Cluster tree. [7]

The main application of WSN in medical monitoring is on non intrusive cases. BSN can be employed either in a stand-alone context or in combination with mobile phones or ambient sensors networks [7].

In the stand-alone context it has usually a processing unit conjointly with the sensing functions. The processing unit reads and records bio-signals or quantities like EMG, ECG, EEG, bloody pressure, and blood flow. Depending on the context, theses signals can be used together with signals provided by other types of sensors like accelerometers, thermometers or gyro-meters. The star topology is the most widely employed in these applications, being necessary an intelligent central unit. Mesh topologies can be found in the same applications in continuous non-invasive monitoring, but in this case it becomes necessary to endow the sensors with some intelligence to operate independently from a central unit.

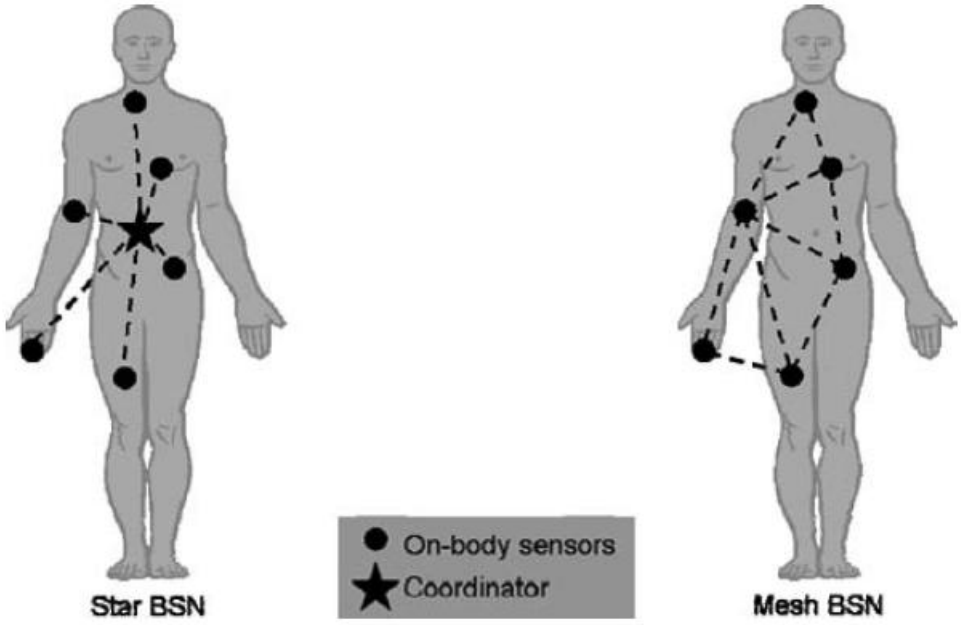

Figure 14 - "*Star vs. mesh-based body sensor network.*"[7]

Figure 14 presents a comparison between the most used topologies. The star topology takes advantage over mesh by its simplicity, low power consumption, high bandwidth and low latency. On the other hand, the mesh topology takes advantages considering fault communications robustness, reliability and large spatial coverage [7].

In the star topology, the central unit assumes the role of processing and communication master and needs, sometimes, an additional hardware as a bridge. In the mesh topology the communication with every sensors implies a higher bandwidth and processing overhead, being advisable to choose one sensor to act as bridge.

3.2. NETWORK CONFIGURATION

The star topology has clear advantage over the mesh topology when low power consumption is mandatory. Additionally, the use of the MCU acting like coordinator in a single node fits the requirements of the system based on a star topology. Figure 15 is an illustration of a MCU based BSN in which electrodes, sensors and CU are the participants. In this configuration the CU is the master and electrodes and sensors act as slaves. The master provides the clock and controls the data flow. The MCU endows the CU with enough ability to act as a bridge, linking parts of networks. The BSN is part of a WSN in which the CU co-participates. In Figure 15 the external participant to the BSN is a PC connected in a *Peer-to-Peer* (P2P) communication mode. MCUs usually are not featured with wireless connectivity and it is necessary to add a peripheral communication module to establish a link. The CU can act like a server in the WSN but in the most common configuration the external participants are responsible to initiate the link.

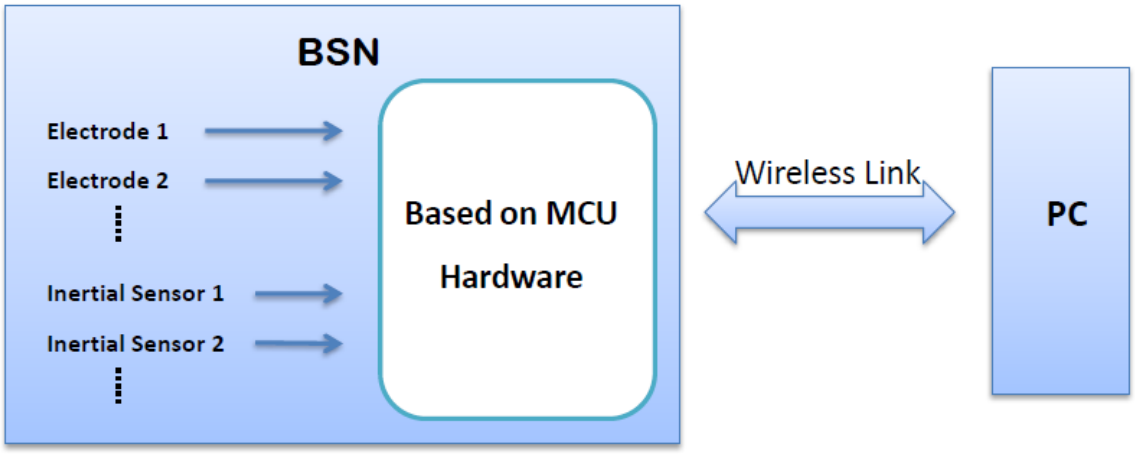

Figure 15 – WSN and the participants. The node is composed by CU that acts like a bridge.

Figure 15 is the first high level scheme of the planned system. For the present work it is proper to use a cheap and low-power transceiver for low and moderate data rates. As far as communication standards are concerned there are some short-range standards to ensure the interoperability and flexibility of the devices, such as *Bluetooth Low Energy* (BT-LE), IEEE802.15.4 (ZigBee) and IEEE802.15.6 (*Medical Body-Area Networks* - MBAN).

3.3. WIRELESS LINK AND PROTOCOLS

> "In order to achieve cost-effective, flexible and preferably interoperable solutions, it is almost a necessity to abandon proprietary technological approaches and instead choose standardized wireless technology as the basis of a BSN."[7]

The use of radio frequency spectrum is internationally regulated after the communication ranges of the specific applications. Not specified applications are located in restricted ranges of the spectrum. The devices operating in these intervals have limitations in power, range and bandwidth. The most important frequency ranges for BSNs are *Very High Frequency* (VHF) (< 300 MHz), *Ultra High Frequency* (UHF) (*e.g.* 315, 433, 868 – 928 MHz), the worldwide 2.4 GHz *Industrial, Scientific and Medical* band (ISM), the worldwide 5 GHz band, and, for *Ultra Wideband* (UWB), the 3 – 10.6 GHz band [7].

WLAN and WPAN are issued by IEEE 802.11 and IEEE 802.15 specifications respectively that establish standards for short range wireless networks. They define the *Physical* (PHY) and *Medium Access Control* (MAC) layers for wireless communications over an action range around 10 – 100 m. Four main standards based on these specifications are available in the market. The Wi-Fi standard is based on the IEEE 802.11 specification and is thought to relative high rate data flow. Three other standards, Bluetooth, ZigBee and UWB, are based on IEEE 802.15, targeting WPAN. Each one has a dedicated IEEE Task Group that defines its own specification: IEEE 802.15.1 for Bluetooth, IEEE 802.15.3 for UWB and IEEE 802.15.4 for ZigBee. Generally the WPAN is more restricted than WLAN in covering power consumption and data flow. The characteristics of these standards are given in the Table 4.

The UWB is designed for high data rate being suitable for multimedia stream. Its architecture allows significant power economy regarding the amount of data processing. Bluetooth is meant to medium data rate using cheap low power devices. It is the most complex protocol as it implies 188 primitives and events in total. Thus, it has higher latency among these four standards.

Table 4 - Comparison of the Bluetooth, UWB, ZigBee, and Wi-Fi protocols [23]

Standard	Bluetooth	UWB	ZigBee	Wi-Fi
IEEE specification	802.15.1	802.15.3a*	802.15.4	802.11a/b/g
Frequency band	2.4 *GHz*	3.1 – 10.6 GHz	868/915 MHz; 2.4 GHz	2.4 GHz; 5 GHz
Max signal rate	1 Mbps	110 Mbps	250 kbps	54 Mbps
Nominal range	10 m	10 m	10 – 100 m	100 m
Nominal TX power	0 – 10 dBm	-41.3 dBm/MHz	(-25) – 0 dBm	15 – 20 dBm
Number of RF channels	79	(1 – 15)	1/10; 16	14 (2.4 GHz)
Channel bandwidth	1 MHz	500 MHz – 7.5 GHz	0.3/0.6 MHz; 2 MHz	22 MHz
Modulation type	GFSK	BPSK, QPSK	BPSK(+ASK), O-QPSK	BPSK, QPSK, COFDM, CCK, M-QAM
Spreading	FHSS	DS-UWB, MB-OFDM	DSSS	DSSS, CCK, OFDM
Coexistence mechanism	Adaptive freq. hopping	Adaptive freq. hopping	Dynamic freq. selection	Dynamic freq. selection, transmit power control (802.11h)
Basic cell	Piconet	Piconet	Star	BSS
Extension of the basic cell	Scatternet	P2P	Cluster tree, Mesh	EES
Max number of cell nodes	8	8	>65000	2007
Encryption	E0 stream cipher	AES block cipher (CTR, counter mode)	AES block cipher (CTR, counter mode)	RC4 stream cipher (WEP), AES block cipher
Authentication	Shared secret	CBC-MAC (CCM)	CBC-MAC (ext. of CCM)	WAP (802.11i)
Data protection	16-bit CRC	32-bit CRC	16-bit CRC	32-bit CRC

* Unapproved draft.

Acronyms: ASK (amplitude shift keying), GFSK (Gaussian frequency SK), BPSK/QPSK (binary/quadrature phase SK), O-QPSK (offset-QPSK), OFDM (orthogonal frequency division multiplexing), COFDM (coded OFDM), MB-OFDM (multiband OFDM), M-QAM (M-ary quadrature amplitude modulation), CCK (complementary code keying), FHSS/DSSS (frequency hopping/direct sequence spread spectrum), BSS/ESS (basic/extended service set), AES (advanced encryption standard), WEP (wired equivalent privacy), WPA (Wi-Fi protected access), CBC-MAC (cipher block chaining message authentication code), CCM (CTR with CBC-MAC), CRC (cyclic redundancy check).

ZigBee is the simplest protocol. It is suitable for low data rate, what allows operating with lower power consumption and provides the smaller latency [7]. Their limited memory and computational capacity restrings its application to sensor networking.

Wi-Fi is meant for high data rate to expansion of Internet [23]. “IEEE 802.11b transceivers are far more power-hungry, with typical power consumptions between 400 mW and 1500 mW.”[7] The performance of each protocol regarding the power consumption is shown in Figure 16, in which the power is given in mW. Figure 17 shows the energy in mJ required to transmit 1 Mb of data.

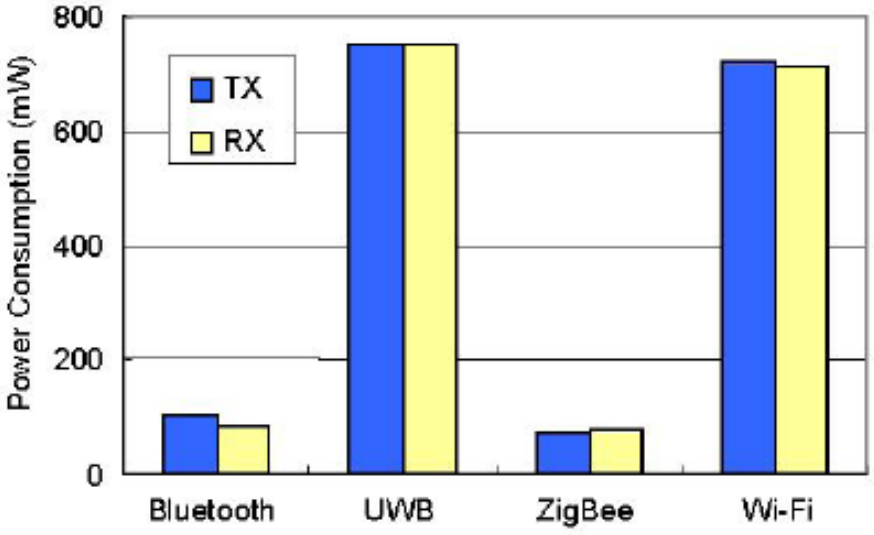

Figure 16 – “Comparison of the power consumption for each protocol.” [23]

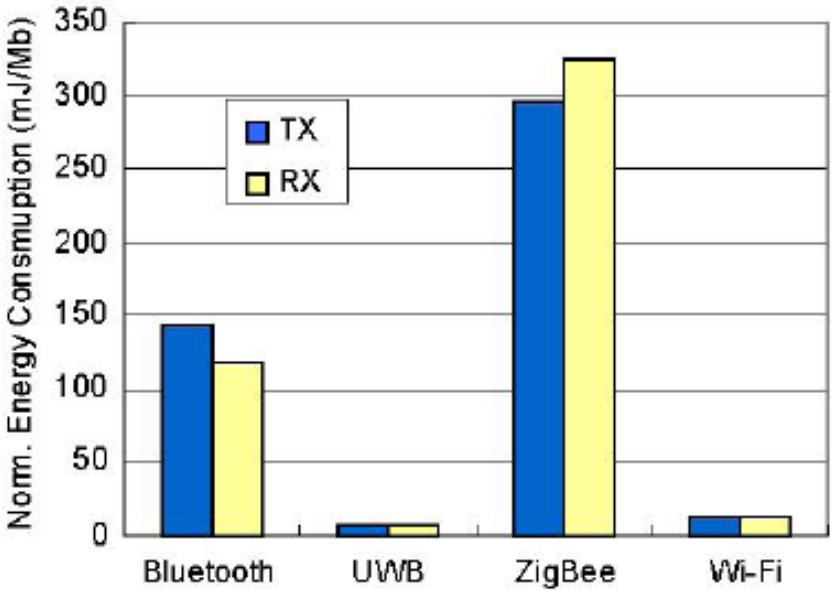

Figure 17 – “Comparison of the normalized energy consumption for each protocol.”[23]

It is possible to conclude from these two graphs that Bluetooth and ZigBee are suitable for low data rate applications with limited battery power, conditions imposed by a sensor network. Also ZigBee has slight advantage over Bluetooth in power consumption, lower latency, flexibility and simplicity but is limited when higher data rates are necessary, what is the case if it is meant to operate like a gateway of an external network. Considering this last scenario, one can conclude that Bluetooth is then the better quoted candidate when the function exceeds the operation in a BSN.

3.4. BLUETOOTH ARCHITECTURE

The Bluetooth standard has been developed by a *Special Interest Group* (SIG), a gathering of thousands of companies that keep as an opened industrial specification, allowing all members using it freely in their products. The idea is creating a universal standard that allow the operation among different devices regarding the powering and expensiveness issues. This standard has been used in a wide sort of applications as mobile telephony, mice, keyboards, PCs, cars, cameras, audio helmets, remote services as banking payment and so on. Its operation is ensured by a basic layer that supports all protocols from higher layers and provides services to the applications. In accordance to the application, it is specified a profile, which "gives details about protocols parameters and settings for the device to be able to discover these applications and to communicate in a uniform way" [24]. The most common profiles are:

- *Generic Access Profile* (GAP)
- *Service Discovery Application Profile* (SDAP)
- *Cordless Telephony Profile* (CTP)
- *Intercom Profile* (IP)
- *Serial Port Profile* (SPP)
- *Headset* (HS)
- *Dial-up Networking Profile* (DNP)
- *Fax Profile* (FP).
- *Local Area Network Profile* (LAP)
- *Generic Object Exchange Profile* (GOEP)

- *File Transfer Profile* (FTP)[3]
- *Synchronization Profile* (SP)

The protocol stack is organized in four layers which are opened to other protocols allowing their interoperability with a sort of communication standards, including with not specified Bluetooth protocols. Bluetooth has as a principle the maximum reusing of existent protocols to ensure the smooth operation and interoperability of these applications [25]. The protocol stack is vertically structured like shown in Figure 18.

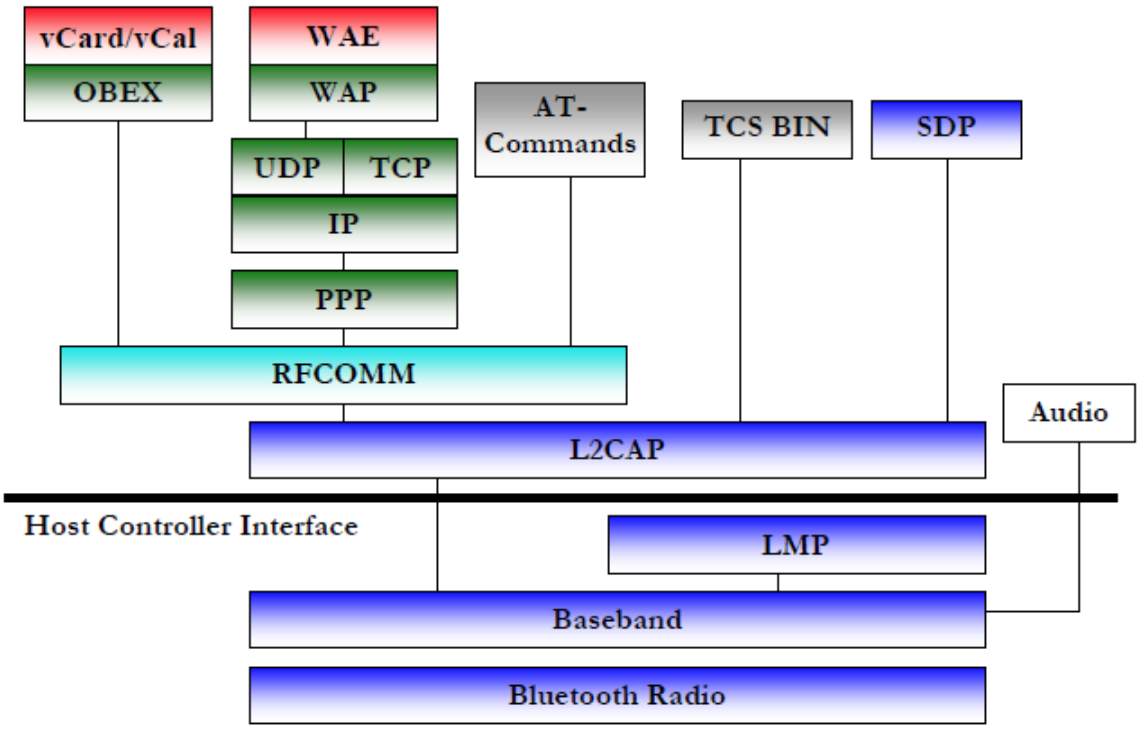

Figure 18 - The Bluetooth protocol stack. [25]

The first layer is the "Bluetooth Core Protocol" comprising four protocols: Baseband, *Link Manager Protocol* (LMP), *Logical Link and Control Adaptation Protocol* (L2CAP) and *Service Discovery Protocol* (SDP). The second layer is the "Cable Replacement Protocol" that uses the RFCOMM, which is a protocol that emulates a serial line over Bluetooth baseband, with RS232 control and data signals. The third layer is the "Telephony Control Protocol" that comprises *Telephony Control Specifications* (TCS) – Binary, a bit-oriented protocol that is used in speech and data exchange services, and AT – commands for FAX services. Finally,

[3] It does not mean *File Transfer Protocol* (FTP), although this protocol is being included in the profile's protocol stack.

the fourth layer is the “Adopted Protocols” that encompasses protocols like *Point-to-Point Protocol* (PPP), *User Datagram Protocol* (UDP), *Transport Control Protocol* (TCP) *over Internet Protocol* (IP), and other involved in Internet communication, *Object Exchange Protocol* (OBEX) a session protocol to simple and reliable communication and *Wireless Application Protocol* (WAP). Other not specified protocols like vCard, vCal, *Infrared Mobile Communication* (IrMC) and *Wireless Application Environment* (WAE) are also seen in Figure 18. [25]

3.5. BLUETOOTH OPERATION

The Bluetooth specification determines some versions and classes of devices according their operation. The range reached depends on the class of the devices that is defined from the transmission power. The version is defined from the bandwidth: Bluetooth 1.0 achieves less than 1 Mbps at 10 m and version 2.0 achieves from 2 to 3 Mbps. The class is determined by the power measured at the input antenna, which must have power sensitivity ≤ - 70 dBm:

- Class1 – 20 dBm (100 mW) at ~100 m
- Class2 – 4 dBm (2,5 mW) at ~10 m
- Class3 – 0 dBm (1 mW) at ~1 m

The communication is based on a master-slave architecture and forms a network with up to seven slaves, known as *piconet*. The establishment of the communication starts with the discovering of the devices, unique phase in which the slaves can communicate directly with others. “Channel allocation and communication establishment are under the responsibility of the master” [24], as well the polling nodes, allocation bandwidth and clock synchronization.

The pseudo-random frequency hopping is used in the channel establishment and is unique for each piconet. The channel is chosen among 79 or 23 channels available in a band of 2.4 GHz and is divided into slots of time. Each interval of time uses its own frequency, having the master clock as a basis. This division in time allows the multiplexing of different devices

when they share the same Bluetooth channel. The nominal hopping frequency is 1600 hop/s in data transfer and 3200 hop/s for connection phases (inquiry and page) [25].

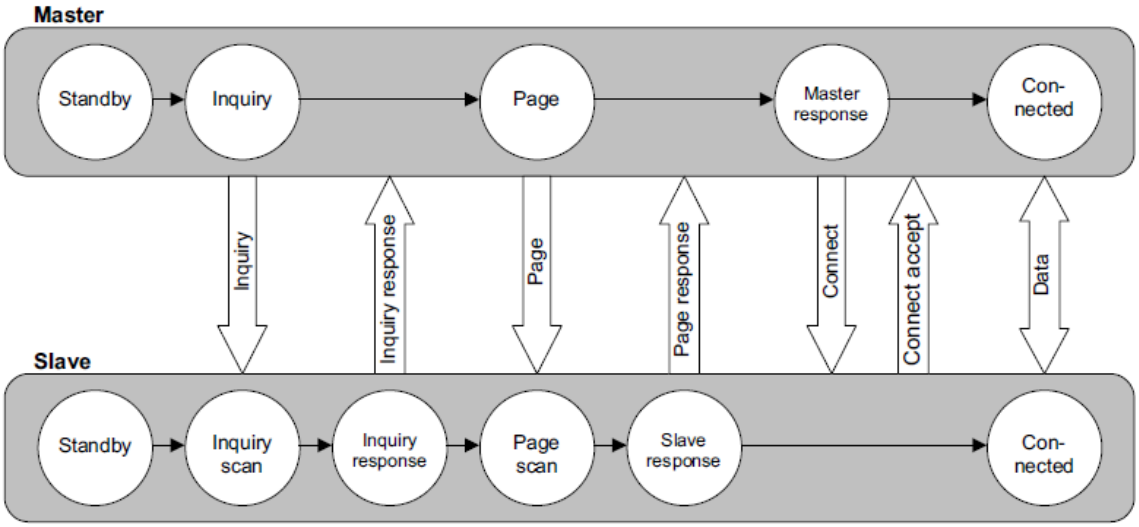

Figure 19 - "Bluetooth connection setup" [7]

Figure 19 depicts the basic procedures for the establishment of a connection. It starts by Inquiry, phase in which a device initiates a search for a link. The search can be done in function of a specific feature like class, service, device name or MAC address. Also, it involves the negotiation of the operation frequency, clock frequency, power management scheme or sequence in the frequency hopping. In the page stage the devices position on the piconet is defined. After that a connection is established and the devices can start the data transfer. Not all defined protocols are used in a link and these phases determine the stack protocol structure.

Other phases are also specified like standby, when the device waits for a scan, park, when the device is connected listening for data transfer in a piconet, or sniff, when the device is in a low power state. The active and hold modes are also specified, the last one being used in asynchronous services in which the device doesn't need to be active all the time.

Lower layer protocols have an important role in the connection process. The Baseband layer determines the clock, data packet formats, master/slave roles, connection/sleep state machine management, link control, audio connection and error control policies, that is based on *Forward Error Correction* code (FEC). The Baseband allows two types

of connection in two different physical links: *Synchronous Connection-Oriented* (SCO) and *Asynchronous Connectionless* (ACL).

LMP sets up, authenticates and configures the link. The Inquiry is not a state managed by the LMP, made by a higher layer protocol HCI. The LMP procedures include the connection phase, the detach phase, power control and adaptive frequency hopping, important to the power control procedure. The page process is necessary in the inquiry state to recognize a possible device that wants to establish a connection, substituting its address. If none connection is needed, the node goes automatically to the standby state. The LMP works with the L2CAP to adapt the upper layer protocols to the Baseband. The SDP provides information about devices, services and characteristics of services necessary to the establishment of the link.

3.6. THE BLUETOOTH MODULE RN41

RN41 is a certified Bluetooth radio transceiver meant for low power applications. It delivers up to 3 Mbps data rate for distances over 100 m thanks to an on chip high performance antenna. The output transmitter power is 12 dBm and the typical receive sensitivity value is -80 dBm. This device pertains to the class 1 radio and supports versions 2.1, 2.0, 1.2, 1.1 and 2.1 with *Enhanced Data Rate* (EDR). The frequency of operation ranges between 2402 MHz and 2480 MHz in which FHSS/GFSK modulation is used with 79 channels at 1 MHz intervals. The embedded stack protocol includes GAP, SDP, RFCOMM and L2CAP with SSP/DUN and HID profiles. Also it supports HCI interface protocol[26]. The device will be presented in Figure 24.

3.7. THE PROCESSOR

The MCU performs the role of master and its functions are: organizing the data in the sampling process, receiving data in orderly way, multiplexing data before being sent by the transceiver. In synchronous tasks the MCU also provides the clock, having as the source either an internal or external oscillator. A MCU combines in the same chip a microprocessor and the relevant peripherals, what freed the hardware from additional external circuitry.

Low power systems imply minimal hardware as well as a minimal processing. In this regard, the intention is not to use buffered data that would imply additional read and write routines and also the use of additional memory. This approach is feasible if the data sending happens at the same rate as it is sampled. Some applications require increased number of input for the sampling process, as in the case of a BSN, for example. It is recommended using a MCU with additional number of ADC inputs, which avoids using an external ADC module.

Regarding a BSN, the sampling process is maybe the principal task of the MCU together with the multiplexing. Both are relatively simple tasks and dispense powerful processors. If more complex data treatment is necessary and it is possible to transfer the processing task to another point not battery powered, this may be regarded. Otherwise more powerful processors like a DSP can be adopted, but this should be avoided due their relative high consumption [15].

3.8. THE PIC18F14K22

The PIC18F14K22 makes part of the midrange MCU of Microchip™, a family of devices that allies high computational performance and low pin counting. Also they are featured with high endurance Flash program memory what increases their life. The incorporation of *nano Watt XLP* technology reduces significantly the power consumption featuring these devices with multiple Idle modes, means that the power consumption can be reduced to 4% of normal operation. In particular, the PIC18F14K22 high performance is ensured by a *Reduced Instruction Set Computer* (RISC) *Central Processing Unit* (CPU) capable to execute 16 MIPs and an internal oscillator that affords eight options of frequency, ranging between 31 kHz and 16 MHz. The frequency can be multiplied by 4 with a *Phase Lock Loop* (PLL) and reach 64 MHz using the internal oscillator. Two programmable I/Os for external oscillator for customized frequency with equal upper limit of 64 MHz are also available [27].

This MCU counts with an ADC module with 12 input channels and 10 bits resolution; with an analog comparator; with 17 I/O pins; with 4 timers / counters, of which 3 with 16 bit – prescaler and 1 with 8 bit – pre/postscaler; with Enhanced Capture / Compare / *Pulse*

Width Modulation (PWM) - (ECCP) up to 4 PWM outputs; with a *Master Synchronous Serial Port* (MSSP) module with SPI and I²C in master and slave modes; and with an *Enhanced Universal Synchronous Asynchronous Receiver Transmitter* module (EUSART). Also it is featured with program memory with 16 kbytes and data memory with 512 bytes. The devices also present 30 interrupt sources with two levels of priority. The device scheme can be sow in Figure 22.

3.9. SENSING DEVICES AND INTERFACE

Two types of sensors satisfy the requirements of this project: surface electrodes and accelerometers. The walking task does not demand a powerful accelerometer. The SCA3000-D01 is a three axes accelerometer targeted for battery operated devices that requires low power consumption. The acceleration is measured by a capacitive sense element that consists of three acceleration sensitive masses. The measurement axes are rotated 45° compared to the conventional orthogonal (**x**, **y**, **z**) coordinate system. The signal is filtered and mapped onto the orthogonal coordinates after an AD conversion and multiplexing. This device is also featured with an internal oscillator and a non-volatile memory that provides some autonomy. The SCA3000-D01 ensures high performance even in low power systems thanks to a “robust, stable and low noise and power capacitive sensors” [28].

This accelerometer is featured with a SPI interface and allows for a master and slave mode operation. It has the option of being used in the measurement mode, in which returns the acceleration value, in motion detection mode, in which an interrupt is generated when a threshold level is exceed, and in free – fall detection modes, that works similarly to the motion detection mode, differing by the availability of acceleration data readings. An internal temperature sensor also enhances the accelerometer and it is available to external reading. The device is presented in Figure 23 [29].

Figure 20 shows the surface electrodes used for general biosignal capturing. Three electrodes collect one sampling point. The electrodes have the central part within conductive gel. The EMG conditioning module (*Analog Front End* - AFE) shown in Figure 25 has been used to interface the acquired signal to the system. This module was

developed in *INESC – Porto*, being constituted by an input instrumentation amplifier with gain of 5 followed by two amplification stages: the first is a low-pass filter with gain of 20 and cut-off frequency about 480 Hz; the second is an amplifier with variable gain limited onto 10. The circuit presents an alternative low-pass filtered output, beyond the not filtered output, with cut-off frequency about 1.6 kHz.

Figure 20 – Top and bottom view of electrodes used in EMG.

4. THE DESIGN OF THE SYSTEM

This chapter discusses the three main topics involved in the integration of the final system. The initial section describes the steps to design the hardware, detailing the electrical requirements to link and interconnect the devices, when the final hardware is presented. The devices need to be configured and correctly programmed to establish communications and to comply with the system constraints and requirements, being the firmware another important aspect to be discussed. Finally, the last subject to be addressed is the software deployment and the interaction with the firmware.

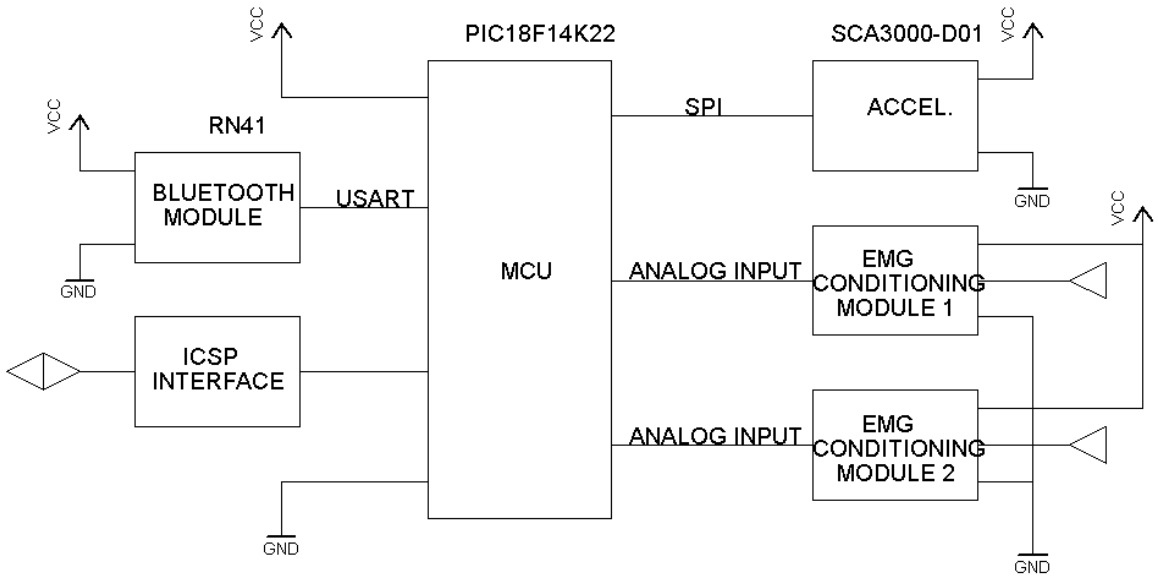

Figure 21 – Block diagram to the intended hardware system.

4.1. THE HARDWARE

The system in Figure 21 is proposed following the usual architecture described in Figure 12. The hardware core is composed by the microcontroller PIC18F14K22 and by the Bluetooth module RN41 linked through an USART interface. The system periphery is composed by sensors (accelerometers and electrodes). The accelerometer SCA3000-D01 communicates with the MCU by a SPI interface. The ADC available in the MCU is used to sample and to convert the EMG signal, which is previously conditioned in the EMG

conditioning module. Additional circuitry allows programming the MCU. The ICSP is the interface used between the programmer device and the MCU. Other required circuits are the power supply voltage regulator and the power on reset.

To interconnect the devices it is necessary to use a communication protocol. SPI is the serial communication protocol used to interface the accelerometer to the MCU. Between the transceiver and MCU the USART protocol is used. The ICSP is the physical interface used to program the MCU.

4.1.1. THE PIC18F14K22 CHARACTERISTICS

All functions of the PIC18F14K22 MCU are distributed over 20 programmable pins, as shown in Figure 22. The pin diagram is summarized in Table 6 and the main features and electrical characteristics are given in Table 5 [27].

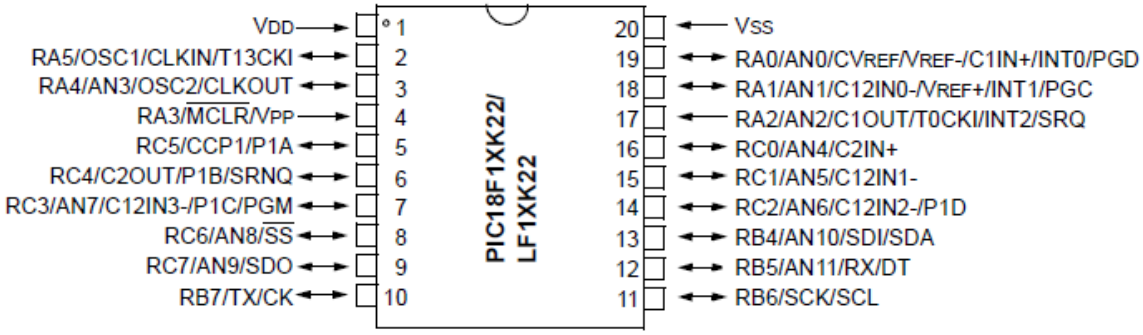

Figure 22 – PIC18F14K22 pinouts [27].

Table 5 – Main features and electrical characteristic of PIC18F14K22.

Description	Features/Characteristic
Extended Voltage Range	1.8 V – 5.5 V (± 0.3 V)
Program memory	16 kbytes
Data Memory	512 Bytes
Operating Frequency	DC – 64 MHz
Max current (run)	14.6 mA (at 5 V and 64 MHz)
Current (sleep mode)	34 nA
Max current I/Os (skin/source)	25 mA
I/O ports	A, B and C
Serial communication	MSSP (SPI, I²C™), EUSART
Timers	4
ADC module	12 channels
ECCP module	1

Table 6 - PIC18F14K22 pin summary.

Pin name	Description	Pin number
V_{DD}	Ground ref. for logic and I/O	1
RAx / RBx / RCx	Digital I/O	2, 3, 4, 5, 6, 7, 8, 9, 10, 11, 12, 13, 14, 15, 16, 17, 18, 19
ANx	ADC channel	3, 7, 8, 9, 12, 13, 14, 15, 16, 17, 18, 19
OSCx	Oscillator crystal / external clock input	2, 3,
CLKIN	External clock source input.	2
CLKOUT	OSC2 pin outputs CLKOUT	3
TxxCKI	Timer external clock input	2, 17
MCLR	Active-low Master Clear	4
V_{PP}	High voltage programming input	4
CCP1	Capture/Compare/PWM	5
P1A / P1B / P1C / P1D	Enhanced CCP1 PWM output	5, 6, 7, 14
CxOUT	Comparator output	6, 17,
SRNQ / SRQ	SR latch output	6, 17
C12INx-	Comparator C1 and C2 non-inverting input	7, 14, 15, 18
PGM	ICSP™ programming clock pin	7
SS	SPI slave select input	8
SDO	SPI data out	9
TX	EUSART asynchronous transmit	10
CK	EUSART synchronous clock	10
SCK / SCL	Synchronous serial clock input/output (SPI and I^2C modes)	11
RX	EUSART asynchronous receive	12
DT	EUSART synchronous data	12
SDI	SPI data in	13
SDA	I^2C™ data I/O	13
CxIN+	Comparator non-inverting input	16, 19
INTx	External interrupt	17, 18, 19
PGC	ICSP™ programming data pin	18
V_{REF+}	ADC and DAC high reference voltage	18
V_{REF-}	ADC and DAC low reference voltage	19
CV_{REF}	DAC reference voltage output	19
PGD	ICSP™ programming data pin	19
V_{SS}	Ground ref. for logic and I/O pins	20

4.1.2. THE ACCELEROMETER ELECTRICAL CHARACTERISTICS

The application requires that the accelerometer being used operates in the measurement mode. In this mode each axis is read with a resolution of 12 bits. A 13^{th} bit is used as sign. Therefore two bytes are used to read an entire axis being the three least significant bits

(LSb) not used. A complete reading of one point, what means the three axes, uses six bytes. Thus it is possible to read a range between -2 G and +2 G with 1333 counts/G. These parameters are summarized in Table 7, together with other relevant features [28].

Table 7 – SCA3000-D01 electrical characteristic [29] [28].

Description		Value
Supply voltage		2.35 V – 3.6 V
I/O voltage		1.7 V – 3.6 V
Current consumption	at 2.5 V	480 µA (typ)
	at 3.3 V	650 µA (typ)
Measuring range		± 2 G
Resolution		0.75 mG / 0.04°
Sensitivity		1333 counts / G
Output buffer		64 samples / axis
Max. SPI clock rate		1.6 MHz

Table 7 also shows the main electrical characteristic of the device that drains relatively low power, requiring a supply source ranging between 2.35 V and 3.6 V. The maximum clock rate allowed in communication with others device is 1.6 MHz. The SCA3000-D01 is available in a package with eighteen pins, being eight of them used. Figure 23 shows this device soldered on a *Printed Wire Board* (PWB) and the pinout description is given in Table 8.

Table 8 – Accelerometer PWB pinout.

Pin Number	Pin Name	Description
1	VIN	Supply Input
2	RST	Reset
3	INT	Interrupt
4	MOSI	Data Out
5	MISO	Data In
6	SCK	Serial Clock
7	CSB	Chip Select
8	GND	Ground

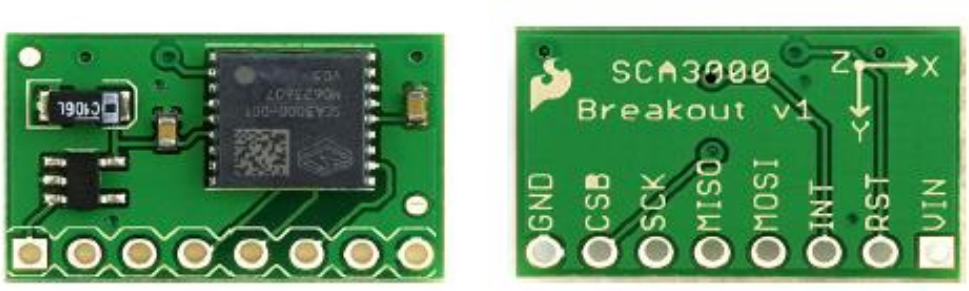

Figure 23 – SCA3000-D01 embedded on a PWB and its pinout.

4.1.3. THE RN41 CHARACTERISTICS

The Bluetooth transceiver chip contains 30 pins and is available in a socket module counting six pins for UART or RS232 interface. The UART interface can be used to configure the device as well over-the-air RF configuration. It works at standard serial baud rate speed: from 1200 bps up to 921 kbps. However, non-standard baud rates can be also programmed. Figure 24 shows the device with the socket module pinout (a) and its top view (b). The pinout description is given in Table 9.

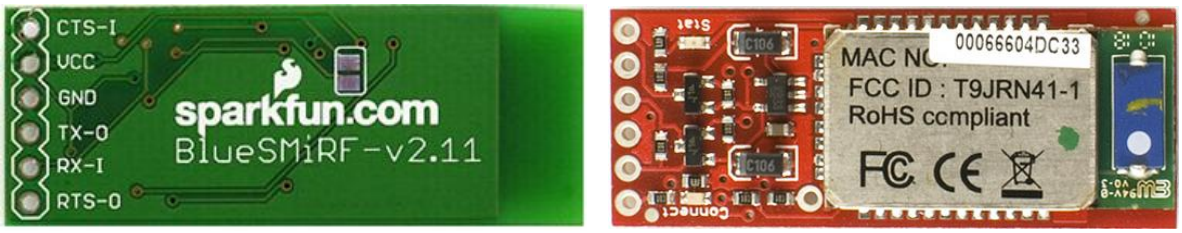

(a) (b)

Figure 24 – The Bluetooth module RN41 on bottom view (a) and on top view (b). [30]

Table 9 – RN41 socket module pinout.

Pin Number	Pin Name	Description
1	CTS – I	Clear-to-Send – Serial flow control
2	VCC	Supply source
3	GND	Ground
4	TX – 0	Serial transmission
5	RX – I	Serial reception
6	RTS – 0	Ready-to-Send – Serial flow control

The electrical characteristics of this module are summarized in Table 10 where one can find the power consumption required for transmission and reception conditions. This devices drain energy when it is connected even without transmission. According to the Bluetooth specification, the RN-41 is featured with power saving modes that reduce the standby consumption. In the Sniff mode the device wakes in specific intervals from sleeping. In the Deep Sleep mode the device is shut-down and the firmware stops its operation until an external order. The current value for each mode is given in Table 11 [31].

Table 10 – RN41 electrical characteristic [26].

Parameter	Min.	Typ.	Max.
Supply Voltage (DC)	3.0 V	3.3 V	5.0 V
RX supply current	-	35 mA	60 mA
TX supply current	-	65 mA	100 mA
RF transmit power		12 dBm	
Sensitivity		-80 dBm	
Data rate		1200 bps ~ 921 kbps	
Frequency		2402 ~ 2480 MHz	

Table 11 – Average power consumption regarding the operation mode [26].

Operation Mode	Average Power Consumption
Standby/Idle (default settings)	25 mA
Standby/Idle (deep sleep enable)	250 µA (min.); 2.5 mA (typ.)
Connected (normal mode)	30 mA
Connected (low power sniff)	8 mA

4.1.4. EMG CONDITIONING MODULE

The EMG conditioning module delivers a filtered and amplified analog signal to the MCU. The accepted amplification level can be programmed on the MCU. Figure 25 (a) is the top view of the module, in which it is possible to identify a four connections terminal. Terminal 1 (red marked) is one pole of the EMG input. The other pole is connected in input 3. The fourth input connects the reference electrode and the second input is meant to the cable's shield. Figure 25 (b) shows the bottom view of the module in which six terminals can be identified. These terminals are used to communicate with other devices

and each function is described in the Table 12. The two first pins are voltage input and reference to supply the module. The following pins are outputs to be used in ADC function in MCU. The third pin delivers the high voltage reference for the A/D converter. The low voltage reference is taken in pin four. The fifth pin is the EMG analog output and the sixth is the filtered EMG signal.

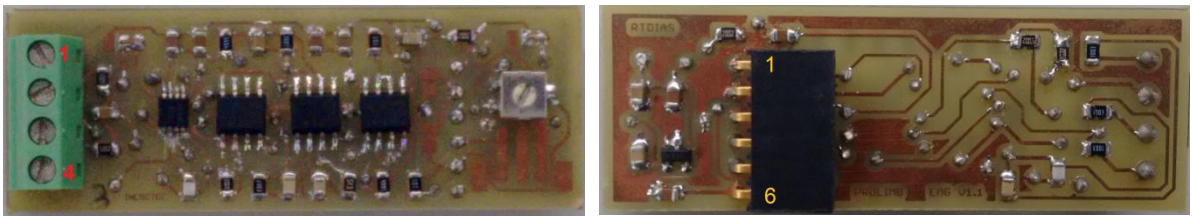

(a) (b)

Figure 25 – EMG conditioning module (a) top view (b) bottom view.

Table 12 – I/O reference to the EMG conditioning module.

Pin	Direction	Function	Feature
1	Input	Vin	3.3 V
2	Input	Ground	-
3	Output	Vref	3.3 V
4	Output	Vref / 2	1.15 V
5	Output	Va/D1	Not low filtered
6	Output	Va/D2	Low filtered

4.1.5. SPI INTERFACE

The SPI protocol is the serial interface used between MCU and accelerometer. The SPI is a full-duplex synchronous communication. It requires 4 lines, in which 2 lines for data transfer: *Master Input / Slave Output* – MISO and *Master Output / Slave Input* – MOSI. Another line is used as a Chip Select (SSx) and the last one is the clock. The data MISO/MOSI and CLK are available for all slave devices through the bus and the data is transferred when the SS of one device goes to logical level '0'. Figure 26 shows the configuration to multiple slaves.

To link the accelerometer to the MCU it is recommended to use pull-up and pull-down resistors [27] [28]. Table 13 gives the pull-up / pull-down resistors values and the available commercial values [28]. The SDA3000-D01 documentation omits any

recommendation to a pull resistor at MISO line. However, this recommendation is provided in the MCU documentation, in which the MCU port current value is used to compute the pull-down resistor value [27].

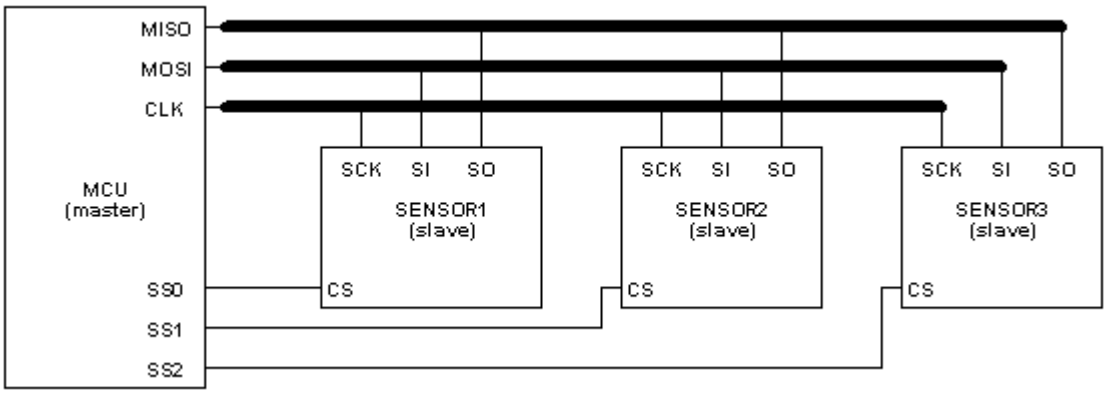

Figure 26 – SPI configuration for multiple slaves. The MISO, MOSI and CLK signal are available on a bus.

Table 13 – Recommended resistor value for stable operation.

Pin	Direction	Resistor	V	Imax(mA)	R(kΩ) = V/Imax	R-comercial (kΩ - 1/4W)
CSB	input	pull-up	3.3	0.05	66	68 / 62
XRESET	input	pull-up	3.3	0.01	330	330
MOSI	input	pull-down	3.3	0.05	66	68 / 62
SCK	input	-			-	
MISO*	output	pull-down*	3	0.250	12	12
INT	output	-			-	
* Value recommend to MCU by its datasheet [27].						

The communication is made over a 16 bits frame format (Figure 27). The six first bits are the address of the register to be accessed. The 7th bit defines if the operation is read (‘0’) or write (‘1’). The eighth bit is not used and is read as ‘0’. If a write operation is performed, the following eight bits contain data; otherwise, if it is a read operation, these bits are ignored. These operations are initiated by the master and are done over MOSI line. At the slave side the first byte answers the previous SPI frame with an error frame at second bit. The seventh bit is always ‘1’ and the eight bit is the odd parity. The following byte over MISO line contains the data captured following the read operation. Bits from the MOSI line are sampled in on the rising edge of SCK and bits to MISO line are latched out on falling edge of SCK. The read and write operations occurs as shown in Figure 27.

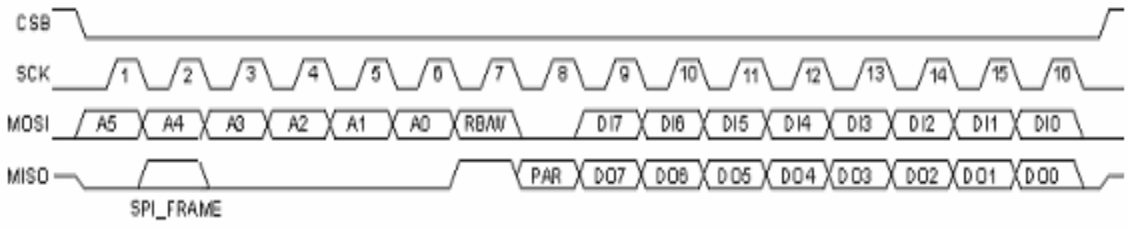

Figure 27 – SPI line operations [28].

The read can be made directly in each register or continuously using the decrement register read. Table 14 details the registers addresses for each byte of specific axes of the SCA3000-D01. This is the value to be written over MOSI line to do a read operation.

Table 14 – Registers addresses for read operation to SCA3000-D01.

Address	Axis	Frame
04h	X	LSB
05h	X	MSB
06h	Y	LSB
07h	Y	MSB
08h	Z	LSB
09h	Z	MSB

4.1.6. USART INTERFACE

The USART is a serial I/O communications protocol used among peripherals, also known as *Serial Communications Interface* (SCI). It uses four lines in the synchronous mode to emulate RS232 communications and two lines in the asynchronous mode. In the synchronous mode the communication is done in half-duplex way. The TX is used as a bidirectional data line and RX is used as a synchronous clock line. The CTS and RTS are used to control the data flow. In the asynchronous mode the communication is done in full-duplex way and CTS and RTS lines are not used. These pins from the RN41 are directly connected when it operates in asynchronous mode. The MCU's TX signal is linked to the RX-I pin of the Bluetooth module and the MCU's RX signal is connected to the TX-O of the RN41.

The EUSART transmits and receives the LSb first. The format *Non-Return-to-Zero* (NRZ) is used in the transmission and in the reception. An NRZ transmission port idles in the mark state. Each character transmission consists of one Start bit followed by eight or nine data

bits and is always terminated by one or more Stop bits. The Start bit is always a space and the Stop bits are always marks. The most common data format is 8 bits. These parameters must have the same configuration in both sides of the line, as well the frequency of operation.

4.1.7. *IN-CIRCUIT SERIAL PROGRAMMING* (ICSP™)

The ICSP™ is the interface used to program PIC microcontrollers and other Microchip devices in circuit. The programming is done using a device programmer, PICKit2 or PICKit3 for instance, that downloads the program from the developing environment to the target circuit. The interface requires five signals: V_{PP}, ICSPCLK or PGC, ICSPDAT or PGD, V_{DD}, V_{SS} [32].

- V_{PP}: Is the Programming Voltage that is about +12 V. When applied the device goes into programming mode.
- ICSPCLK/PGC: Is a unidirectional synchronous serial clock line from the programmer to the target. This pin needs to be isolated from the application circuit to prevent signal distortion. A series resistor is a possible solution.
- ICSPDAT/PGD: Is a bidirectional synchronous serial programming data line. This pin also needs to be isolated. If it is possible, the PGC and PGD should be dedicated for ICSP.
- V_{DD}: Is the voltage that feeds the target MCU during programming. An external supply source can be used but typically the circuit is powered by the programmer. The V_{DD} is +5 V and an isolation circuit is required if the circuit operates at a different voltage.
- V_{SS}: Is the ground reference that must be at the same potential of the target circuit.

Figure 28 depicts a possible circuit to isolate the target circuit to the difference of voltage of the programmer and preserve the signal features. A resistor or a Schottky – type diode together with a pull-up resistor/capacitor circuit is suggested to isolate the V_{PP} from circuit preventing the voltage conflict. Two serial resistors also isolate the ICSPDAT and the ICSPCLK inputs prevent the programming signal degradation.

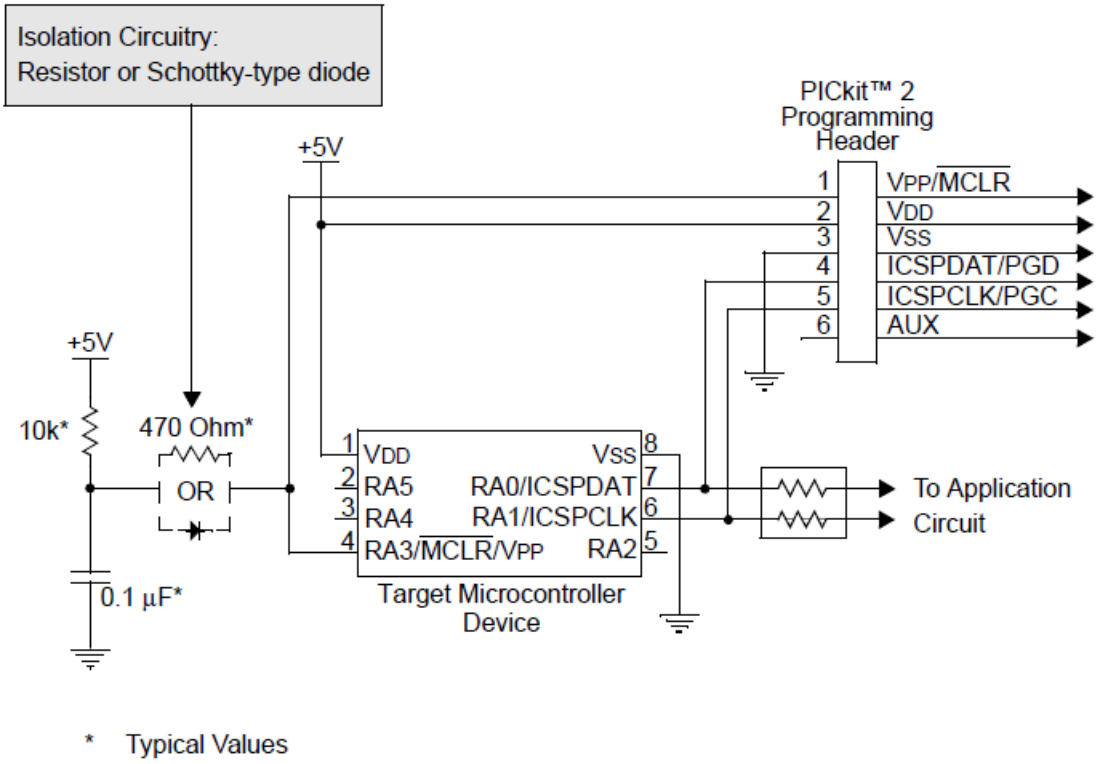

Figure 28 – ICSP circuit interface and isolation circuitry [32].

4.2. THE FINAL HARDWARE

The components were used to assemble the circuit viewed in the Figure 29. There it is possible to identify the MCU (**1**), the Bluetooth module (**2**), the accelerometer (**3**) and the EMG conditioning module (**4**). It is also indicated the ISCP input slot, in which the pin counting starts from the left side to the right, the output to the EMG sensors, to a scope and to the source. Auxiliary circuitries complete the mounting as indicated in figure: (**A**) is the Reset/ICSP isolation circuit. (**D**) and (**E**) are pull-up/pull-down resistors. (**B**) and (**C**) are voltage regulators circuit to 3.3 V and 3.0 V, respectively. The voltage regulator UCC 383-T3 is used to deliver 3.3 V, where the manufacturer recommended value to the associated capacitors [33] of 10 µF and 22 µF are used. The FAN 1581 was used to provide 3.0 V using the manufacturer indicated value to the capacitors of 10 µF and 22 µF. The output voltage is determined by the resistors association. The value of the first resistor and the typical current is suggested by the manufacturer and the second resistor is obtained by a voltage divider [34]. The part signaled with (**F**) is an access point bank for test purpose with two inputs buffered by the AMPOP LM324N [35]. The schematic with complete circuit is presented in the Annex B.

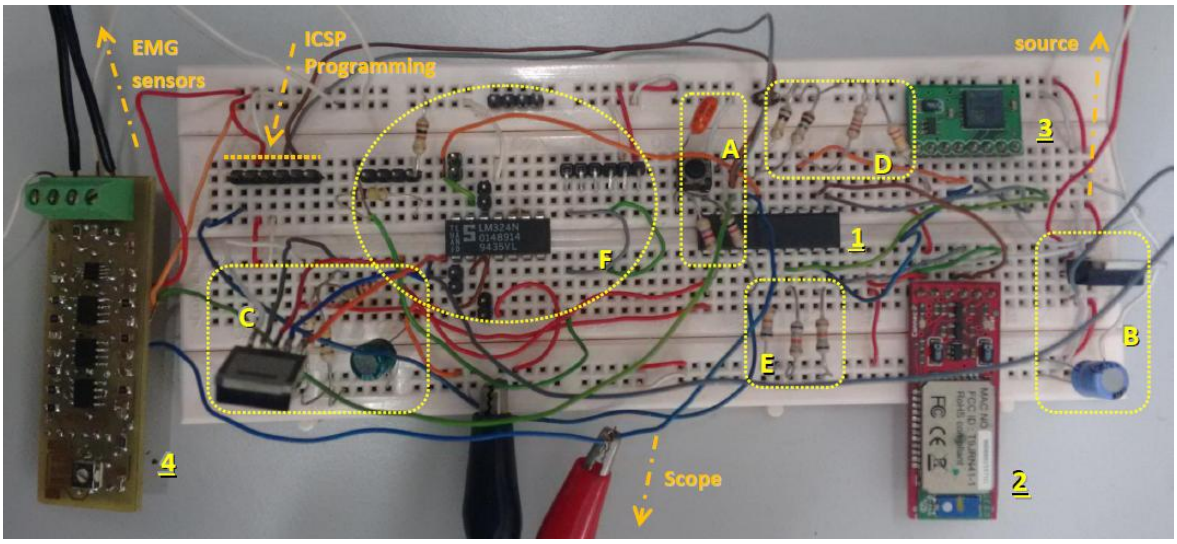

Figure 29 – Hardware assembly.

4.3. BLUETOOTH MODULE CONFIGURATION

To configure the RN41 module it is necessary to assign a COM port on a PC and connect through either the Bluetooth or serial port interface. A simple ASCI command language is used to program and the new configuration take effect after reboot. For over-the-air configuration the device uses the SPP Service. The pairing process is done manually by the user using the default key password "1234". All future connection will be done over the assigned COM port to this SPP profile. Once connected, the RN41 goes into data mode and the user has 60 s to go into command mode. A green LED turns on and the red turns off to indicate that the connection was succeeded [31].

It is in the command mode that all desired configuration and device programming is done. It is possible to enter in the command mode using an over-the-air connection only if the device is on the slave mode (default). The command to go into command mode is "$$$", typed from a terminal like TeraTerm, HyperTerminal or RealTerm. The OS Linux™ incorporates its own terminal, but latter OS Windows™ releasing does not, being necessary to install one of them. Once in command mode the Green LED blinks and the device answers with "CMD". To exit it type "---<cr>" and the device answers with "END" [31].

The configuration is possible if the serial port parameters are the same for both sides. The default serial port configuration to RN41 is: 115200 of baud rate, 8 bits, no parity, 1 stop bit and hardware flow control enabled. Here is present the most important configuration

instructions used in the present circuit among a sort of 61. The syntax is the command followed by a value, both separated by comma. To set the baud rate the command SU,<value> was used, whose value is one of the serial baud rate standards {1200, 2400, 4800, 9600, 19.2, 28.8, 38.4, 57.6, 115 k, 230 k, 460 k, 921 k}. Just the two first characters are typed in the field value, for example, the baud rate of 115200 was programmed by the command 'SU,11'. For non standard baud rates there is the command SZ,<value>, in which **baud rate** × 0.004096 determines value. The command SL,N selects none parity. The module returns "AOK" for a valid command, returns "ERR" for a not valid command and "?" for a not recognized command [31].

There is the possibility of reducing the module power consumption by configuration commands. The SJ,<value> command reduces the time window for page scan process and the SI,<value> command reduces the time window for inquire process. By default, both values correspond to 12.5% of duty cycle. Values below the default can save power but under risk to miss an inquiry or page request, whereby these value was maintained. The activation of the Sniff mode or Deep Sleep mode is the most powerful tool to reduce the consumption. In both modes the device awakes cyclically under minimal interval of 0.625 ms. This value is superior to the desired sampling rate (0.5 ms) and their activation would implies data loosing and was not configured [31].

4.4. THE MCU PROGRAMMING AND CONFIGURATION

The PIC MCU was programmed using C language. The code was developed on the MPLab™ *Integrated Development Environment* (IDE) – v8.36 for Windows OS. The MPLab encompasses the assembler, the linker, the ASM compiler and the simulator in one environment. A third part is necessary to develop and compile the code in C language, whereby the MC18 C compiler, specific to the PIC18 family, was installed. The PICKit2 programmer/debugger was used to load the programming to the MCU.

The programming is done writing proper word over specifics feature registers. Some of them require preprocessing configurations to the MCU start up, what is stored in a non-volatile memory. The main features to be programmed are the voltage of operation, the oscillator to be used, the power consumption mode and policies, and boot options. Other

initial configurations define how peripherals will behave. Their frequencies are generated from the oscillator frequency (F_{OSC}) and their instructions are executed in each cycle period ($T_{CY} = 4 \times T_{OSC}$).

- **Oscillator:**

The oscillator is programmed with 9 registers: CONFIG1H, INTCON, OSCCON, OSCCON2, OSCTUNE, IPR2, PIE2, PIR2, and T1CON2. With these registers one can configure, for instance, the system clock, the clock source, the frequency of operation and the startup mode.

The clock source is chosen among three options, setting the SCS pair bits from the CONFIG1H register. The options are: Primary External Oscillator (SCS: 00), Secondary External Oscillator (SCS: 01) and Internal Oscillator (SCS: 1x). The clock sources can operate in 12 different oscillator modes in which 11 options for external clock source.

As a 13^{th} option the internal oscillator can be clocked out. This oscillator is composed by two independents oscillators: the LFINTOSC, which provides a low frequency of 31 kHz, and the HFINTOSC, a high frequency oscillator which provides a range of eight possible values {16 MHz, 8 MHz, 4 MHz, 2 MHz, 1 MHz, 500 kHz, 250 kHz, 31 kHz}. The frequency of the internal oscillator is set by the bits IRCF<2:0> from OSCCON register. The PLL mode can be activated through PLLEN bit from OSCTUNE register, multiplying by four standard frequencies ($T_{CY} = T_{OSC}$).

All other peripherals share the same clock source, whereby it is necessary to choose the suitable oscillator frequency to match all their needs. These needs are extended for the devices linked to the MCU in master/slave architecture to satisfy equally their constraints.

- **Interrupt sources:**

Twelve registers control the interrupt operation: RCON, INTCON, INTCON2, INTCON3, PIR1, PIR2, PIE1, PIE2, IPR1, and IPR2. Generally the interrupt control and operation are done by three bits: the Flag bit to indicate a changing state, the Enable bit to allow an event to perform an interrupt, and Priority bit to determine the preference on a routine execution.

The PIC18F14K22 peripherals can independently generate interrupt operations in two possible priority levels: Low and High. To turn on an interrupt source, the GIEL bit of the INTCON register must be set (‘1’), beyond the correspondent source peripheral Enable bit. To work with the two priority levels, the IPEN bit of the RCON register must be set (‘1’) together the GIEH bit of the INTCON register. The source priority with the higher priority must have its Priority bit set (‘1’). On the operation, the high priority interrupt level event interrupts the routine flow, even the low priority routine, to perform its instructions and, in the end, returns to the same point that was stopped. Before returning to the routine, the interrupt flag bits must be cleared by software, avoiding the reentrance in the interrupt routine.

- **I/O:**

Three main registers configure the three I/O ports (A, B and C): the TRIS register defines the data direction (‘1’ as input, ‘0’ as output); the PORT register reads the levels on the pins of the device, and the LAT register is the output Latch. Other two registers are available, one to enable (‘1’) or to disable (‘0’) a weak internal pull-up (WPU register) and another to enable (‘1’) or to disable (‘0’) the interrupt on-change function (IOC register). Some port pins share the digital and analog function. When a pin is used as an analog input, it is necessary to disable the digital input buffer setting the appropriated bit at the ANSEL and/or ANSELH register. Otherwise, the digital function just performs correctly with the respectively pin of these registers configured as ‘0’.

- **SPI:**

The MSSP registers configure the SPI interface by four control registers. The SPI function is enabled setting the SSPEN bit at SSPCON1 register. Thus, the serial functions (SCK, SDO, SDI and SS) overlap the I/O port pins. Nevertheless, the respective I/O pin must be configured either as input or output by TRIS register, regarding the SPI function direction. The quartet of bits SSPM of this register selects the role to be performed by MCU and the SPI clock among four options: TMR2/2 (‘0011’), F_{OSC}/64 (‘0010’), F_{OSC}/16 (‘0001’) and F_{OSC}/4 (‘0000’). The polarity of the clock is defined in the same register by the CKP bit. Others clock features are configured at the SSPSTAT register, in which the bits SMP and CKE are used to determine what occasion of the SPI clock cycle the data is sampled and

transmitted. CKE and CKP bits determine what the standard SPI mode the bus has been being configured. Table 15 [27] shows the correspondence between bits configuration and SPI bus mode.

Table 15 – SPI standard bus modes.

Standard SPI Mode Terminology	Control bits State	
	CKP	CKE
0, 0	0	1
0, 1	0	0
1, 0	1	1
1, 1	1	0

- **USART:**

The USART is programmed regarding both, the transmission and the reception functions. They are enabled writing '1' to the TXEN bit of the TXSTA register, to the CREN of the RCSTA register respectively, and to the SPEN bit of the RCSTA register. This last bit enables the EUSART peripheral. The asynchronous communication is configured clearing the SYNC bit of the TXSTA register.

The analog I/O function must be disabled by clearing the ANSEL bit corresponding to the TX/CK and RX/DT pins. The TRIS control bits corresponding to the RX/DT and TX/CK pins should be set to '1'. The peripheral will control automatically the pin direction with EUSART function enabled (SPEN bit set to '1').

The *Baud Rate Generator* (BRG) is a dedicated timer that operates at 8 bits mode or 16 bits mode. The last referred mode is determined by the BRG16 bit of the BAUDCON register set ('1'). The BRGH bit of the TXSTA register set to '1' selects the high baud rate speed. The baud rate period is configured by the SPBRGH:SPBRG register pair, which receives the close integer value to the n, determined by Equation 1. The configuration of BGRH and BGR16 bits determines the k value in the Table 16 to be used in the equation. The desired baud rate is used to obtain the value of n, including non-standard serial values, that is computed regarding the frequency of the internal oscillator.

$$Desired\ Baud\ Rate = Fosc/[k\ (n+1)] \qquad \text{(Equation 1)}$$

Table 16 – Value for *k* in function of the EUSART operation mode.

Configuration Bits			BRG/EUSART Mode	*k*
SYNC	BGR16	BGRH		
0	0	0	8-bit/Asynchronous	64
0	0	1	8-bit/Asynchronous	16
0	1	0	16-bit/Asynchronous	16
0	1	1	16-bit/Asynchronous	4
1	0	-	8-bit/Synchronous	4
1	1	-	16-bit/Synchronous	4

TSR register is the data outgoing register that is not accessible by software. The byte to be transmitted is written into TXREG and transferred to the TSR register if it is empty. The transmission starts when the byte is completely transferred. The TXIF bit is controlled by hardware and is kept cleared while the TSR is busy.

The RSR register is the incoming register that is equally not directly accessible by software. The accessing to the received data is done via the RCREG register. The RCIF bit is set whenever there is an unread byte in the input buffer and is cleared when the byte is read. The RCIF is also controlled by software.

- **ADC:**

The ADC configuration starts defining the pin analog function, with the ANSx bit of ANSEL or ANSELH registers corresponding to the analog input set (‘1’). It writing ‘1’ to the TRISx bit configures the pin as input. The channel to be sampled is determined by the CHS bits of the ADCON0 register [27]. When changing channels, a delay is required before starting the next conversion. The delay is configured by ACQT<2:0> bits of the ADCON2 register among of eight possible multiples to the T_{AD} {0, 2, 4, 6, 8, 12, 16 and 20}. T_{AD} is the time to complete one bit conversion defined in function of the T_{OSC}. 2 T_{AD} wait is required before the next acquisition can be started. The T_{OSC} is configured by ADCS<2:0> bits also from ADCON2 register, choosing among seven possible clock frequencies {$F_{OSC}/2$, $F_{OSC}/4$, $F_{OSC}/8$, $F_{OSC}/16$, $F_{OSC}/32$, $F_{OSC}/64$ or F_{RC}}.

The ADC module is enabled through ADON bit of the ADCON0 register set to ‘1’. The sampling starts writing ‘1’ to the GO/DONE bit of the ADCON0 register. The ADIF bit is automatically set when a conversion is completed and GO/DONE bit is cleared. The ADC

sampling has 10 bits of resolution stored in two register: ADRESL and ADRESH. If the ADFM bit of the ADCON2 register is set, the result is stored in right justified way filling the LSbs, otherwise, if ADFM bit is clear the result is stored in MSbs and the output format is left justified. With this resolution readings of 1024 levels between low and high voltage reference are allowed. The PVCFG and NVCFG bits of the ADCON1 register configure respectively the positive and negative voltage references. “The positive voltage reference can be V_{DD}, FVR or an external voltage source. The negative voltage reference can be either V_{SS} or an external voltage source” [27].

- **CCP:**

The CCP1 Special Event Trigger can be used to execute a periodic sampling. In this case the GO/DONE register of the ADCON0 register is controlled by hardware and the Timer1 or Timer3 is used to trigger event. To configure the sampling using the CPP1 with the Special Event Trigger function, the AD conversion must already be enabled.

To operate in Special Event Trigger mode the CCP1M <3:0> bits of the CCP1CON register must contain the ‘1011’ bits. This configuration allows the ECCP to reset TMR1 or TMR3, start AD conversion and set CC1IF bit. These events happen whenever the running timer value matches to the value written in the CCPR1H and CCPR1L register pair.

- **Timers:**

TMR1 and TMR3 resemble in their features and configuration. Thus anyone can be chosen to be used with the Special Event Trigger mode. The choice is done with the T3CCP1 bit of the T3CON register: ‘1’ selects TMR3 and ‘0’ selects TMR1. Once selected, the timer must be configured to run as timer mode, clearing the TMRxCS of the TxCON register. This configuration also selects the $F_{OSC}/4$ like clock source to the timer. The timer running frequency is selected by the TxCKPS<1:0> pair bits of the TxCON register among four prescale options (1:1, 1:2, 1:4 or 1:8). The RD16 bit of this register configures the 8-bits mode (‘0’) or 16-bits mode (‘1’), depending on the desired running period. The timer is enabled writing ‘1’ in the TMRxON bit, also in this register. The TMRxH and TMRxL registers store the running counting that is compared to the CCPR1H and CCPR1L reference value.

- **Modes of operation:**

There are three possible modes of operation for the MCU, determined by the clock source and by the fed modules: The Run and Idle modes use any of the three available clock sources (primary, secondary or internal oscillator block) and the Sleep mode does not use any clock source. The IDLEN bit of the OSCCON register controls CPU clocking and the clock source is selected by the SCS<1:0> bits of the OSCCON. All clocks stop with IDLEN bit cleared and, with the IDLEN bit set, the clock is disconnected from the CPU and maintained for peripherals.

The power-managed mode is invoked with the 'SLEEP' instruction. An interrupt source can be used to exit from Idle or Sleep mode to the Run mode. The exit sequence is performed when an interrupt flag bit is set, being necessary the suitable interrupt configuration in the INTCON and PIE registers.

4.5. THE FIRMWARE

It is possible to distinguish three main steps inside any firmware: the pre-processing configuration, the initial settings and main code. The pre-processing configurations and the initial peripherals settings obey the requirements of the tasks performed by the main code. Here the tasks can be seen slightly into two states as shown in Figure 30.

Figure 30 – Tasks performed in the two states of the main code.

Figure 31 illustrates the basic message exchange between two sides and the action performed by them. After being turned on and performing the initial settings, the hardware goes to the low power state, waiting for the link establishment. The PC starts the Bluetooth communication. The data transfer between two parts also starts with a

remote order. When a byte is received, the MCU leaves from idle mode and runs a low priority routine. The PC also finishes the communication in the same way. Every time that the low priority routine is called the timer is activated or deactivated by a toggle.

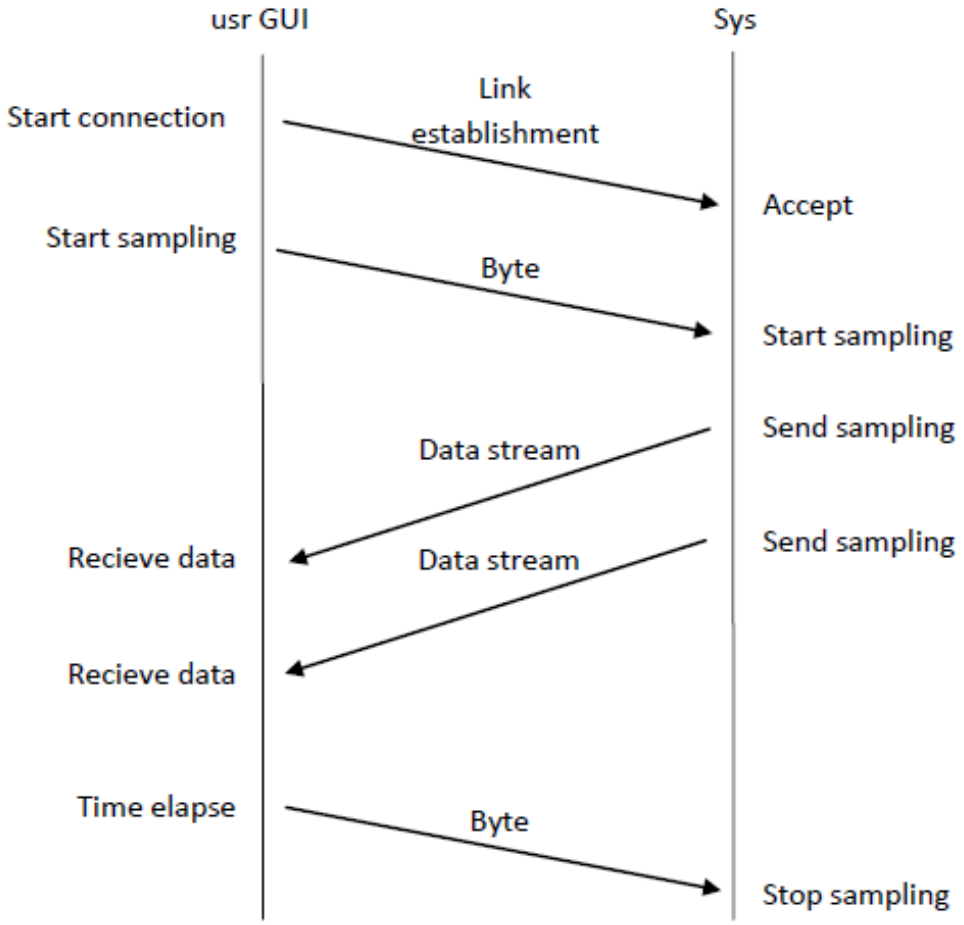

Figure 31 – Handshake diagram between the remote system and the user interface.

Two levels of interrupt priority are defined. The lower level interrupt is called by RC interrupt flag (Figure 32) and the high level is called by CCP interrupt flag. The first is activated by a reception of one byte and the second is activated after a CCP triggering. Once the timer is running, the high priority routine is called whenever a time elapse happens. Inside this routine, the ADC sampling is performed followed by the transmission the converted value; followed then by the capture of the accelerometer data and its transmission. Thus, inside one interrupt routine two bytes are transmitted. The timer is reactivated at the final of the routine, restarting the process. The system returns continuously to the idle mode after an interrupt routine is performed. All the time, the MCU waits by an incoming byte from the PC.

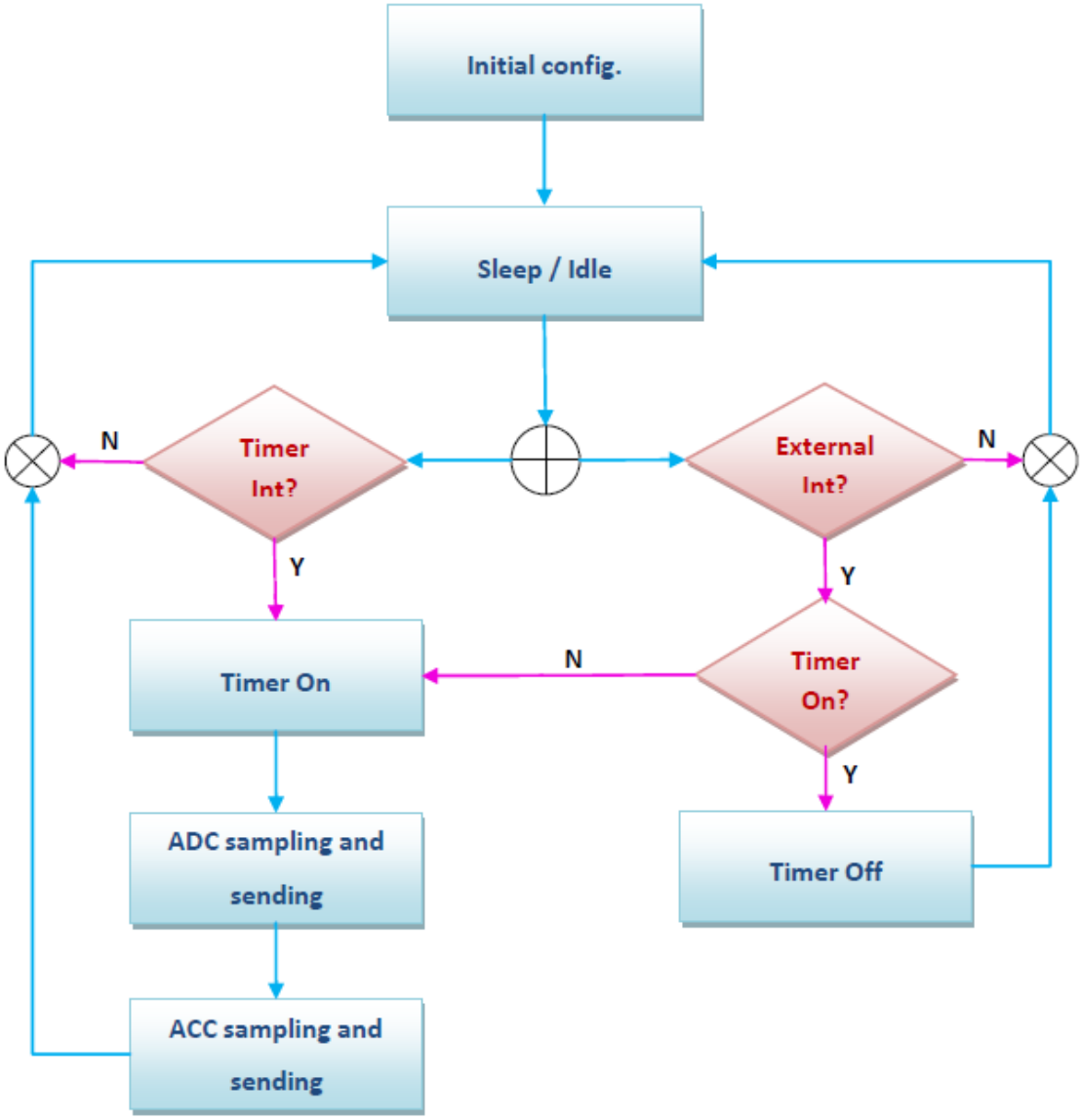

Figure 32 – The firmware block diagram.

On the other side, on the laptop, data is received using a GUI application. The user determines when the link is established and the sampling. The software controls the time and sends an order to the microcontroller to stop the sampling. The data is received continuously and processed before being displayed.

4.5.1. THE PACKAGES FORMATION

The samples are sent byte after byte alternating a sampling from one electrode and a byte from the inertial sensor. The EMG sampling value is sent in one byte. The reading of one axis of the accelerometer is sent in two bytes and the complete reading of one point

is sent in six bytes. Figure 33 illustrates the packet formed by the samplings. **S** represents the sampling from an EMG sensor and **A** represents an accelerometer data byte. The basic frame is formed by two different EMG samplings interspersed by the two bytes of an accelerometer axis. The next EMG reading comes from the following sensor. The readings are done cyclically, returning to the first sensor when the last is reached.

The ADC delivers a sampling with 10 bits of resolution that is carried in two bytes. The last two bits are more liable to noise and were discarded. Thus the EMG sampling information was reduced to one byte with the advantage of reducing the bandwidth.

The first byte of the accelerometer is the least significant and its three least significant bits are not used. These bits are read as '0' and are available to assign an axis and the accelerometer. This mark also assigns the beginning of a packet and is used for synchronism on the reception. The sampling sequence is XYZ and each X axis was marked with a bit '1'. The position of the bit identifies the accelerometer (Figure 33): '...001' to the first sensor (S1), '...010' to the second (S2) and '...100' to a possible third sensor (S3). The MSB of each axis is bolded and the MSB of X axis, which carries the bit of synchronism, is underlined.

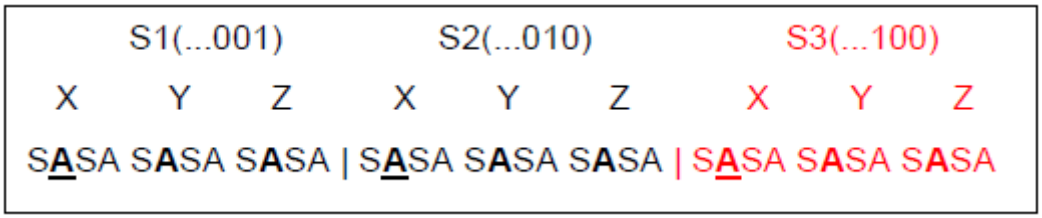

Figure 33 – Packet format and frame sequence.

4.5.2. SYSTEM REQUIREMENTS

The sampling rate is the first requirement to be observed in the system. Regarding Nyquist rate applied to the EMG frequency, each channel is captured with a 500 Hz × 2 like minimal sampling rate, which is equivalent to the frequency of 1000 Hz. Other peripheral frequency values regards this basis value multiplied by the number of input channels. The prototype was conceived to test two input channels, but the analysis was extended for other possible dimensions, targeting the dimension of sixteen channels (Table A. 9 - Annex A).

Under these conditions the sampling process is done at 1/2000 s, or 0.5 ms. This is the interrupt periodic time interval of occurrence, referred as T_{SMP}. The tasks of sampling the analog channel (T_{ADC}), sampling the inertial sensor (T_{SPI}) and send both bytes ($T_{SENDING}$) were calculated to be inside this interval (Equation 2). Additional processing is also regarded and refers to some extra cycles expended to clear an interrupt flag, to perform other computations (T_{PROC}):

$$T_{ADC} + T_{SPI} + 2\times T_{SENDING} + T_{PROC} < T_{SMP} = 0.5 \text{ ms}. \qquad \text{(Equation 2)}$$

The communication frequencies impose their own limitations to the firmware settings. The SPI was limited by the accelerometer to a frequency below 1600 kHz and the EUSART by the sampling rate to the minimal of 384000 bps, which is the closest serial standard value to the 2 kbytes. Table A. 1 of Annex A has the analysis to all standard serial baud rates. The baud rate upper limit is determined by protocol, 115200 for transmission over SPP and about 1 Mbps using other profile like RFCOMM or OBEX. The packet format also limits the transmission, in which one sampling provides two bytes (accelerometer plus EMG). In this regard the minimal transmission rate is 4 kbps, rising the minimal frequency 576000 bps.

A reliable A/D conversion is ideally done inside the range of 1 µs to 4 µs for the T_{AD} [27] (Table A. 6 – Annex A). The T_{ADC} depends on the choice of T_{ACQ} and the frequency of operation (Equation 3). Table A. 7 in the Annex A has the evaluation of the frequency – T_{ACQ} association that returns the better option.

$$T_{ADC} = T_{ACQ} + 11T_{AD} + 2T_{AD} \qquad \text{(Equation 3)}$$

T_{SPI} calculation returns the fastest value of 0,016 ms to a complete cycle of R/W operation. This value is possible to the minimal F_{OSC} of 4000 Hz. Other possible values are given in the Table A. 5 – Annex A, which has the complete analysis for the all range of frequencies available by MCU.

The frequency to the EUSART function was computed using Equation 1 targeting the standard serial baud rate. The resulting value is the *n* to be written in the SPBRGH:SPBRG register pair. Table A. 3 and Table A. 4 of the Annex A provide the complete range of n

values, as well as the percentage error due the rounding. The feasible $T_{SENDING}$ are given in Table A. 2.

It was based on these requirements that the choice for the appropriate oscillator and suitable timer frequencies to feed other functions was done.

4.5.3. FIRMWARE ALGORITHM

The MCU starts up using the internal oscillator as the clock source and the nominal voltage of 3.0 V, both programmed in the configuration bit. Complementary characteristics take place in the main code, in which the frequency was programmed to run at 16 MHz with factory calibration. The oscillator was programmed to clock the peripherals when “Sleep” instruction is called, being lead to the Idle mode.

Both the transmission and reception of the EUSART were enabled and configured to work with a word of 8 bits. RX was programmed to listen continuously and to wake up on a reception event. The Baud Rate Generator used 16 bits in the high speed. The frequency was programmed to 115.2 kbauds/s writing the decimal 34 (22h) to the SPBRGH:SPBRG register pair (Table A. 4 – Annex A). Pin 10 was configured as output to be used like TX and pin 12 was configured as input to be used like RX, being their analog function disabled.

The SPI was programmed in the mode 0,0 (Table 15) and the $F_{OSC}/16$ frequency divider was selected to generate a clock SPI source of 1 MHz. The MCU was programmed to assume the master role and the pin 11 was programmed output to provide the clock. The pin 9 was programmed as output and the pin 13 was programmed as input and the analog function was disabled to work as MOSI and MISO respectively. The function SS was disabled from the pin 8, measure necessary when the SPI function requires more than one slave. Pins 6 and 7 were configured to use the I/O function to works like SS, operating then as output. Also, it was necessary to disable the analog function from pin 7. A third I/O was reserved to a possible inclusion of one slave.

The ADC was programmed to use an external positive voltage reference and ground as the negative reference. The voltage reference was programmed to use the analog module

as source. The word 'FFh' was written in the VREFCON2 register to use the full scale of 3 V. This configuration generates a signal offset equal to half the voltage interval. The sampling was justified to the left to obtain the eight MSbs. The frequency was programmed to run at 4 MHz ($F_{OSC}/4$) and a delay of 12 T_{AD} (Table A. 7 – Annex A) was introduced to ensure the sampling accurate. The pins 16 and 17 were configured as inputs and enabled to operate in the analog mode.

Pin 5 was also configured as an output to disable the CCP external capture and program to be used with a special event trigger. The TIMER3 was programmed to provide the clock source to the CCP module. The frequency was set to run at a scale of 1:2 of the F_{CY}. Regarding the IRC frequency, the TIMER3 frequency is 2 MHz. The CPP module counts 1000 cycles from the TIMER3 to generate an interrupt at 0.5 ms, which is equivalent to writing 03E8h to the CCPR1H:CCPR1L register pair (Table A. 10 – Annex A).

The global peripheral interrupts were enabled allowing the multiple levels of priority. Each specific peripheral interrupt was disabled, except the two desired peripheral interrupts: the CCP and the RC. The first was set to call the high priority routine and the second to call the low priority routine.

The following sequence is performed in the low priority interrupt routine:

- Receive the incoming byte (wait for interrupt flag clearing);
- Set the address to point to the first accelerometer byte (_adsrs = 4);
- Initialize a global counting variable (_commut_SS = 0);
- Commute the TIMER3 operation.

The high priority interrupt routine performs the next routines:

- Clear AD interrupt flag;
- Clear CCP interrupt flag;
- Send the A/D value;
- Wait for the sending finished;
- Commute the analog input channel;
- Verify if the address is the first or the last byte of the accelerometer. If true:
    - Set the address to the first byte (_adsRS = 4);
    - Go to the next accelerometer (_commut_SS = ++_commut_SS & 1);
- Enables the Sensor Chip Select pin (_SS_CH[_COMMUT_SS]);
- Write the address to be read in the accelerometer;

- Wait to read the required value;
- Send the Accelerometer byte;
- Disables all Sensor Chip Select pin;
- Go to the next byte address (_ADSRS ++);

The code was implemented following general rules for soft and power efficient programming [6]: The number of variables was minimized using direct R/W on the registers; the structure of the code was sized for powers of two; it was preferred the types **char**, **int** and **short;** the most probably case is the first into verifications cyclist and the mostly called routines were placed before the less called. The final code is presented in Annex C and the generated program follows in the media digital Annex.

4.6. THE SOFTWARE

The software functions receive and treat the data stream to be displayed in a graphical interface. The software was developed in visual C# using the Microsoft Visual Studio 2010 like IDE. Visual C# is an events object-oriented program language which provides a vast sort of visual libraries that facilitates the programming. The developed application was thought to interact through a clean, intuitive and friendly window, with a first area meant to plot the graphic representation of EMG signal and kinetic activity and a second area reserved to input user commands.

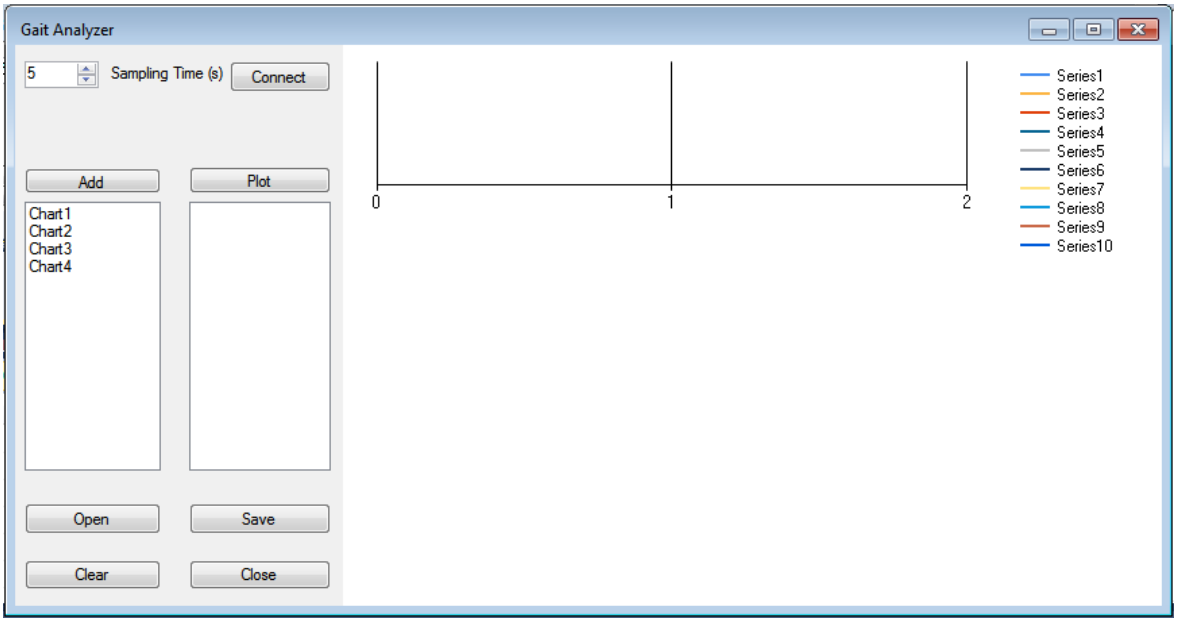

Figure 34 – Form window application fashion.

The application interface is shown in Figure 34. The commands were organized at the left side, where on the top are disposed the commands to determine the duration and to start the sampling. Commands to plot the received data are disposed below, with option to save the data or clear the scream to get another sampling. The data is saved in a file "*.txt" with the possibility to be opened late. Only files that obey the coding rule can be opened. The application also allows saving a plot area as an image file.

The class *serialPort* was used to establish the Bluetooth communication. Its properties configurations are the same for the remote Bluetooth device (baud rate of 115200, none parity, one stop bits). *PortName* property matches with the COMPort previously attributed to the Bluetooth device (COM4). The *ReadBufferSize* property was configured to 1048576 bytes.

The data is received continuously during the time chosen by the user. A Timer class controls the time and finishes the connection when the time elapses. A byte is sent at the connection instant to order the data transfer. The data is copied to an Array and it is verified if the stream is corrupted. The verification is done searching for the occurrence of the two first LSB from the 'X' axis from the inertial sensor. The marked bytes are spaced with 12 bytes. Also it is verified if the fourth byte that came from an accelerometer corresponds to the LSB 'Y' axis. These conditions are the basis to the algorithm:

- The 3 last bits from Byte[index] and from Byte[index + 12] != 0;
- Both three last bits correspond to a counting sequence: (001 -> 010 ->001)
- The 3 last bits from Byte[index + 4] and from Byte[index + 16] == 0;

If one condition is not verified the array is discarded and returns a message error. Otherwise, the data is computed and the code follows verifying the data bloc length. Now, if an error is found, only the wrong bloc is discarded and is rebuilt by the arithmetic mean between the anterior and posterior bloc. This approach is just efficient when few bytes are lost. If two successive blocs show error the array copy is halted.

The treated array contains alternated data types, being divided in other two arrays, a first containing just EMG data and a second with all accelerometer measuring. The first array has data from alternated EMG sensors and a new division for other two arrays is done separating even and odd elements. The sampling position related to the marked byte ('X'

axis) identifies the sensor origin. Each byte was normalized and extracted the offset to recover data before plotting. The multiplication by 3 was done to match to the amplitude reference from EMG module.

- ByteToPlot[index] = 3 × (Byte[index] - 127) / 256;

The second array alternates the LSB and the MSB from all axes of the accelerometers. The accelerometer source alternates for each six bytes. Again the array is divided in other two arrays in accordance with the assigned bit in the marked byte. The information is recovered binding the LSB to the next MSB. The three LSbs are ignored and the LSB is shifted the corresponding positions to the right. The MSB is shifted five positions to the left and finally the MSB and LSB are bound to form the number of counts measured. The division for 1.333 (multiplying by 0.75) returns the value of acceleration in gravity to be plotted in the chart.

- Value = ((LSB >> 3) or (MSB << 5)) × 0.75;

5. TESTS AND VALIDATIONS

This section presents the results obtained to validate the conceived system. The validation is done by comparing results to an expected waveform. Some tests done to verify the right mounting and the fine hardware working flow are also presented. Preliminary tests were made in order to reproduce the conditions of the real EMG signal.

5.1. MODULE BLUETOOTH - MCU COMMUNICATION

The communication was established over SPP through serial port COMM4 on PC. All the devices and the COMPort were set to operate on 9600 kbps and the SPP settings was none parity bit, 1 stop bit.

Three different terminals were used to read incoming data from serial port: Realterm, Indigo and Teraterm. All of them are similar and they are free for download on the web. On the test, a string of characters was sent from the MCU to the Bluetooth module, and then sent to the PC. A single circuit was implemented on a protoboard comprising the Bluetooth module and the MCU programmed with a 'Hello World' firmware. The three terminals displayed the sent string correctly.

The correct reception within the hardware module was tested altering the firmware to send a string after receiving a command from the computer. The command was given by a specific character with the sending occurring after the character is recognized at the MCU. In this situation the string was also displayed correctly and the orders were obeyed as expected. This test also worked to verify the link between module and PC.

5.2. SAMPLING TEST

Two signal generators and a scope were used to test the sampling process. The objective was to sample a known waveform to be recovered in the reception. A new code was loaded to the MCU keeping the serial communications configurations and adding the ADC

settings. The MCU was configured to use the internal voltage reference (FRV) with positive reference at 1.024 V and negative reference at 0 V. The used sampling rate was about 15 kHz (1 M/64). Two input channels were enabled and the code alternates the sampling of the two inputs.

Both signal generators delivered a signal with a frequency of 100 Hz and 0.6 Vpp of amplitude. The voltage value below 1 V avoids the saturation on the receiver. Also it was necessary to introduce a 0.5 V of DC offset. One generator delivered a sinusoidal signal to one input and the other generator delivered a triangular signal to the second input. The MCU input was isolated using a buffered stage with OPAMP LM324N.

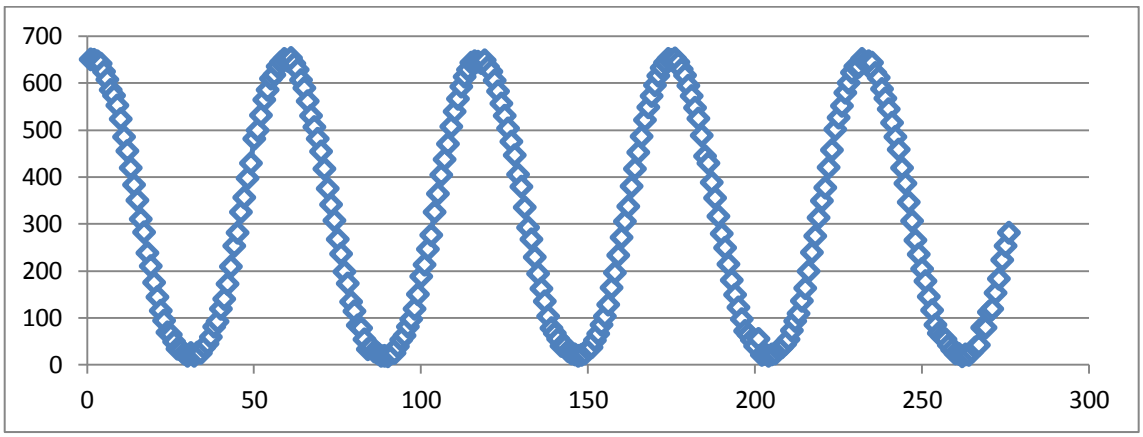

Figure 35 – Sinusoidal signal with frequency of 100 Hz recovered.

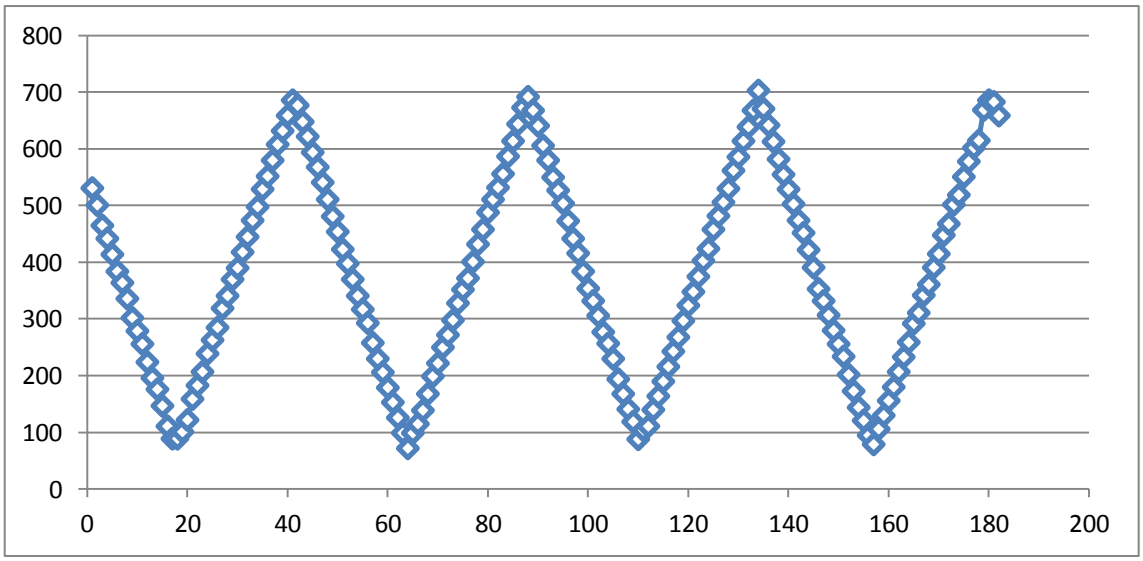

Figure 36 – Triangular signal with frequency 100 Hz recovered.

The captured samples were left justified to ignore the two LSb on the sending. The sampled signals were received in a terminal and stored in a log file. The Office Excel was used to open the file and trace the chart. The sequence was separated in other two by even and odd ordering. Figure 35 and Figure 36 are the obtained waveforms. Both were compared to the waveform seen at the scope and had similar shape, validating the sampling process. The amplitudes presented the expected value for non-normalized voltages and the horizontal axis returns the number of samples index.

The frequency was increased tenfold to test the recovering capability with less sampling. Figure 37 and Figure 38 are the recovered sinusoidal and triangular waveforms respectively. Again it was possible to separate the two signals maintaining their characteristic but with an, expectable, loss of resolution.

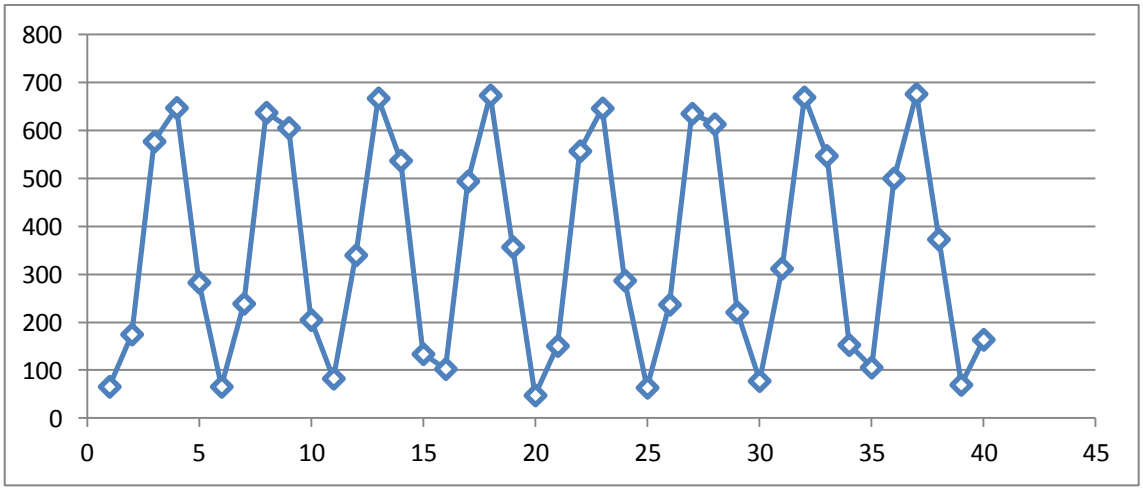

Figure 37 - Sinusoidal signal with frequency of 1 kHz recovered.

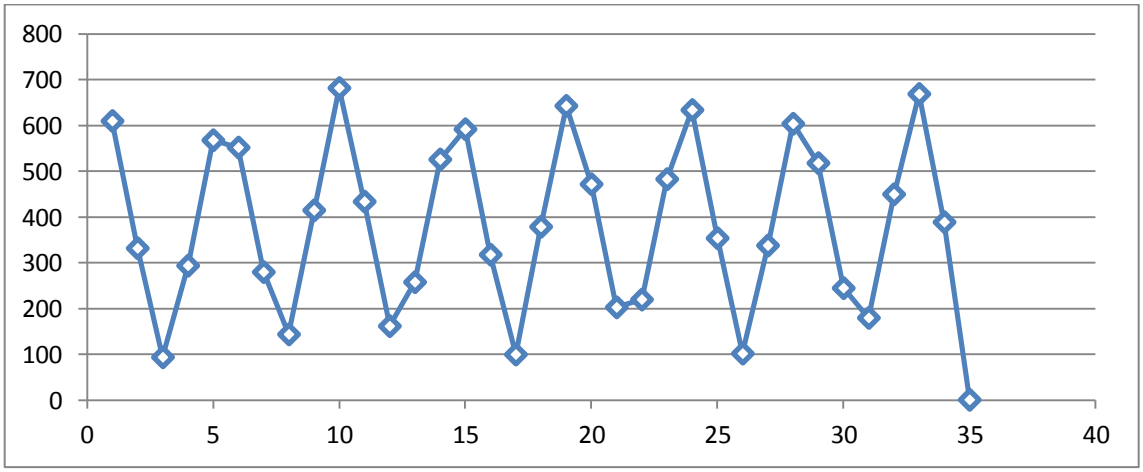

Figure 38 - Triangular signal with frequency of 1 kHz recovered.

5.3. ACCELEROMETER – MCU SPI COMMUNICATION

The firmware was altered to send the SPI data instead of the ADC sampling. The peripheral was programmed to use two slaves alternately. The frequency used was (FOSC = 1M) / 4. A scope was used to verify the clock waveform delivered to the slaves. The scope was also used to verify the SS switching. In these tests the clock presented the expected waveform and frequency and both SS behaved as desired, switching between the low and high level alternating the two SS outputs.

The MatLab was used to receive and treat the data from the accelerometer. A *.m file was prepared to communicate through the serial port and reorder the bytes sequence to present the sampled acceleration value on the screen. As just one accelerometer was available, only one channel a time was tested. In this regard, it was expected reading values '0' for the isolated sensor input. For the axis in vertical position it was expected a value of about 1333 counts. The opposite value was expected varying the axis position by 180°.

Table 17 – Acceleration value measured for each axis in the vertical position.

	Sensor 1			Sensor 2		
Position	**X**	**Y**	**Z**	**X**	**Y**	**Z**
X - 0°	-1307	-1	-21	0	0	0
X - 180°	1345	66	60	0	0	0
Y - 0°	38	-1179	583	0	0	0
Y - 180°	-31	1372	-37	0	0	0
Z - 0°	15	129	1364	0	0	0
Z - 180°	-17	64	-1306	0	0	0
X - 0°	0	0	0	-1311	-3	-26
X - 180°	0	0	0	1348	59	42
Y - 0°	0	0	0	34	-1281	168
Y - 180°	0	0	0	-7	1363	-19
Z - 0°	0		0	7	121	1366
Z - 180°	0	0	0	-15	84	-1300

Table 17 is composed by the first obtained values on a set of 64 samples. As the samples were obtained in hold position, all 64 values are closed. The axis tested was on vertical

position, in order to be parallel to the gravity acceleration vector. The color orange highlights the varied axis and the gray indicates the inactive sensor. The obtained values are inside the expected values, showing that sensors and the microcontroller output operate properly.

5.4. TEST TO THE FINAL SYSTEM

The system was programmed to run with final configuration values for all peripherals, with the purpose of performing a last test before coupling the EMG sensor. The intention is verifying the joint operation and the fidelity on recovering a waveform in the presence of the AFE module. A function generator delivers a known waveform in the minimal allowed voltage (0.1 Vpp). A sinusoidal wave with 1 kHz frequency was applied. The signal passes through a voltage divider to reduce the input voltage to about 1/10 the maximum range to avoid saturation. Here the amplification stage was also tested.

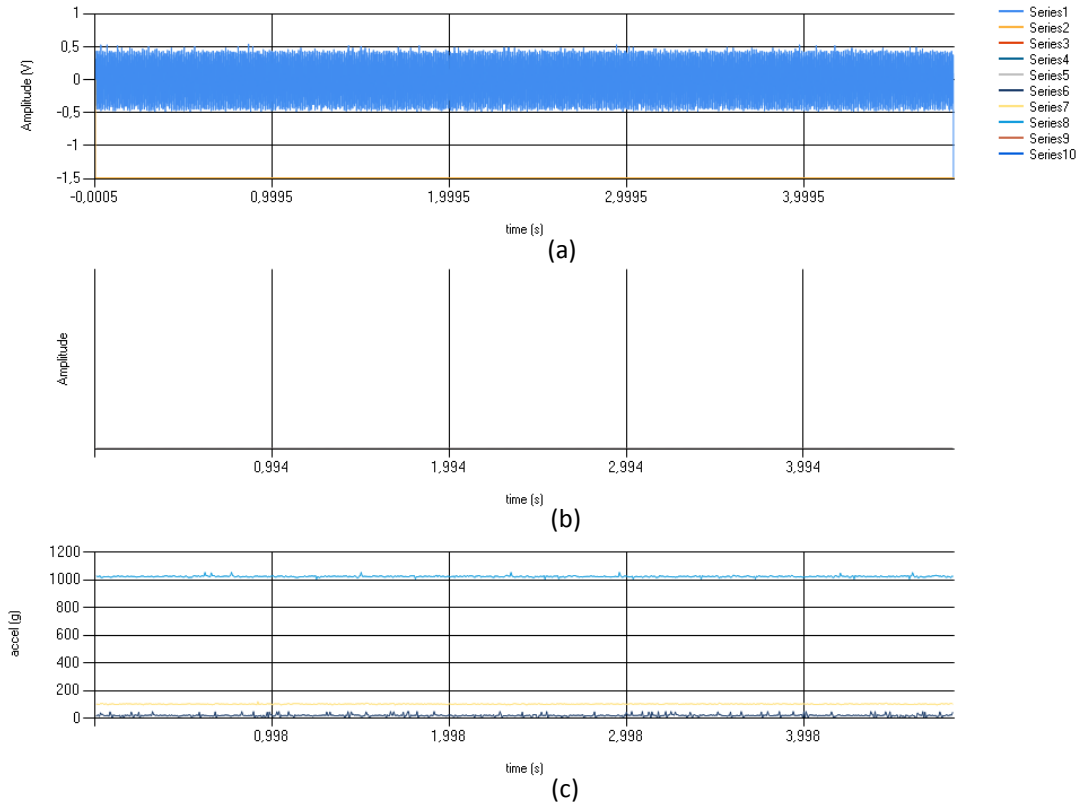

Figure 39 – The waveform obtained from the test to the complete system, displayed on the developed GUI: (a) shows the sinusoidal wave from signal generator; (b) is an unused input meant to the accelerometer data; (c) shows a 2nd input with three axes accelerometer data.

The waveform was displayed in the application developed for user interface. Just one signal was captured with the system because only one AFE module was available. The other analog input was connected to the ground. The same procedure was adopted previewing the insertion of a second accelerometer allowing the code to run for two analog inputs and for two SPI inputs without changes.

Figure 39 shows the obtained result from the test. The first trace is the recovered sinusoidal wave. This signal is expanded in Figure 40 to highlight the waveform, in which the sinusoidal waveform becomes evident. The second chart does not present a visible trace because it was meant to a second accelerometer. The third chart presents three traces equivalents to the X, Y and Z axes. This test was performed in static position justifying the obtained values. The waves were separated and recovered adequately, inside the expected values and shape, proving the code effectiveness.

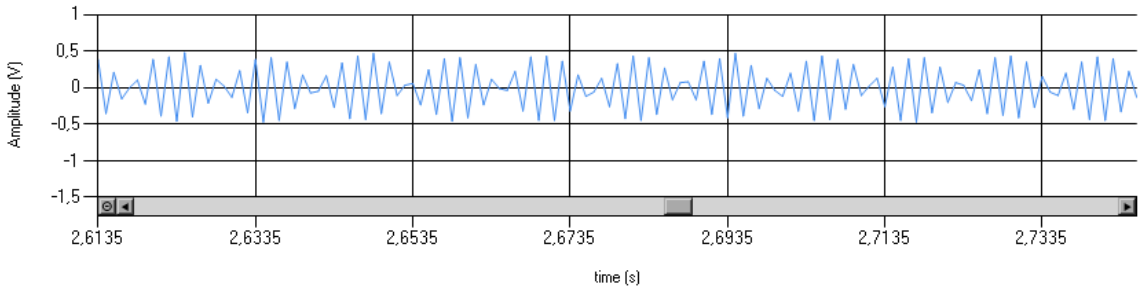

Figure 40 – Sinusoidal recovered signal expanded.

5.5. FUNCTIONAL TESTING

The scope was replaced by three electrodes to realize ultimate test. The muscle Biceps Brachii was chosen to perform the test due to its easy accessibility, thin fat layer and low presence of bristles. The reference electrode was placed on the olecranon and the two polar electrodes were placed on the medial third of the anterior face of the muscle, at 5 cm of distance from one to the other. Cables were used to connect the electrodes directly to the AFE module, which had its gain adjusted to the minimum possible.

The circuit on a protoboard limits the test in the stand situation. The gain of the AFE module was adjusted increasing up to find the limit of the wave saturation. Figure 41 shows the waveform obtained for some isometric contractions. The first trace is the raw

EMG signal, the second trace is the signal treated with a RMS time window of 50 ms and the third trace is the measured acceleration for each axis.

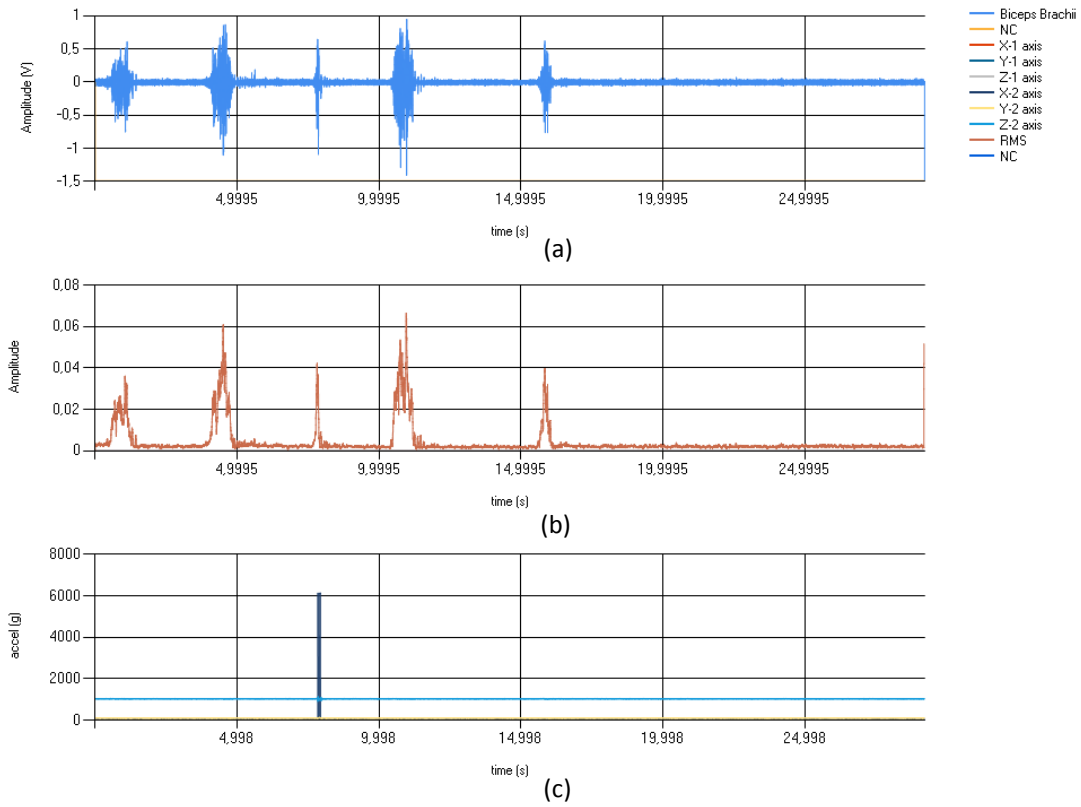

Figure 41 – EMG signal and acceleration shown in the GUI: (a) shows a raw EMG in some isometric contractions performance; (b) shows the EMG smoothened with a 50 s RMS time window; (c) shows the three axes acceleration data.

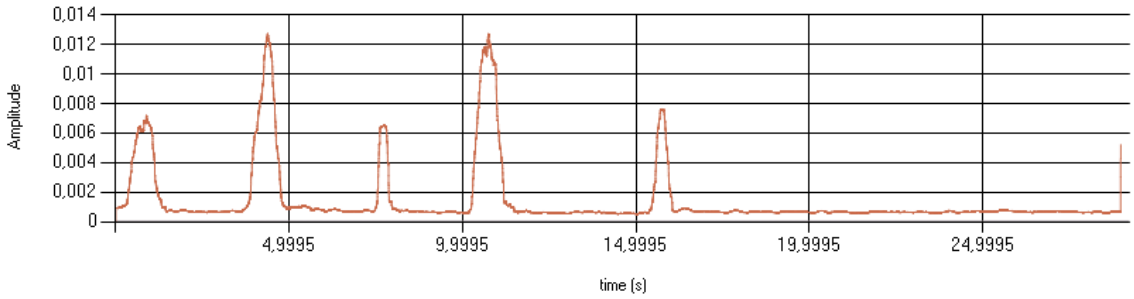

Figure 42 – EMG outline for 500 s RMS time window.

The RMS waveform is repeated in the Figure 42, but with a time window of 500 ms, showing better resolution and smoother form. The graphic is expanded in the Figure 43 for one contraction peak, increasing the resolution and highlight the higher frequency components from the wave.

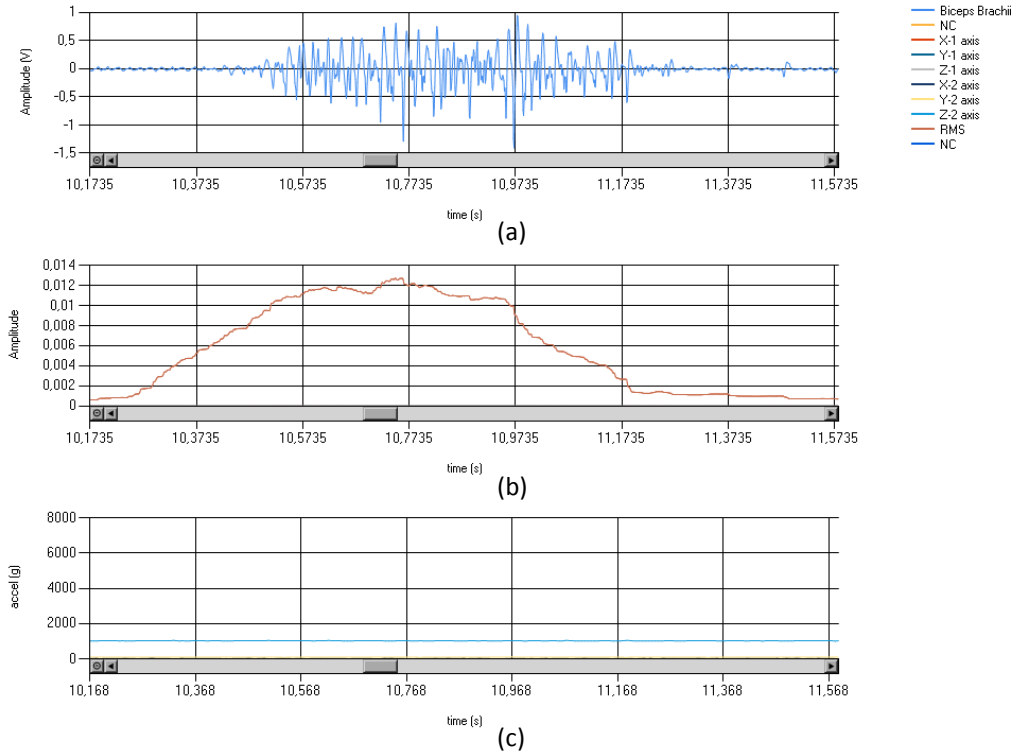

Figure 43 – Signal expanded on the time scale: (a) is a raw EMG contraction; (b) shows the contraction smoothened; (c) shows the acceleration data.

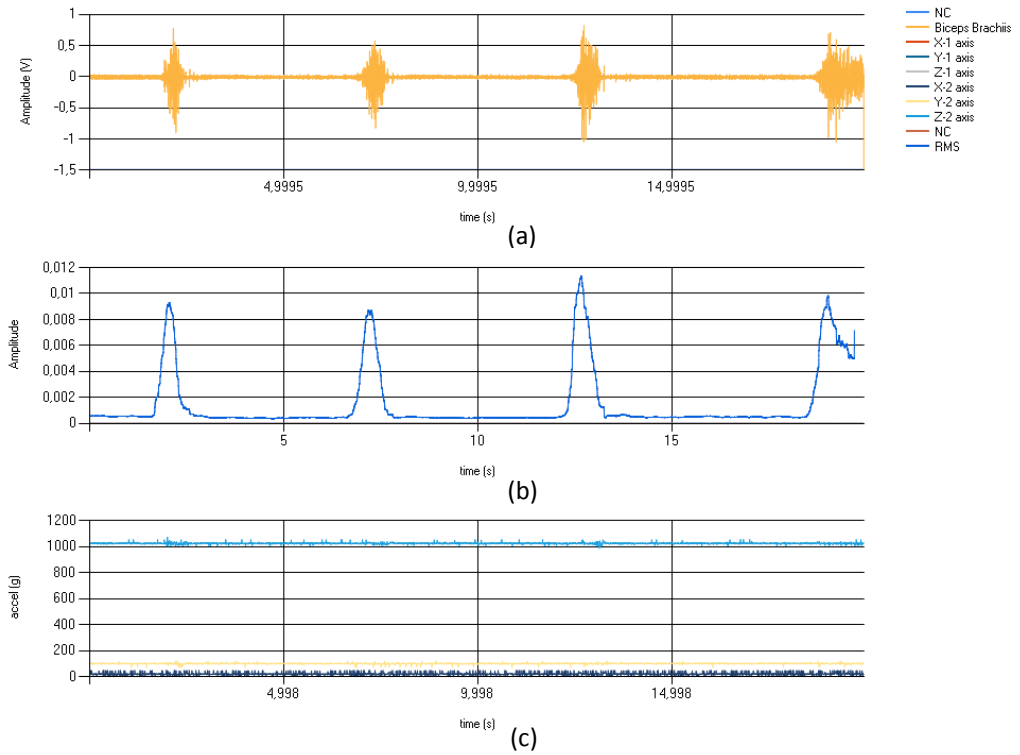

Figure 44 – EMG signal at the second channel and the acceleration chart: (a) shows a raw EMG in some isometric contraction; (b) shows the EMG smoothened with a 500 s RMS time window; (c) shows the three axes acceleration data.

The test was repeated for the second channel as shown in the Figure 44 and returns similar waveform. The difference here is that it was applied a time window of 500 ms for the RMS. Figure 45 shows the signal expanded on the time axis highlighting the higher frequency components.

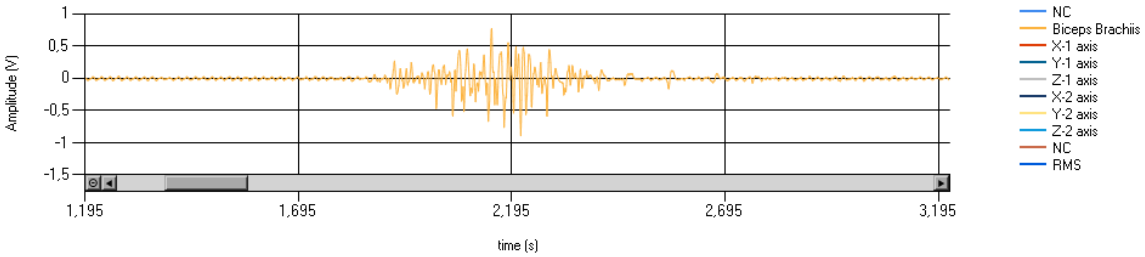

Figure 45 – Time expanded EMG signal for the second channel.

The tests were realized with a gain of about 200. This gain was measured connecting the signal generator with a known input voltage and comparing with the read voltage in the scope.

The obtained waveform is the result expected from the system in its full performance. Figure 46 is a waveform obtained from a similar system and the comparison with the results serves to the validation. The system has presented the expected behavior and returns the desired waveform for EMG. The acceleration also has presented the expected value for the static situation.

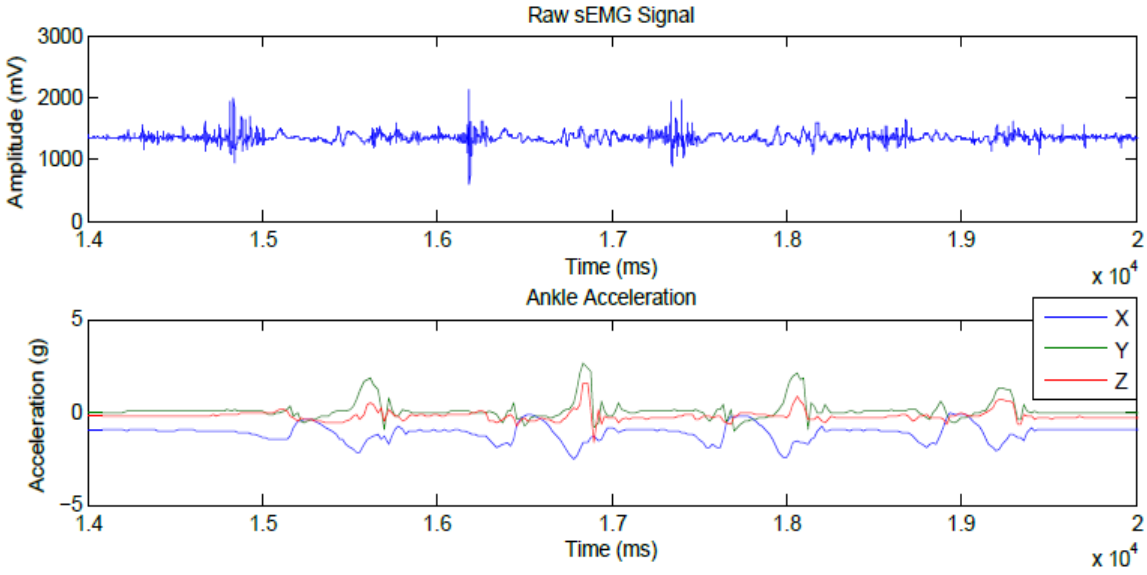

Figure 46 – EMG waveform and acceleration obtained from a similar system. [36]

5.6. EVALUATION OF THE POWER CONSUMPTION

Some tests were made to evaluate the power consumption of the system and the impact of each component in its performance. The traditional method uses the voltage and current values to calculate the power. The use of an amperimeter is not a suitable method when the current shows a transient behavior. An alternative solution is to use the scope to measure the RMS voltage value over a known series resistor and use these values to calculate the RMS current value. The transient behavior is due to the code execution and continuous alternation between the sleep and awaken states. Figure 47 is an example of the voltage captured waveform. Here it was measured the full system consumption when in Idle, it means, the system wait for an order to follow running in full performance.

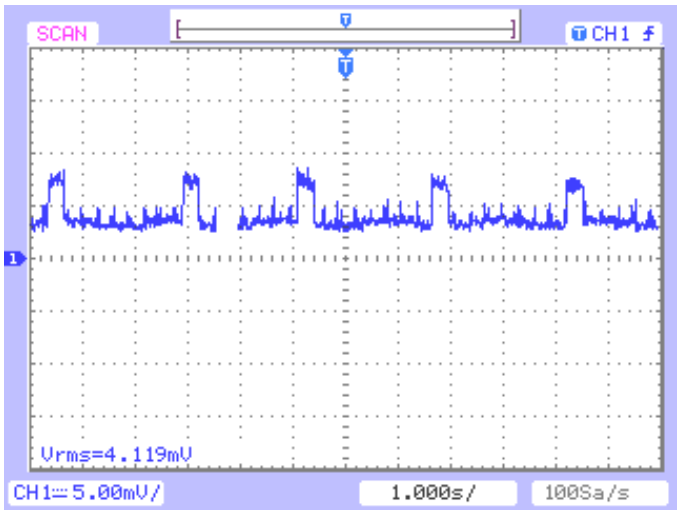

Figure 47 – Waveform of the power supply voltage obtained from a digital scope.

The first procedure was to read the voltage with a multimeter in the voltage regulator output. A 1.2 Ω resistor was introduced in series with the regulator output. The V_{RMS} was read over this resistor during a time window of 1 s. The division of V_{RMS} with resistor value returns the desired current value that was used with the voltage to calculate the power. The procedure is repeated individually to all active elements of the circuit, getting the voltage and opening the circuit at the respective V_{in} to put the resistor in series. The values read in the idle situation are presented in Table 18. The test was repeated in the run situation, generating the values shown in Table 19.

Table 18 – System power consumption at idle and contribution from each component.

Idle	V	Vrms(mV)	I (mA)=Vrms/R	P = V × I (mW)	%
Full System	3.26	3.93	3.27	10.49	-
MCU	3.25	0.346	0.288	0.937	8.93
Bth Module	3.23	1.77	1.47	4.76	45.37
ACC	3.24	0.348	0.29	0.94	8.96
Analog Module	2.80	0.4	0.375	1.10	10.48
Ckt test	3	0.28	0.233	0.7	6.67
				Σ = 8.437	Ɛ% = - 19.59

Table 19 - System power consumption at run mode and contribution from each component.

On the fly	V	Vrms(mV)	I (mA)=Vrms/R	P = V × I (mW)	%
Full System	3.2	6.8	5.666	18.13	-
MCU	3.22	0.447	0.372	1.2	6.62
Bth Module	3.12	4.7	3.916	12.22	67.40
ACC	3.25	0.4	0.333	1.083	5.97
Analog Module	3.24	0.4	0.333	1.08	5.95
Ckt test	3.25	0.282	0.235	0.763	4.21
				Σ = 16.346	Ɛ% = - 5.64

The individual power values were summed to compare with the value measured for the full system. The sums are seen in the pink cells in both tables. Some difference is expected because the read is done under certain inaccuracy and the passive components influence was not regarded. The coherence is met because the summed values are nearly below to the measured value. Also it was calculated the percentage of contribution of each component to the total consumption. The cells shadowed by green in the tables present the difference between the calculated value and the 100 %. As it was expected the total percentage value was below the 100 % in both situations.

The Bluetooth module was responsible for the higher consumption in two the situations evaluated. It was responsible for almost half of the power demanded with the circuit in idle and reaching 67 % in the full performance. The values in the two tables show also significant difference of consumptions between the two situations. Other devices have

little or none difference, even the MCU that enters in a low power state during idle situation. The Bluetooth module also is responsible for signal pattern seen in the Figure 47 like the great contributor and whose presents great oscillation.

The read power values were compared with the expected values provided by manufactures: For the Bluetooth module the values obtained in the two situations were considerably lower than the expected ones in an order of 10 × (Table 11), being close to the values to the power saving modes. The value measured for the accelerometer's current is of the same order of magnitude of the expected value (Table 7) but lower. The MCU documentation presents the electrical characteristic for each specific configuration [27]. For the system conditions (RC mode, 16 MHz, 3 V) the typical current ranges between 3.9 mA and 4.6 mA in run mode, and between 1.65 mA and 2.05 mA in idle mode.

6. CONCLUSIONS

This work aimed at developing a system to analyze disorders associated to the human gait. The analyses are done inspecting the kinetic data and the EMG signals. Autonomous systems became a response for the need to replace cables in modern approaches and the power constraint is a question to be observed.

The developed work comprised the design of the hardware, the firmware deployment and the development of a graphic user interface. The system was conceived taking into account power constraints, using solutions available in the market in order to minimizing the power demand. To achieve the minimal power consumption the development strategy sought the minimal solutions for the hardware and minimal code processing, regarding topologies, architecture and protocols. For the core of the system the PIC18F14K22, which pertains to the midrange Microchip family, meant to systems that requires some versatility in applications with power constraints, was used. Sensors were linked using a star topology, which primes for the simplicity and low power in place to the trust. The inertial sensor SCA3000 is also meant for low power applications. Bluetooth is the protocol that presents the best consumption characteristics inside the target baud rate, being the RN41 used to establish the link between the capturing module of and the PC.

The total consumption obtained was lower than the sum of the nominal values. The Bluetooth module was the major power consumer, being responsible by more than half of the power consumed. The Bluetooth module has its own microprocessor to run a relatively hard task, characteristic of the specifications of the protocol, which contributes to its high power demand. Important resources to the power saving could not be used, although appealing, because the demanded high rate of the system: the Sniff mode and the Deep Sleep mode. Regarding the percentage reducing with the nominal electrical specifications like reference, the usage of these modes could represent less than half of the power consumed (~ 55 %) in the two system situations (idle and running). One

possible approach that would turn possible the using of these modes without losing information would be working with large block of information, storing the data before sending. The inclusion of a module of memory can be advantageous regarding that the increased power demand would be considerable inferior than the power decreased by using of the power safe modes. For example, the SRAM memory 23LC1024 from Microchip [37] has capability to 1024 Kbits, which represents one minute of sampling (Annex A - digital). It is meant for low power applications, presenting the nominal consume of 4 µA at standby and 3 mA at the read operation, which is inferior to the values in the Table 11.

The inclusion of an external memory would imply a modification on the code including routines to control the R/W processes. In this regard two approaches can be adopted: the first is storing all data before sending and the second is sending the data continuously in place of performing the sleep instruction in the main. This would jeopardize the availability of the number of channels. If reaching the number of 16 channels becomes mandatory, the alternative is choosing for another MCU. For example, the PIC24F16KA304 has similar features than the used devices with increased number of channels and peripherals, reaching the pin count of 44 [38]. Futures studies could use these hardware modifications and compares to the actual system to evaluate the impact on the performance and consumption.

The configuration adopted has the capability of meeting the system requirements. For two ADC channels it is possible to achieve twenty four samples, requiring 0.0476 ms of sampling period. Over this number of samples, the minimal time value for transmission calculated in Table A. 8 from Annex A is exceeded. If all 12 ADC channels available on the µC were used, the maximum number of samples got is four. As calculated in Table A. 9 from Annex A, this represents a sampling period of 0.0416 ms or, in other words, a sampling frequency of 24 KHz that, summed with accelerometers data, occupies 48 KHz of the transmission band. These limits situations are just feasible with the oscillator at 32 MHz at least.

The transmission over Bluetooth is the great bottleneck of the system. The usage of SPP limits the transmission to the baud rate of 115200 kbps. This limit was not determined by

the serial protocol but by the device drive of the computer peripheral, when was attributed a COM port. An alternative to increase the transmission rate is using another Bluetooth profile, passing over the COM port. The programming, however, would turn harder when using Bluetooth Application Programming Interface (API) [39] or Windows sockets [40], both solutions from Microsoft, or alternatively the free library 32feet.NET [41]. The system was also limited by the number of data transferred that limits the sampling rate, probably by a limitation of the buffer length allowed by device drive, but this hypothesis depends on more test to be confirmed.

To develop this works new concepts and techniques were learned, especially at the programming field, dealing with different languages. The time spent in the learning curve was extended due to the lack of full time dedication impairs reaching the target deadline. The tests were not directly applied to the target test by limitation of mounting in a protoboard instead in a PBC. During programming was necessary to be alert for some details not documented. The V_{DD} reference of the ADC set using the default library does not work, being necessary to impose the desired value. Inspecting the library 'adc.h' the value does not correspond to the expected value, but in the last version of MPLab this library was discontinued.

The results obtained by tests showed that the developed system executes its function adequately, reproducing the EMG waveform as expected. Two EMG channels and other two channels from accelerometers were multiplexed and the data from each one were separated and recovered correctly on the destination. More channels could be inserted and the both codes of the firmware and of the software were implemented foreseeing the inclusion of a third accelerometer. The code and handshake structures would be maintained adding more channels, with due observation to the bandwidth capacity and the limits of the frequency. The conceived system gathers important concepts and methods to achieve the maximum power safe. The methods used along the work can be applied to the other system with power constraints for improvement.

Bibliography

[1] D. Jennings, A. Flint, B. C. H. Turton and L. D. M. Nokes, Introduction to Medical Eletronics Aplications, London: Edward Arnold, 1995.

[2] M. Pozzo, "Electromyography (EMG), electrodes and equipments for," *Encyclopedia of Biomedical Engineering,* vol. 6, pp. 1386-1397, 2006.

[3] C. Frigo and P. Crenna, "Multichannel SEMG in clinical gait analysis: A review and state-of-the-art," *Clinical Biomechanics,* no. 24, pp. 236 - 245, 2009.

[4] M. Kutz, Standard handbook of biomedical engineering and design, New York: McGraw-Hill, 2003.

[5] E. Jovanov, A. Milenkovic, C. Otto and P. C. de Groen, "A wireless body area network of intelligent motion sensors for computer assisted physical rehabilitation," *Journal of NeuroEngineering and Rehabilitation,* vol. 2, no. 6, pp. 1-10, 2005.

[6] K. Deshmukh, D. Patel, N. Gupta and S. Kumar, "Efficient Coding Mechanism for Low Power Consumption in Wireless Programmable Devices," *International Journal of Soft Computing and Engineering,* vol. 1, no. 1, pp. 57-61, 2011.

[7] J. Espina, T. Falck and O. Mülhens, "Network Topologies Communication Protocols," in *Body Sensor Networks*, London, Springer, 2006, pp. 145-182.

[8] IEEE 802.15, "IEEE 802.15 Wireless Next Generation Standing Communitee," IEEE, 09 01 2011. [Online]. Available: http://www.ieee802.org/15/pub/TG6.html. [Accessed 14 02 2014].

[9] C. L. Vaughan, B. L. Davis and J. C. O'Connor, Dynamics of human gait, Cape Town: Kiboho, 1999.

[10] J. M. Hausdorff and N. B. Alexander, Gait Disorders, Evaluation and Management, Boca Raton: Taylor & Francis Group, 2005.

[11] M. Meng, Q. She, Y. Gao and Z. Luo, "EMG Signals Based Gait Phases Recognition Using Hidden Markov Models," in *International Conference on Information and Automation*, Harbin, 2010.

[12] P. Wang and H. K. Low, "Qualitative Evaluations of Gait Rehabilitation via EMG Muscle Activation Pattern: Repetition, Symmetry, and Smoothness," in *International Conference on Robotics and Biomimetics*, Guilin, 2009.

[13] C. J. De Luca, "Physiology and Mathematics of Myoelectric Signals," *IEEE Transactions on Biomedical Engineering,* pp. 313-325, June 1979.

[14] P. Konrad, The ABC of EMG: A Practical Introduction to Kinesiological Electromyography, Scottsdale: Noraxon U.S.A. Inc., 2006.

[15] J. Moore and G. Zouridakis, Biomedical technology and devices handbook, Boca Raton: CRC Press LLC, 2004.

[16] M. Akay, Wiley Encyclopedia of Biomedical Engineering, New Jersey: John Wiley & Sons, 2006.

[17] J. D. Bronzino, The Biomedical Engineering HandBook, Second Edition, Boca Raton: CRC Press LLC, 2000.

[18] H. Huang, F. Zhang, Y. L. Sun and H. He, "Design of a robust EMG sensing interface for pattern classification," *Journal of Neural Engineering,* no. 7, 2010.

[19] R. Shiavi, "Quantitative representation of electromyographyc patterns generated during human locomotion," IEEE Engeneering in medicine and biology magazine, 1990.

[20] M. C. Garcia and T. M. Vieira, "Surface electromyography: Why, when and how to use it," *Revista Andaluza de Medicina del Deporte,* vol. 4, no. 1, pp. 17-28, 2011.

[21] J. Espina, T. Falck and O. Mülhens, "Wireless Sensor Development Platforms," in *Body Sensor Network*, London, 2006, pp. 403-493.

[22] S. Sudevalayam and P. Kulkarni, "Energy Harvesting Sensor Nodes: Survey and Implications," *IEEE Communications Surveys & Tutorials,* vol. 13, no. 3, pp. 443-461, 2011.

[23] J.-S. Lee, Y.-W. Su and C.-C. Shen, "A Comparative Study of Wireless Protocols: Bluetooth, UWB, ZigBee, and Wi-Fi," in *The 33rd Annual Conference of the IEEE Industrial Electronics Society (IECON)*, Taipei, 2007.

[24] H. Labiod, H. Afifi and C. De Santis, Wi-Fi, Bluetooth, Zigbee and WiMax.

[25] SIG-Nokia, "Bluetooth Protocol Architecture.pdf," 29 09 1999. [Online]. Available: http://www.bluetooth.org. [Accessed 10 06 2011].

[26] Roving Networks, "DS-RN41-V3.1," 19 February 2010. [Online]. Available: http://www.rovingnetworks.com. [Accessed 22 February 2011].

[27] Microchip Technology Inc., "DS41365D," 01 May 2010. [Online]. Available: http://www.microchip.com. [Accessed 23 March 2011].

[28] VTI technologies Oy, "Doc.Nr. 8257300A.06," 30 Octuber 2007. [Online]. Available: http://www.vti.fi. [Accessed 22 February 2011].

[29] VTI Technologies Oy, "Doc. Nr. 8255700B.01," 08 September 2009. [Online]. Available: http://www.vti.fi. [Accessed 24 March 2011].

[30] Sparkfun, "RN41 - BlueSMiRF," [Online]. Available: https://www.sparkfun.com/products/12582. [Accessed 28 10 2014].

[31] "RN-Bluetooth-um Version 4.77," 02 March 2011. [Online]. Available: http://www.rovingnetworks.com. [Accessed 2011 August 13].

[32] Microchip Technology Inc., "DS51553A," 20 April 2005. [Online]. Available: http://www.microchip.com. [Accessed 22 February 2011].

[33] Texas Instruments Co., "UCC383-5," 2 2004. [Online]. Available: www.ti.com. [Accessed 18 1 2012].

[34] FairChild Semiconductor Corporation, "FAN1581," 11 06 2003. [Online]. Available: www.fairchildsemi.com. [Accessed 16 07 2014].

[35] FairChild Semiconductor Corporation, "LM324A," 19 11 2002. [Online]. Available: www.fairchildsemi.com. [Accessed 21 10 2011].

[36] F. Derogarian, R. Dias, J. C. Ferreira, M. G. V. Tavares and J. M. da Silva, "Using a Wired Body Area Network for Locomotion Data Acquisition," in *Conference on Design of Circuits and Integrated Systems (DCIS)*, Porto, 2014.

[37] Microchip, "23A/LC1024," 01 2015. [Online]. Available: http://ww1.microchip.com/downloads/en/DeviceDoc/20005142C.pdf. [Accessed 06 06 2015].

[38] Microchip, "PIC24F16KA304," 19 03 2013. [Online]. Available: http://ww1.microchip.com/downloads/en/DeviceDoc/39995d.pdf. [Accessed 06 06 2015].

[39] Microsoft, "MSDN," [Online]. Available: https://msdn.microsoft.com/en-us/library/windows/desktop/aa362942%28v=vs.85%29.aspx. [Accessed 06 06 2015].

[40] Microsoft, "MSDN Winsoc," [Online]. Available: https://msdn.microsoft.com/en-us/library/windows/desktop/aa363059%28v=vs.85%29.aspx. [Accessed 06 06 2015].

[41] In The Hand ltd, "32feet," 18 12 2013. [Online]. Available: https://32feet.codeplex.com/. [Accessed 06 06 2015].

[42] S. Katzen, The Essential PIC18® Microcontroller, London: Springer-Verlag, 2010.

[43] D. Ibrahim, Advanced PIC Microcontroller Projects in C: From USB to RTOS with the PIC18F Series, Oxford: Elsevier, 2008.

[44] J. L. Semmlow, Biosignal and Biomedical Image Processing: MatLab-Based Applications, New York: Marcel Dekker, 2004.

[45] J. D. Enderle, S. M. Blanchard and J. D. Bronzino, Introduction to Biomedical Engineering, San Diego: Elsevier Inc., 2005.

[46] B. Gyselinckx, C. V. Hoof, J. Ryckaert, R. F. Yazicioglu, P. Fiorini and V. Leonov, "Human++: Autonomous Wireless Sensors for Body Area Networks," IMEC, Leuven.

[47] K. Bervet, M. Bessette, L. Godet and A. Crétual, "KeR-EGI, a new index of gait quantification based on electromyography," *Journal of Electromyography and Kinesiology,* vol. 23, pp. 930-937, 2013.

[48] G. A. Bekey, C.-W. Chang, J. Perry and M. M. Hoffer, "Pattern Recognition of Multiple EMG Signals

Applied to the Description of Human Gait," *PROCEEDINGS OF THE IEEE,* pp. 674-681, May 1977.

[49] T. D' Alessio and S. Conforto, "Extraction of the Envelope from Surface EMG Signals: Attempting to Solve Estimation Problems with an Adaptive Procedure for Dynamic Protocols," IEEE ENGINEERING IN MEDICINE AND BIOLOGY, Roma, 2001.

Annex A – Calculations

Annex A has the calculations of the parameters of the system, being presented in a written part and in a digital part, where one can find other calculations. The calculations are presented in ten tables from Microsoft Excel, in which are determined the requirements of the system.

Table A.1 was computed using the equation: Tdata = 10 × Tbit = (1 / f) × 1000

Table A. 1 – Time to send a bit and send a word for each serial baud rate standard.

frequency(Baud)	Tbit(ms)	Tdata(ms)
921600	0,001085069	0,010850694
460800	0,002170139	0,021701389
230400	0,004340278	0,043402778
115200	0,008680556	**0,086805556**
57600	0,017361111	0,173611111
38400	0,026041667	0,260416667
19200	0,052083333	0,520833333
9600	0,104166667	1,041666667
4800	0,208333333	2,083333333
2400	0,416666667	4,166666667
1200	0,833333333	8,333333333

Table A.1 legend:

Tdata < Tsmp

Table A. 2 – Time to send data through USART

Tsending (ms) = Tdata + 1Tcy	Fosc/4 = Fcy(kHz)									
frequency(Baud)	**16000***	**8000***	**4000**	**2000**	**1000**	**500**	**250**	**125**	**62,5**	**7,75**
921600	**0,0109132**	**0,0109757**	**0,0111007**	**0,011351**	**0,011851**	**0,012851**	**0,014851**	**0,018851**	**0,026851**	**0,139883**
460800	**0,0217639**	**0,0218264**	**0,0219514**	**0,022201**	**0,022701**	**0,023701**	**0,025701**	**0,029701**	**0,037701**	**0,150734**
230400	**0,0434653**	**0,0435278**	**0,0436528**	**0,043903**	**0,044403**	**0,045403**	**0,047403**	**0,051403**	**0,059403**	**0,172435**
115200	**0,0868681**	**0,0869306**	**0,0870556**	**0,087306**	**0,087806**	**0,088806**	**0,090806**	**0,094806**	**0,102806**	**0,215838**
57600	**0,1736736**	**0,1737361**	**0,1738611**	**0,174111**	**0,174611**	**0,175611**	**0,177611**	**0,181611**	**0,189611**	**0,302643**
38400	**0,2604792**	**0,2605417**	**0,2606667**	**0,260917**	**0,261417**	**0,262417**	**0,264417**	**0,268417**	**0,276417**	**0,389449**
19200	0,5208958	0,5209583	0,5210833	0,521333	0,521833	0,522833	0,524833	0,528833	0,536833	0,649866
9600	1,0417292	1,0417917	1,0419167	1,042167	1,042667	1,043667	1,045667	1,049667	1,057667	1,170699
4800	2,0833958	2,0834583	2,0835833	2,083833	2,084333	2,085333	2,087333	2,091333	2,099333	2,212366
2400	4,1667292	4,1667917	4,1669167	4,167167	4,167667	4,168667	4,170667	4,174667	4,182667	4,295699
1200	8,3333958	8,3334583	8,3335833	8,333833	8,334333	8,335333	8,337333	8,341333	8,349333	8,462366

Table A.2 legend:

< 0,5 ms	< 0,0833 ms	< 0,033 ms
< 0,25 ms	< 0,0625 ms	**Satisfy to Tsmp > Tspi = 0,016**
< 0,125 ms	< 0,05 ms	**Satisfy to Tsmp > Tspi = 0,032**

Table A. 3 – Value for n to determine the frequency of EUSART and associated error when [SYNC:BRG16:BRGH] = [0:0:0].

n for [SYNC:BRG16:BRGH] = [0:0:0]	Fosc(KHz)									
frequency(Baud)	64000	32000	16000	8000	4000	2000	1000	500	250	31
921600	0,085069	-0,45747	-0,72873	-0,86437	-0,93218	-0,96609	-0,98305	-0,99152	-0,99576	-0,99947
460800	1,170139	0,085069	-0,45747	-0,72873	-0,86437	-0,93218	-0,96609	-0,98305	-0,99152	-0,99895
230400	3,340278	1,170139	0,085069	-0,45747	-0,72873	-0,86437	-0,93218	-0,96609	-0,98305	-0,9979
115200	7,680556	3,340278	1,170139	0,085069	-0,45747	-0,72873	-0,86437	-0,93218	-0,96609	-0,9958
57600	16,36111	7,680556	3,340278	1,170139	0,085069	-0,45747	-0,72873	-0,86437	-0,93218	-0,99159
38400	25,04167	12,02083	5,510417	2,255208	0,627604	-0,1862	-0,5931	-0,79655	-0,89827	-0,98739
19200	51,08333	25,04167	12,02083	5,510417	2,255208	0,627604	-0,1862	-0,5931	-0,79655	-0,97477
9600	103,1667	51,08333	25,04167	12,02083	5,510417	2,255208	0,627604	-0,1862	-0,5931	-0,94954
4800	207,3333	103,1667	51,08333	25,04167	12,02083	5,510417	2,255208	0,627604	-0,1862	-0,89909
2400	415,6667	207,3333	103,1667	51,08333	25,04167	12,02083	5,510417	2,255208	0,627604	-0,79818
1200	832,3333	415,6667	207,3333	103,1667	51,08333	25,04167	12,02083	5,510417	2,255208	-0,59635
921600	8,506944	-45,7465	#DIV/0!	#DIV/0!	#DIV/0!	#DIV/0!	#DIV/0!	#DIV/0!	#DIV/0!	#DIV/0!
460800	8,506944	8,506944	-45,7465	#DIV/0!	#DIV/0!	#DIV/0!	#DIV/0!	#DIV/0!	#DIV/0!	#DIV/0!
230400	8,506944	8,506944	8,506944	-45,7465	#DIV/0!	#DIV/0!	#DIV/0!	#DIV/0!	#DIV/0!	#DIV/0!
115200	-3,54938	8,506944	8,506944	8,506944	-45,7465	#DIV/0!	#DIV/0!	#DIV/0!	#DIV/0!	#DIV/0!
57600	2,124183	-3,54938	8,506944	8,506944	8,506944	-45,7465	#DIV/0!	#DIV/0!	#DIV/0!	#DIV/0!
38400	0,160256	0,160256	-6,99405	8,506944	-18,6198	-18,6198	#DIV/0!	#DIV/0!	#DIV/0!	#DIV/0!
19200	0,160256	0,160256	0,160256	-6,99405	8,506944	-18,6198	-18,6198	#DIV/0!	#DIV/0!	#DIV/0!
9600	0,160256	0,160256	0,160256	0,160256	-6,99405	8,506944	-18,6198	-18,6198	#DIV/0!	#DIV/0!
4800	0,160256	0,160256	0,160256	0,160256	0,160256	-6,99405	8,506944	-18,6198	-18,6198	#DIV/0!
2400	-0,07994	0,160256	0,160256	0,160256	0,160256	0,160256	-6,99405	8,506944	-18,6198	#DIV/0!
1200	0,040016	-0,07994	0,160256	0,160256	0,160256	0,160256	0,160256	-6,99405	8,506944	#DIV/0!

Table A. 4 - Value for n to determine the frequency of EUSART and associated error when [SYNC:BRG16:BRGH] = [0:0:1] or [0:1:0].

n for [SYNC:BRG16:BRGH] = [0:0:1] or [0:1:0]	Fosc(kHz)									
frequency(Baud)	64000	32000	16000	8000	4000	2000	1000	500	250	31
921600	3,340278	1,170139	0,085069	-0,45747	-0,72873	-0,86437	-0,93218	-0,96609	-0,98305	-0,9979
460800	7,680556	3,340278	1,170139	0,085069	-0,45747	-0,72873	-0,86437	-0,93218	-0,96609	-0,9958
230400	16,36111	7,680556	3,340278	1,170139	0,085069	-0,45747	-0,72873	-0,86437	-0,93218	-0,99159
115200	33,72222	16,36111	7,680556	3,340278	1,170139	0,085069	-0,45747	-0,72873	-0,86437	-0,98318
57600	68,44444	33,72222	16,36111	7,680556	3,340278	1,170139	0,085069	-0,45747	-0,72873	-0,96636
38400	103,1667	51,08333	25,04167	12,02083	5,510417	2,255208	0,627604	-0,1862	-0,5931	-0,94954
19200	207,3333	103,1667	51,08333	25,04167	12,02083	5,510417	2,255208	0,627604	-0,1862	-0,89909
9600	415,6667	207,3333	103,1667	51,08333	25,04167	12,02083	5,510417	2,255208	0,627604	-0,79818
4800	832,3333	415,6667	207,3333	103,1667	51,08333	25,04167	12,02083	5,510417	2,255208	-0,59635
2400	1665,667	832,3333	415,6667	207,3333	103,1667	51,08333	25,04167	12,02083	5,510417	-0,19271
1200	3332,333	1665,667	832,3333	415,6667	207,3333	103,1667	51,08333	25,04167	12,02083	0,614583
921600	8,506944	8,506944	8,506944	-45,7465	#DIV/0!	#DIV/0!	#DIV/0!	#DIV/0!	#DIV/0!	#DIV/0!
460800	-3,54938	8,506944	8,506944	8,506944	-45,7465	#DIV/0!	#DIV/0!	#DIV/0!	#DIV/0!	#DIV/0!
230400	2,124183	-3,54938	8,506944	8,506944	8,506944	-45,7465	#DIV/0!	#DIV/0!	#DIV/0!	#DIV/0!
115200	-0,79365	2,124183	-3,54938	8,506944	8,506944	8,506944	-45,7465	#DIV/0!	#DIV/0!	#DIV/0!
57600	0,644122	-0,79365	2,124183	-3,54938	8,506944	8,506944	8,506944	-45,7465	#DIV/0!	#DIV/0!
38400	0,160256	0,160256	0,160256	0,160256	-6,99405	8,506944	-18,6198	-18,6198	#DIV/0!	#DIV/0!
19200	0,160256	0,160256	0,160256	0,160256	0,160256	-6,99405	8,506944	-18,6198	-18,6198	#DIV/0!
9600	-0,07994	0,160256	0,160256	0,160256	0,160256	0,160256	-6,99405	8,506944	-18,6198	#DIV/0!
4800	0,040016	-0,07994	0,160256	0,160256	0,160256	0,160256	0,160256	-6,99405	8,506944	#DIV/0!
2400	-0,02	0,040016	-0,07994	0,160256	0,160256	0,160256	0,160256	0,160256	-6,99405	-19,2708
1200	0,010001	-0,02	0,040016	-0,07994	0,160256	0,160256	0,160256	0,160256	0,160256	-19,2708

Table A.3 and A.4 legend:

Values out of range

Table A. 5 – Time to R/W in function of the SPI scale.

Scale	oscillator frequency - FOSC (KHz)									
	64000	32000	16000	8000	4000	2000	1000	500	250	31
64	1000	500	250	125	62,5	31,25	15,625	7,8125	3,90625	0,484375
16	4000	2000	1000	500	250	125	62,5	31,25	15,625	1,9375
4	16000	8000	4000	2000	1000	500	250	125	62,5	7,75
	period - Tb(ms)									
64	0,001	0,002	0,004	0,008	0,016	0,032	0,064	0,128	0,256	2,064516
16	0,00025	0,0005	0,001	0,002	0,004	0,008	0,016	0,032	0,064	0,516129
4	0,0000625	0,000125	0,00025	0,0005	0,001	0,002	0,004	0,008	0,016	0,129032
	Period to R/W - Tspi (ms) = Tb x 16 bits									
64	0,016	**0,032**	0,064	0,128	0,256	0,512	1,024	2,048	4,096	33,03226
16	0,004	0,008	**0,016**	0,032	0,064	0,128	0,256	0,512	1,024	8,258065
4	0,001	0,002	0,004	0,008	0,016	0,032	0,064	0,128	0,256	2,064516

Table A.5 legend:

Exceeds the Tsmp (< 0,5 ms)

Exceeds the Tmin

Fmax (kHz)	Tmin (ms)
1600	0,000625

Table A. 6 – Time to one bit AD conversion.

FOSC (kHz)	64000	32000	16000	8000	4000	2000	1000	500	250	31
scale ADCON2 register	TAD (ms)									
2	0,00003125	0,0000625	0,000125	0,00025	0,0005	0,001	0,002	0,004	0,008	0,064516
4	0,0000625	0,000125	0,00025	0,0005	0,001	0,002	0,004	0,008	0,016	0,129032
8	0,000125	0,00025	0,0005	0,001	0,002	0,004	0,008	0,016	0,032	0,258065
16	0,00025	0,0005	0,001	0,002	0,004	0,008	0,016	0,032	0,064	0,516129
32	0,0005	0,001	0,002	0,004	0,008	0,016	0,032	0,064	0,128	1,032258
64	0,001	0,002	0,004	0,008	0,016	0,032	0,064	0,128	0,256	2,064516

Table A.6 legend:

Recommended values
Limit values
Not feasible

Table A. 7 – Total time to ADC process for each acquisition time waiting.

Tadc (ms)	64000	32000	16000	8000	4000	2000	1000	500	250	31
scale ADCON2 register	Tacq = 4 Tad									
2	0,00053125	0,0010625	0,002125	0,00425	0,0085	0,017	0,034	0,068	0,136	1,096774
4	0,0010625	0,002125	0,00425	0,0085	0,017	0,034	0,068	0,136	0,272	2,193548
8	0,002125	0,00425	0,0085	0,017	0,034	0,068	0,136	0,272	0,544	4,387097
16	0,00425	0,0085	0,017	0,034	0,068	0,136	0,272	0,544	1,088	8,774194
32	0,0085	0,017	0,034	0,068	0,136	0,272	0,544	1,088	2,176	17,54839
64	0,017	0,034	0,068	0,136	0,272	0,544	1,088	2,176	4,352	35,09677
	Tacq = 8 Tad									
2	0,00065625	0,0013125	0,002625	0,00525	0,0105	0,021	0,042	0,084	0,168	1,354839
4	0,0013125	0,002625	0,00525	0,0105	0,021	0,042	0,084	0,168	0,336	2,709677
8	0,002625	0,00525	0,0105	0,021	0,042	0,084	0,168	0,336	0,672	5,419355
16	0,00525	0,0105	0,021	0,042	0,084	0,168	0,336	0,672	1,344	10,83871
32	0,0105	0,021	0,042	0,084	0,168	0,336	0,672	1,344	2,688	21,67742
64	0,021	0,042	0,084	0,168	0,336	0,672	1,344	2,688	5,376	43,35484

Tadc (ms)	64000	32000	16000	8000	4000	2000	1000	500	250	31
	Tacq = 16 Tad									
2	0,00090625	0,0018125	0,003625	0,00725	0,0145	0,029	0,058	0,116	0,232	1,870968
4	0,0018125	0,003625	0,00725	0,0145	0,029	0,058	0,116	0,232	0,464	3,741935
8	0,003625	0,00725	0,0145	0,029	0,058	0,116	0,232	0,464	0,928	7,483871
16	0,00725	0,0145	0,029	0,058	0,116	0,232	0,464	0,928	1,856	14,96774
32	0,0145	0,029	0,058	0,116	0,232	0,464	0,928	1,856	3,712	29,93548
64	0,029	0,058	0,116	0,232	0,464	0,928	1,856	3,712	7,424	59,87097

	Tacq = 0 Tad									
2	0,00040625	0,0008125	0,001625	0,00325	0,0065	0,013	0,026	0,052	0,104	0,83871
4	0,0008125	0,001625	0,00325	0,0065	0,013	0,026	0,052	0,104	0,208	1,677419
8	0,001625	0,00325	0,0065	0,013	0,026	0,052	0,104	0,208	0,416	3,354839
16	0,00325	0,0065	0,013	0,026	0,052	0,104	0,208	0,416	0,832	6,709677
32	0,0065	0,013	0,026	0,052	0,104	0,208	0,416	0,832	1,664	13,41935
64	0,013	0,026	0,052	0,104	0,208	0,416	0,832	1,664	3,328	26,83871

Tadc (ms)	64000	32000	16000	8000	4000	2000	1000	500	250	31
scale ADCON2 register					Tacq = 2 Tad					
2	0,000469	0,000938	0,001875	0,00375	0,0075	0,015	0,03	0,06	0,12	0,967742
4	0,000938	0,001875	0,00375	0,0075	0,015	0,03	0,06	0,12	0,24	1,935484
8	0,001875	0,00375	0,0075	0,015	0,03	0,06	0,12	0,24	0,48	3,870968
16	0,00375	0,0075	0,015	0,03	0,06	0,12	0,24	0,48	0,96	7,741935
32	0,0075	0,015	0,03	0,06	0,12	0,24	0,48	0,96	1,92	15,48387
64	0,015	0,03	0,06	0,12	0,24	0,48	0,96	1,92	3,84	30,96774

					Tacq = 6 Tad					
2	0,000594	0,001188	0,002375	0,00475	0,0095	0,019	0,038	0,076	0,152	1,225806
4	0,001188	0,002375	0,00475	0,0095	0,019	0,038	0,076	0,152	0,304	2,451613
8	0,002375	0,00475	0,0095	0,019	0,038	0,076	0,152	0,304	0,608	4,903226
16	0,00475	0,0095	0,019	0,038	0,076	0,152	0,304	0,608	1,216	9,806452
32	0,0095	0,019	0,038	0,076	0,152	0,304	0,608	1,216	2,432	19,6129
64	0,019	0,038	0,076	0,152	0,304	0,608	1,216	2,432	4,864	39,22581

Tadc (ms)	64000	32000	16000	8000	4000	2000	1000	500	250	31
	Tacq = 12 Tad									
2	0,000781	0,001563	**0,003125**	0,00625	0,0125	0,025	0,05	0,1	0,2	1,612903
4	0,001563	**0,003125**	0,00625	0,0125	0,025	0,05	0,1	0,2	0,4	3,225806
8	**0,003125**	0,00625	0,0125	0,025	0,05	0,1	0,2	0,4	0,8	6,451613
16	0,00625	0,0125	0,025	0,05	0,1	0,2	0,4	0,8	1,6	12,90323
32	0,0125	0,025	0,05	0,1	0,2	0,4	0,8	1,6	3,2	25,80645
64	0,025	0,05	0,1	0,2	0,4	0,8	1,6	3,2	6,4	51,6129

	Tacq = 20 Tad									
2	0,001031	0,002063	0,004125	0,00825	0,0165	0,033	0,066	0,132	0,264	2,129032
4	0,002063	0,004125	0,00825	0,0165	0,033	0,066	0,132	0,264	0,528	4,258065
8	0,004125	0,00825	0,0165	0,033	0,066	0,132	0,264	0,528	1,056	8,516129
16	0,00825	0,0165	0,033	0,066	0,132	0,264	0,528	1,056	2,112	17,03226
32	0,0165	0,033	0,066	0,132	0,264	0,528	1,056	2,112	4,224	34,06452
64	0,033	0,066	0,132	0,264	0,528	1,056	2,112	4,224	8,448	68,12903

Tacq < 140 ns

Tadc > 0.5 ms

Tacq < 2 Tad

Table A. 8 – Minor time got to execute a sampling and sending cycle.

Fosc	Minor Tadc (ms)	Minor Tsending (ms)	Minor Tspi (ms)	Tsmp (ms)
64 MHz	0,003125	0,0109132	0,016	0,0409514
32 MHz	0,003125	0,0109757	0,032	0,0570764

Table A. 9 – Time to sample relating the number of channels to the number of samplings.

Tsmp (ms)	Sample amount											
channels amount	**2**	**4**	**6**	**8**	**10**	**12**	**14**	**16**	**18**	**20**	**24**	**28**
2	**0,5**	**0,25**	**0,166667**	**0,125**	0,1	**0,083333**	0,071429	**0,0625**	0,055556	0,05	0,041667	0,035714
3	0,333333	**0,166667**	**0,111111**	**0,083333**	0,066667	0,055556	0,047619	0,041667	0,037037	**0,033333**	0,027778	0,02381
4	**0,25**	**0,125**	**0,083333**	0,0625	0,05	0,041667	0,035714	0,03125	0,027778	0,025	0,020833	0,017857
5	0,2	**0,1**	0,066667	0,05	0,04	0,033333	0,028571	0,025	0,022222	0,02	0,016667	0,014286
6	**0,166667**	**0,083333**	0,055556	0,041667	0,033333	0,027778	0,02381	0,020833	0,018519	0,016667	0,013889	0,011905
7	0,142857	0,071429	0,047619	0,035714	0,028571	0,02381	0,020408	0,017857	0,015873	0,014286	0,011905	0,010204
8	**0,125**	0,0625	0,041667	0,03125	0,025	0,020833	0,017857	0,015625	0,013889	0,0125	0,010417	0,008929
9	**0,111111**	0,055556	0,037037	0,027778	0,022222	0,018519	0,015873	0,013889	0,012346	0,011111	0,009259	0,007937
10	**0,1**	0,05	0,033333	0,025	0,02	0,016667	0,014286	0,0125	0,011111	0,01	0,008333	0,007143
11	0,090909	0,045455	0,030303	0,022727	0,018182	0,015152	0,012987	0,011364	0,010101	0,009091	0,007576	0,006494
12	**0,0833**	0,041667	0,027778	0,020833	0,016667	0,013889	0,011905	0,010417	0,009259	**0,0083**	0,006944	0,005952
13	0,076923	0,038462	0,025641	0,019231	0,015385	0,012821	0,010989	0,009615	0,008547	0,007692	0,00641	0,005495
14	0,071429	0,035714	0,02381	0,017857	0,014286	0,011905	0,010204	0,008929	0,007937	0,007143	0,005952	0,005102
15	0,066667	0,033333	0,022222	0,016667	0,013333	0,011111	0,009524	0,008333	0,007407	0,006667	0,005556	0,004762
16	**0,0625**	0,03125	0,020833	0,015625	**0,0125**	0,010417	0,008929	0,007813	0,006944	**0,0063**	0,005208	0,004464

Table A.9 was computed using the equation: $T_{SMP} = 1 / (0.5 \times nºch \times nºsamples)$

Table A.9 legend

Lower than the possible max sending rate (Table A.8)
Lower than the T_{SPI}
Unfeasible without buffer for F< 921600

Table A.10 was computed using the equation: $t = 65535 \times scale \times (1 / FOSC/4)$

Table A. 10 – Time counted regarding the frequency and the timer scale.

tmr1 & tmr3 (2 bytes) count: 65535	maximum time allowed FOSC/4 (ms)									
	16000	8000	4000	2000	1000	500	250	125	62,5	7,75
8	32,7675	65,535	131,07	262,14	524,28	1048,56	2097,12	4194,24	8388,48	67649,03
4	16,38375	32,7675	65,535	131,07	262,14	524,28	1048,56	2097,12	4194,24	33824,52
2	8,191875	16,38375	32,7675	65,535	131,07	262,14	524,28	1048,56	2097,12	16912,26
1	4,0959375	8,191875	16,38375	32,7675	65,535	131,07	262,14	524,28	1048,56	8456,129

Annex B - Schematic

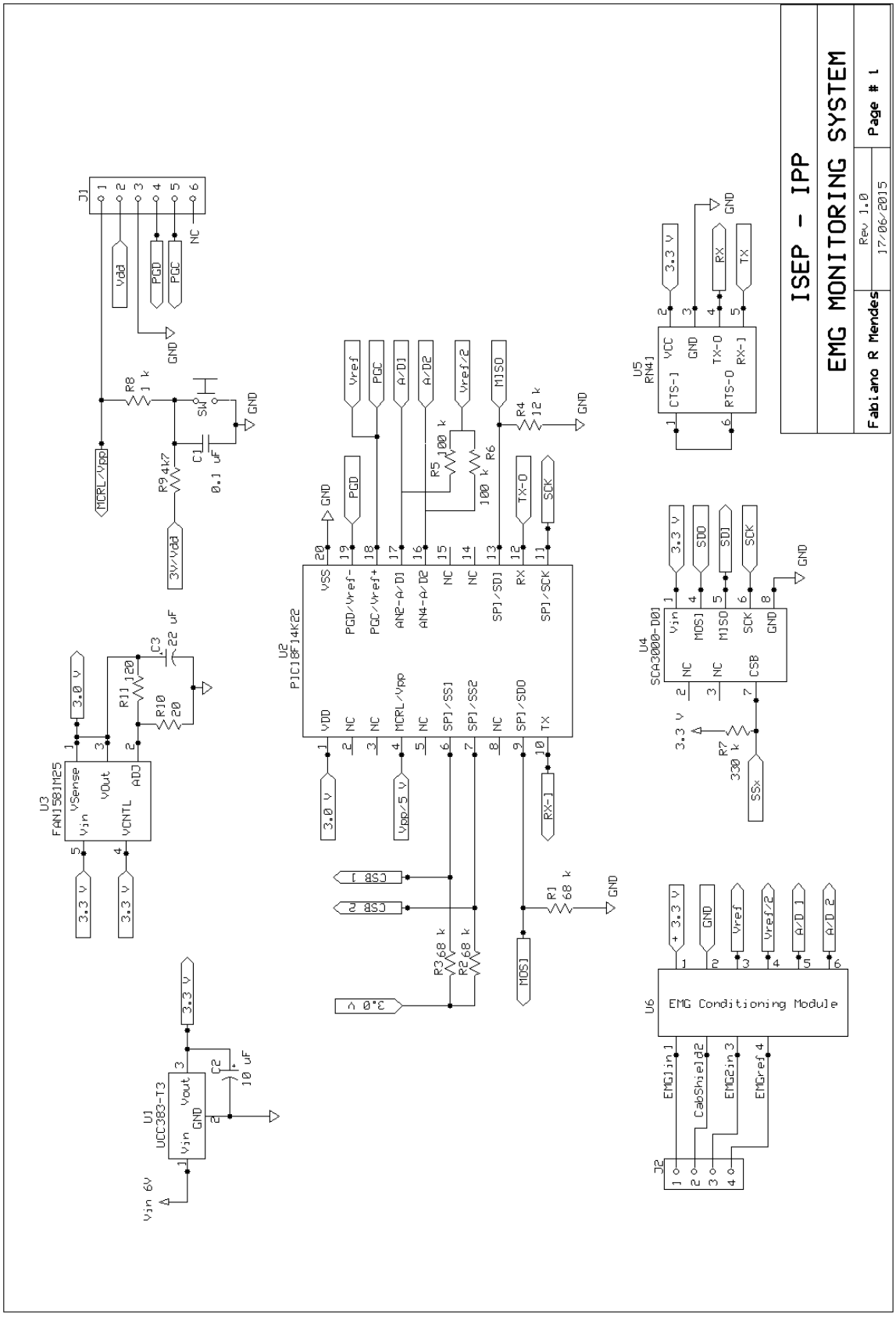

Annex C – Programming Codes

The Annex C is presented in a written part, containing the code of the firmware, and a digital part containing the codes of the firmware and the software as well the executable generated.

```
#include<p18f14k22.h>
#include<spi.h>
//#include<usart.h>

//#define _SS1 PORTCbits.RC4
//#define _SS2 PORTCbits.RC3
//#define _SS3 PORTCbits.RCx

#define _CH1 0x09
#define _CH2 0x11

unsigned char _Rcpt_Con;// _count_time = 0x00;
volatile unsigned char _SS_CH[] = {0b11101111,0b11110111};
static unsigned char _adsRS = 4, _comut_SS = 0;// i=0;

void _int_High_Handler();
void _int_Low_Handler();

/*************************** configuration bits ****************************/

#pragma config FOSC = IRC, PLLEN = OFF, PCLKEN = OFF, FCMEN = OFF, IESO = OFF
#pragma config PWRTEN = OFF, BOREN = OFF, BORV = 30
#pragma config WDTEN = OFF, WDTPS = 32768
#pragma config MCLRE = ON, HFOFST = OFF
#pragma config STVREN = OFF, BBSIZ = ON, LVP = OFF, XINST = OFF
#pragma config CP0 = OFF, CP1 = OFF
#pragma config CPB = OFF, CPD = OFF
#pragma config WRT0 = OFF, WRT1 = OFF
#pragma config WRTB = OFF, WRTC = OFF, WRTD = OFF
#pragma config EBTR0 = OFF, EBTR1 = OFF
#pragma config EBTRB = OFF

/*************************** pre processing code ****************************/

                /// high priority irq

#pragma code high_vector = 0x0008
        void high_vector(void)
        {
                _asm GOTO _int_High_Handler _endasm
        }
#pragma code

                /// high priority irs

#pragma interrupt _int_High_Handler
```

```
        void _int_High_Handler()
        {
//                      PORTAbits.RA5 = ~PORTAbits.RA5;

                if(PIR1bits.CCP1IF)
                {
//                      PORTAbits.RA5 = ~PORTAbits.RA5;

//                      PIR2bits.TMR3IF = 0;

                        PIR1bits.ADIF = 0;              // ADC Interrupt Flag (R/W)
                        PIR1bits.CCP1IF = 0;            // CCP Interrupt Flag (R/W)

                        TXREG = ADRESH;                 // puts the content of ADRESH register as
char on output register
                        while (!PIR1bits.TXIF);
                        PIR1bits.ADIF = 0;              // ADC Interrupt Flag (R/W)

                        if(ADCON0 == _CH1)              // commutates the ADC channel
                                ADCON0 = _CH2;
                        else
                                ADCON0 = _CH1;

                        if (_adsRS == 10 || _adsRS == 4)
                        {
                                _adsRS = 4;                     // first address
                                _comut_SS = ++_comut_SS & 1;    // commutates the index

                                PORTC &= _SS_CH[_comut_SS];     // enables SS

//                              PORTCbits.RC4 =~ PORTCbits.RC4;
//                              PORTCbits.RC3 =~ PORTCbits.RC3;

                                WriteSPI(_adsRS<<2);            // indicate the address to be read
                                while(!DataRdySPI());           // ensure the read to be completed
                                TXREG = ReadSPI() | 1<<_comut_SS;       // read a byte to variable
Val_SPI
                                PORTC |= 0b00011000;            // disables SS
                                _adsRS++;                       // goes to the next address
                        }
                        else
                        {
                                PORTC &= _SS_CH[_comut_SS];
                                WriteSPI(_adsRS<<2);            // indicate the address to be read
                                while(!DataRdySPI());           // ensure the read to be completed
                                TXREG = ReadSPI();              // read a byte to variable Val_SPI
                                PORTC |= 0b00011000;            // disables SS
                                _adsRS++;                       // goes to the next address
                        }

//                      PORTAbits.RA5 = ~PORTAbits.RA5;

                }
        }

                /// low priority irq

#pragma code low_vector = 0x0018
        void low_vector(void)
        {
                _asm GOTO _int_Low_Handler _endasm
        }
```

```
#pragma code

                /// low priority irs

#pragma interruptlow _int_Low_Handler
        void _int_Low_Handler()
        {
                if(PIR1bits.RCIF)
                {
//                      PORTAbits.RA5 = ~PORTAbits.RA5;

                        _Rcpt_Con = RCREG;              // Receives an incoming byte
                        while (!PIR1bits.RCIF);         // wait for complete reading

                        _adsRS = 4;                     // initializes the accel address
                        _comut_SS = 0;                  // initializes the SS pin
//                      _count_time = 1;

//                      PIR2bits.TMR3IF = 0;
                        T3CONbits.TMR3ON =~ T3CONbits.TMR3ON;     // turn on/off the timer
//                      VREFCON1bits.D1EN =~ VREFCON1bits.D1EN;
                }
        }

void main(void)
{

/****************** initializations *****************/

        TRISBbits.TRISB6 = 0;           // SCK output
        TRISCbits.TRISC6 = 1;           // SS disable
        // SS3 output - to be addressed
        TRISCbits.TRISC4 = 0;           // SS2 output - (ST)
        TRISCbits.TRISC3 = 0;           // SS1 output - (ST)

//      TRISCbits.TRISC2 = 0;           // SSx output - (ST)

        TRISAbits.TRISA5 = 0;           // SS_SDCard output - (TTL)
        TRISCbits.TRISC7 = 0;           // MOSI output
        TRISBbits.TRISB4 = 1;           // MISO input
        PORTC |= 0b00011000;            // Set all SS disabled

        TRISBbits.TRISB5 = 1;           // USART input  -- this need to be configured as input --  !!!
        TRISBbits.TRISB7 = 0;           // USART output

        TRISAbits.TRISA2 = 1;           // AN2 input
        TRISCbits.TRISC0 = 1;           // AN4 input
        TRISCbits.TRISC5 = 0;           // CCP1 output

//      ANSELbits.ANS6 = 0;

        ANSELHbits.ANS11 = 0;           // disable the analog function and enable USART function
        ANSELHbits.ANS10 = 0;           // disable the analog function and enable SPI function
        ANSELbits.ANS7 = 0;             // disable the analog function and enable SPI function

        ANSELbits.ANS2 = 1;             // configure as analog input
        ANSELHbits.ANS8 = 1;            // configure as analog input

//      _SS1 = 1;
//      _SS2 = 1;
//      _SS3 = 1;
//      _SS_SDCARD = 1;
```

```
//      PORTAbits.RA5 = 1;
//      PORTCbits.RC6 = 1;
//      PORTCbits.RC4 = 1;
//      PORTCbits.RC3 = 1;

/************************** Set up oscillator ********************/

        OSCTUNE &= 0x80;                // Oscillator, module works at factory calibrated frequency
and with 16MHz HFINTOSC reference source

//      OSCTUNEbits.PLLEN = 1;          // enables the 4xPLL = 64MHz / 32MHz      -- 139->115200
(limit of 127)

        OSCCON |= 0b11110010;           // define the frequency in 16MHz  -- 34->115200; 103->34800--
0b11110110 - sleep instruction enter in idle mode

//      OSCCON |= 0b11100000;           // define the frequency in 8MHz
                                        -- 0b11100010 - sleep instruction enter in idle mode
//      OSCCON &= 0b11101111;

//      OSCCON |= 0b11010000;           // define the frequency in 4MHz
                                        -- 0b11010010 - sleep instruction enter in idle mode
//      OSCCON &= 0b11011111;

//      OSCCON &= 0b11001111;           // define the frequency in 2MHz
                                        -- 0b11000010 - sleep instruction enter in idle mode
//      OSCCON |= 0b11000000;


/************************ Global interrupt ***********************/

        RCONbits.IPEN = 1;              // Enables the usage of priority levels on interrupts
//      INTCONbits.GIE = 1;             // Enables all interrupts
        INTCONbits.GIEH = 1;            // Enables all interrupts == GIE
//      INTCONbits.PEIE = 1;            // Enables all peripherals interrupts
        INTCONbits.GIEL = 1;            // Enables all peripherals interrupts == PEIE

/************************** USART ***********************/

        SPBRG = 0x22;
        SPBRGH = 0x22 >> 8;             // Initialize the SPBRGH:SPBRG with 34 decimal value: FOSC =
16MHz and Baud Rate = 115,2 KHz (pg. 191)

//      SPBRG = 0x01;
//      SPBRGH = 0x01 >> 8;             // Initialize the SPBRGH:SPBRG with 1 decimal value: FOSC =
32MHz and Baud Rate = 921,6 KHz (pg. 191)

//      SPBRG = 0x03;
//      SPBRGH = 0x03 >> 8;             // Initialize the SPBRGH:SPBRG with 3 decimal value: FOSC =
64MHz and Baud Rate = 921,6 KHz (pg. 191)

//      SPBRG = 0x1F;
//      SPBRGH = 0x1F >> 8;             // Initialize the SPBRGH:SPBRG with 31 decimal value: FOSC =
16MHz and Baud Rate = 128 KHz (pg. 191)
        TXSTA = 0x26;                   // TX is actually enabled, Asynchronous mode, 8 bits, BRGH in
High speed
        RCSTA = 0x90;                   // RX is continuously enabled, 8 bits rcpt, receives
continuously
        BAUDCON = 0x4A;                 // * Auto baud detection disabled, Wake-up event on reception
enabled, Baud Rate Generator in 16 bits mode
        PIE1bits.RCIE = 1;              // enables interrupts on reception
```

```
        IPR1bits.RCIP = 0;              // EUSART RX Interrupt high priority
        PIE1bits.TXIE = 0;              // EUSART TX Interrupt disabled
        IPR1bits.TXIP = 0;              // EUSART TX Interrupt low priority

/************************** SPI **************************/

        SSPSTATbits.SMP = 0;            // the data is sampled at middle
        SSPSTATbits.CKE = 1;            // transmission occurs on transition from active to idle clock
state
//      SSPCON1 = 0x02;                 // no collision, no overflow, idle at low level, clk = FOSC/64
        SSPCON1 = 0x01;                 // no collision, no overflow, idle at low level, clk = FOSC/16
//      SSPCON1 = 0x00;                 // no collision, no overflow, idle at low level, clk = FOSC/4

        SSPCON1bits.SSPEN = 1;          // Enables SPI

        PIE1bits.SSPIE = 0;             // disables (external) SPI Interrupt
        IPR1bits.SSPIP = 0;             // SPI Interrupt low priority

/************************** ADC **************************/

//      VREFCON0 = 0xD0;                // It set and enable this register to works with Fixed
Reference Voltage of 1,024 V
//      while(VREFCON0bits.FVR1ST);     // Wait the internal reference stabilization

//      VREFCON1 = 0x60;                // Enables internal voltage reference and disables output
reference
        VREFCON1 = 0x44;                // Disables internal voltage reference and disables output
reference
        VREFCON2 = 0XFF;                // Vref = Vsource

//      ADCON1 = 0x00;                  // Positive reference as internal (Vdd) and negative reference
as Vss - configure VREFCON1
        ADCON1 = 0x04;                  // Positive reference as external (Vref) and negative
reference as Vss - configure VREFCON1

//      ADCON1 = 0x08;                  // Positive reference as internal (FVR) and negative reference
as Vss - configure VREFCON0
//      ADCON2 = 0x0D;                  // Configure the register ADRES as left justified, TAD
multiplied by 2 and the clock as FOSC/16 -> 0x0D / 0x0E -> FOSC/64
        ADCON2 = 0x2C;                  // FOSC/4, 12 TAD, left justified.

        ADCON0 = _CH1;                  // determines the channel and active ADON bits to star
conversion

        ADCON0bits.ADON = 1;            // Enable ADC

                // --- !!! Uncomment the ANSEL and TRIS register in initializations !!! ---

        PIE1bits.ADIE = 0;              // ADC Interrupt enable
        IPR1bits.ADIP = 0;              // ADC Interrupt as high priority

/************************** CCPM1 **************************/

        CCP1CON = 0x0B;                 // Compare mode with a special event trigger

//      CCPR1H = 0x00;                  // Value to be compared  --- !!! does not work properly at
this sampling frequency !!! ---
//      CCPR1L = 0xC8;                  // = 12,5 us / 50 us     --- !!! not feasible with serial
port! excides the sampling time !!! ---

//      CCPR1H = 0x01;                  // Value to be compared  --- !!! overflow at 25s !!! ---
//      CCPR1L = 0x90;                  // = 200 us
```

```
//      CCPR1H = 0x03;                  // Value to be compared  --- !!! overflow at 30s !!! ---
//      CCPR1L = 0x20;                  // = 400 us

//      CCPR1H = 0x00;                  // Value to be compared  --- !!! !!! ---
//      CCPR1L = 0x7D;                  // = 125 us

//      CCPR1H = 0x01;                  // Value to be compared          ---
//      CCPR1L = 0xF4;                  // = 250 us

        CCPR1H = 0x03;                  // Value to be compared          ---
        CCPR1L = 0xE8;                  // = 500 us

//      CCPR1H = 0x07;                  // Value to be compared          ---
//      CCPR1L = 0xD0;                  // = 1000 us


        PIR1bits.CCP1IF = 0;            // CCP Interrupt Flag (R/W)
        PIE1bits.CCP1IE = 1;            // CCP Interrupt disabled
        IPR1bits.CCP1IP = 1;            // CCP Interrupt priority

/************************** Timer3 **************************/

        T3CON = 0b10011100;             // operation with 16 bits, prescale 1:2, TMR3 as clk for CCP,
IRC, actually off

//      TMR3L = ;                                       // NOT USED !!!
//      TMR3H = ;                                       // NOT USED !!!

        PIR2bits.TMR3IF = 0;            // TIMER3 Interrupt Flag (R/W)
        PIE2bits.TMR3IE = 0;            // TIMER3 Interrupt enable
        IPR2bits.TMR3IP = 0;            // TIMER3 Interrupt priority

/*****************************************************************************/
/**/
        while(1)
        {
                Sleep();
        }
}
```